

PERTURBATIVE AND NON-PERTURBATIVE PHYSICS FROM  
SINGULARITIES



by

Cihan Pazarbaşı

B.S., Physics, Boğaziçi University, 2012

M.S., Physics, Boğaziçi University, 2015

Submitted to the Institute for Graduate Studies in  
Science and Engineering in partial fulfillment of  
the requirements for the degree of  
Doctor of Philosophy

Graduate Program in Physics

Boğaziçi University

2022



*“On all essential problems,  
there are probably but two methods of thought:  
The method of La Palisse and the method of Don Quixote.  
Solely the balance between evidence and lyricism can  
allow us to achieve simultaneously emotion and lucidity.”*

*Albert Camus*

## ACKNOWLEDGEMENTS

A part of the research about this thesis was pursued during my visit to North Carolina State University. This visit was supported by TUBITAK 2214-A Research Fellowship Programme for PhD Students.

PhD is a long journey. For me it was a transformative one, not only academically but also mentally. With its all ups and downs, it was a great journey and I am grateful to many for their contribution to my academic and social life.

First of all, it has been a pleasure for me to study under the guidance of my supervisor Dieter Van den Bleeken for last 9 years. During this time, he has been an inspirational role model as a researcher that I learned a lot while I was developing as an independent researcher. Starting from the beginning of my master thesis research, his guidance helped me not to lose my path and his faith and support gave me courage to continue when I started to lose my confidence. I am also grateful for the freedom and his patience during all the discussions while I am looking around to find my research path.

Next, I would like to thank Mithat Ünsal for the opportunity to visit NSCU for one year and the enlightening research experience during this time. Along with the academic part of this experience, I am also grateful for his encouragements that actually started via e-mails before we met in person and continued since then whenever we interact.

In addition to my research collaborators and mentors, I would like to thank Can Kozçaz and Ilmar Gahramanov for various conversations on physics that also shaped my research. I want to add a special thank you note to Can Kozçaz for the suggestion to contact Mithat Ünsal for collaborating with him before I dared to think about it.

I also thank Mansur İsgenderoğlu and Cemsinan Deliduman for accepting to be in the thesis committee and their helpful comments on the thesis.

When it comes to friendship, during my PhD journey, I am very lucky to be surrounded by many friends to talk about physics but more importantly to have great times and a lot of fun that help me to shake off the stress of PhD research. Here, I would like to express my special gratitudes to Şelale and Berare for being there when I fell. I also thank Birses, Ceyda, Emre for many rehabilitating conversations. There is also “Fizikçi gençler”, viz. Cem, Kerem, Narçiçeği, Ömer, Sinan and Şelale, I thank them for many “mind opening” conversations.

And I am grateful to my mother for supporting me as I walked through this journey. Thank you so much, mom.

Finally, Hasret! Thank you so much for all the endless love, support and courage along this journey. Your presence brings joy and serenity to my life.

## ABSTRACT

# PERTURBATIVE AND NON-PERTURBATIVE PHYSICS FROM SINGULARITIES

A function that representing a physical quantity has singularities which contain perturbative or non-perturbative information about the physical system under investigation. Moreover, the theory of resurgence tells us that these perturbative and non-perturbative parts are intimately connected and it is possible to use one of them to obtain the other one. In this thesis, we combine these two ideas with a focus on the functions formulated in integral representations. Specifically, first considering two different examples on the semi-classical expansion in quantum mechanics and the pair production problem in electromagnetic backgrounds, we will concentrate on the quantum action which we express in the Schwinger's integral representation. We will show that the perturbative and non-perturbative information about the physical system is hidden in singularities of the propagator  $\text{Tr}U(t)$ . The way we obtain the non-perturbative one is very similar to the Borel method which is used to handle the divergent perturbation series. Contrary to the Borel method, by probing the singularities of  $\text{Tr}U(t)$  directly and using the  $i\varepsilon$  prescription, we will be able to prevent the Borel ambiguity problem in the physical cases that it leads to the violation of the unitarity. Later, we will turn our attention to the renormalon problem in non-relativistic quantum mechanics. After presenting the existence of the renormalon divergence in a scattering problem with a background potential consisting of 2D  $\delta$ -potential perturbed with a tilted 1D  $\delta$ -potential, we will argue that the Borel ambiguity in the summation of the divergent series can be prevented again by a careful application of the  $i\varepsilon$  prescription and the resulting non-perturbative contribution due to the renormalon obeys the causality condition.

## ÖZET

### TEKİLLİKLERDEN ELDE EDİLEN PERTÜRBATİF VE PERTÜRBATİF OLMAYAN FİZİK

Fiziksel bir niceliği temsil eden bir fonksiyon, incelenmekte olan fiziksel sisteme hakkında pertürbatif veya pertürbatif olmayan bilgiler içeren tekilliklere sahiptir. Bununla birlikte resurgence teorisi bize bu tedirgin ve tedirgin olmayan kısımların yakından bağlantılı olduğunu ve bunlardan birinin diğerini elde etmek için kullanımının mümkün olduğunu söyler. Bu tezde, integral temsillerinde formüle edilen fonksiyonlara odaklanarak bu iki fikri birleştiriyoruz. Spesifik olarak, öncelikle kuantum mekaniğindeki yarı-klasik açılım ve elektromanyetik arkaplanında çift üretim problemi ile ilgili iki farklı örneği ele alarak, Schwinger'in integral temsilinde ifade ettiğimiz kuantum eylemine odaklanacağız. Fiziksel sistem hakkındaki pertürbatif ve pertürbatif olmayan bilginin  $\text{Tr}U(t)$ 'nin tekilliklerinde saklı olduğunu göstereceğiz. Pertürbatif olmayan kısmı elde etme yöntemimiz, iraksak perturbasyon serilerini üstesinden gelmek için kullanılan Borel yöntemine çok benzemektedir. Borel yönteminin aksine,  $\text{Tr}U(t)$ 'nın tekilliklerini doğrudan araştırarak ve  $i\varepsilon$  reçetesini kullanarak, üniterliğin ihlal edildiği fiziksel sistemlerde Borel belirsizliği sorununun önüne geçebileceğiz. Daha sonra dikkatimizi relativistik olmayan kuantum mekaniğindeki renormalon problemine çevireceğiz. Renormalon iraksamasının, eğilmiş bir 1D  $\delta$ -potansiyeliyle pertürbe edilmiş 2D  $\delta$ -potansiyelinden oluşan bir arka plan potansiyeline sahip bir saçılma probleminde var olduğunu gösterdikten sonra, iraksak serilerin toplamında ortaya çıkan Borel belirsizliğinin yine  $i\varepsilon$  reçetesinin dikkatli bir şekilde uygulanmasıyla önlenebileceğini ve renormalon sebebiyle ortaya çıkan pertürbatif olmayan katkılardan nedensellik koşulunu sağladıkların iddia edeceğiz.

## TABLE OF CONTENTS

ACKNOWLEDGEMENTS . . . . .	iv
ABSTRACT . . . . .	vi
ÖZET . . . . .	vii
LIST OF FIGURES . . . . .	xi
LIST OF TABLES . . . . .	xiii
LIST OF SYMBOLS . . . . .	xiv
LIST OF ACRONYMS/ABBREVIATIONS . . . . .	xvi
1. INTRODUCTION . . . . .	1
1.1. About the Thesis . . . . .	5
1.2. Outline of the Thesis . . . . .	7
2. PRELIMINARY DISCUSSION . . . . .	9
2.1. Divergence of Perturbation Series in Physics . . . . .	9
2.2. Divergent Series and Borel Summation . . . . .	13
2.2.1. An Analysis of Divergent Series: . . . . .	13
2.2.2. The Euler Equation . . . . .	14
2.2.3. Borel Summation . . . . .	16
2.2.4. Borel Ambiguity and Its Resolution . . . . .	19
2.3. Physics from Analytic Structure . . . . .	22
2.3.1. Integrals and Their Singularities . . . . .	24
2.3.2. Geometry and WKB Method . . . . .	27
3. THE SEMI-CLASSICAL EXPANSION IN ARBITRARY DIMENSION . .	34
3.1. Spectral Problem . . . . .	35
3.2. Expansion in $D$ Dimensions . . . . .	36
3.2.1. Recursion Relation . . . . .	40
3.3. An Example: Anharmonic Oscillators in Quantum Mechanics . . . . .	44
3.4. WKB Expansion = Derivative Expansion . . . . .	47
3.5. Discussion . . . . .	49
4. PAIR PRODUCTION WITHOUT BOREL AMBIGUITY . . . . .	51

4.1. Background Discussion . . . . .	51
4.2. Pair Production Problem and Resolution of Ambiguity . . . . .	56
4.2.1. Ambiguity and Its Resolution in Uniform Electromagnetic Background . . . . .	58
4.3. Unambiguous Pair Production from Perturbative Expansions . . . . .	64
4.3.1. Time Dependent Electric Fields: . . . . .	68
4.3.2. Space Dependent Electric Fields: . . . . .	71
4.4. Connection to Semi-Classics . . . . .	72
4.4.1. Duality from WKB Cycles: . . . . .	73
4.4.2. Non-cancellation from Lefschetz Thimbles: . . . . .	76
4.5. Discussion . . . . .	80
5. RENORMALONS IN QUANTUM MECHANICS . . . . .	83
5.1. Background Discussion . . . . .	83
5.2. Quantum Mechanics with a 2D $\delta$ -potential . . . . .	86
5.2.1. One Loop . . . . .	87
5.2.2. All Order . . . . .	89
5.2.3. Exact Solution . . . . .	91
5.3. A Renormalon Diagram in Quantum Mechanics . . . . .	92
5.4. Renormalons: All Order Perturbation Theory . . . . .	96
5.4.1. First Order in $\kappa$ . . . . .	96
5.4.2. Second Order in $\kappa$ . . . . .	99
5.4.3. Concrete Example . . . . .	100
5.4.4. Borel Summation: Ambiguity and Resolution . . . . .	102
5.5. Rederivation Using Exact Green's Operator . . . . .	105
5.5.1. Operator Formalism and the Born Series . . . . .	105
5.5.2. Operator Formalism and the $\lambda$ -Exact Series . . . . .	106
6. CONCLUSION . . . . .	109
REFERENCES . . . . .	111
APPENDIX A: NOTATIONS AND CONVENTIONS . . . . .	123
APPENDIX B: ASYMPTOTICS OF A KEY RENORMALON INTEGRAL .	124
APPENDIX C: NUMERICAL RESULTS . . . . .	126

C.1. Cubic Oscillator: . . . . .	126
C.2. Quartic Oscillator: . . . . .	127
C.3. Quintic Oscillator: . . . . .	127

## LIST OF FIGURES

Figure 2.1. Left: A renormalized 1-loop diagram with logarithmic momentum dependence. Right: $n$ renormalized diagram inserted in a larger loop. . . . .	12
Figure 2.2. Contours for the Borel summation integral. . . . .	17
Figure 2.3. The Borel summation integral contours in the limit $\theta_1 \rightarrow 0$ and $\theta_2 \rightarrow 0$ . . . . .	19
Figure 2.4. Double-well potential. . . . .	20
Figure 2.5. Deformation of contour as the singularity at $z_1$ moves on a circle. . . . .	25
Figure 2.6. Formation of torus from a two sheeted Riemann surface. . . . .	29
Figure 4.1. Complex $t$ planes. (Left) Real time cases. (Right) Imaginary time case. . . . .	59
Figure 4.2. Possible paths to probe the singularity on the real axis. This picture describes for the electric poles in the Euclidean case and the magnetic poles in the real time case. . . . .	61
Figure 4.3. Contours for the real time integrals in Electric case. Left: Contours for $\Gamma^+$ . Right: Contours for $\Gamma^-$ . . . . .	62
Figure 4.4. Lefschetz thimbles for the magnetic case. . . . .	78
Figure 4.5. Lefschetz thimbles for the electric case. . . . .	79

Figure 5.1. Left: Renormalon type diagrams in 2-particle scattering violate particle number conservation. Right: In 4-particle scattering particle number can be conserved. . . . .	84
Figure 5.2. Support of our example potential. The blue line, which coincides with the $z$ -axis, corresponds to $V_\star = \delta(x)\delta(y)$ , while the red plane corresponds to $V_* = \delta(\cos \theta z - \sin \theta y)$ . . . . .	93
Figure 5.3. A renormalon-type diagram. On the left the diagram describing one-particle scattering off a potential. On the right a corresponding diagram in the language of 4-particle scattering. . . . .	94

## LIST OF TABLES

Table 5.1.	Expressions for all 8 types of diagrams at order $\kappa^2$ . Only the diagrams in the last four rows can lead to renormalons. . . . .	98
------------	--	----

## LIST OF SYMBOLS

$a(u)$	WKB action
$a^D(u)$	Dual WKB action
$A_\mu$	Gauge potential
$\mathcal{A}$	Vacuum vacuum amplitude
$B$	Magnetic field strength
$\mathcal{B}$	Borel transformation
$D(u)$	Fredholm determinant
$E$	Energy of scattering states
$E_b$	Bound state energy of 2D $\delta$ -potential
$e$	Charge of the scalar particle
$E_\alpha(z)$	The generalized exponential function
$\mathcal{E}$	Electric field strength
$g_{\mu\nu}$	Lorentzian metric
$G(u)$	Green's function
$H$	Hamiltonian
$\mathsf{H}$	Hamiltonian Operator
$\mathcal{J}$	Integration cycles corresponding to Lefschetz thimbles
$\mathcal{K}$	Integration cycles dual to Lefschetz thimbles
$m$	Mass of the scalar charged particle
$\mathbf{p}$	Momentum vector in euclidean signature
$p_\mu$	Momentum vector in Lorentzian signature
$\mathcal{P}$	Pair production probability
$s$	Imaginary (Euclidean) time
$S$	S-matrix
$\mathcal{S}[f(x)]$	Borel summation of $f(x)$
$t$	Real time
$T(\mathbf{p})$	Generalized kinetic term
$\mathsf{T}(\mathbf{p})$	Operator valued function for the generalized kinetic term

$\mathcal{T}$	Time ordering
$\mathbf{T}(z)$	Off-shell T-matrix
$u$	Energy eigenvalue
$U(t)$	Time dependent quantum propagator
$\mathbf{V}(\mathbf{x})$	Operator valued function for the potential
$V(\mathbf{x})$	Classical Potential
$\hat{V}(\mathbf{p})$	Potential in momentum space
$\mathbf{V}_I$	Potential operator in the interaction picture
$\mathbf{x}$	Position vector in Euclidean signature
$x_\mu$	Position vector in Lorentzian signature
$\beta$	Beta function
$\Gamma$	Quantum action/Effective Action
$\Lambda$	Renormalization invariant scale
$\mu$	Renormalization energy scale
$\tau$	On-shell T-matrix
$\omega$	Frequency of electromagnetic field
$\Omega$	UV cutoff

## LIST OF ACRONYMS/ABBREVIATIONS

1D	One Dimensional
2D	Two Dimensional
3D	Three Dimensional
LSZ	Lehmann-Symanzik-Zimmerman
QCD	Quantum Chromodynamics
QED	Quantum Electrodynamics
QFT	Quantum Field Theory
QM	Quantum Mechanics
UV	Ultraviolet
WKB	Wentzel-Kramers-Brillouin

## 1. INTRODUCTION

Physics is an experimental and observational science which can only be understood by using the language of mathematics. The underlying mathematics of physical theories can be used to understand the physical phenomenon known to exist or to make predictions for future experiments. On the other hand, often than not it is better to analyze the mathematical structure of a theory beyond its predictive scheme. In this way, we might further appreciate the beauty of the physical phenomenon. In addition to that, it is also possible to uncover previously unnoticed relations and solve the completeness and consistency problems already exists in a physical theory. Motivated from the intimate relationship between perturbative and non-perturbative sectors in quantum theories, this thesis is about such a journey which focuses on obtaining both perturbative and non-perturbative physical information from the singularities of quantum propagators.

The association of the analytical structure of a function to some physical information is not a new concept for quantum physics. It is well known that the singularities of the Green's function,  $G(\lambda) = (\lambda - H)^{-1}$ , which also serves as quantum propagator, are associated to the eigenvalues of the Hamiltonian. Similarly, in a scattering problem, bound states (or masses in QFT) can be probed by looking to the analytical structure of  $S$ -matrix. The latter one is, in fact, the main approach of  $S$ -matrix theory which was initiated in early days of relativistic quantum theories [1, 2]. However, knowing these facts does not help in practical considerations since obtaining the complete Green's function or the  $S$ -matrix is not possible except in very few special cases. At this point, one might think that approximation methods might help to compute physical quantities. However, a perturbative expansion is just a polynomial series, so only its summation can probe the singularities of the functions that they suppose to represent. While this is an option which we will use in this thesis, it is also possible to devise other formulations for quantum theories.

In both non-relativistic and relativistic quantum theories, there are several approaches which transform the problem in a more favorable form. For example in non-relativistic regimes, we have the Schrödinger equation whose solutions provide all the information about the spectrum. On the relativistic side, with the help of LSZ reduction, we can obtain physical information about masses or coupling constants by computing correlation functions of relativistic fields. However, again except few special cases, approximation methods would be needed. At least in these cases, perturbative techniques yield physical information directly but they hide non-perturbative information such as the mass gap in non-abelian gauge theories, topological effects or bound states.

One way to obtain non-perturbative information is using specialized approximation methods based on the underlying classical motion associated to the Lagrangian of the physical system [3–5]. In this way, it is possible to associate non-perturbative information with the action of the classical motion of real or pseudo particles.

Another way to get the non-perturbative information is summing the perturbation series, which is one of the main focuses of this thesis. This is possible due to the fact that the perturbative and non-perturbative sectors of a physical theory are intimately connected. This connection exists because, as we will see in different examples in this thesis, both sectors arise from the same (or at least related) singularities of the function representing a physical quantity. In this sense, we can interpret the perturbative and non-perturbative parts as different aspects of the information arising from the same singularity. Moreover, using this connection, it is also possible to obtain one of these sectors from the other one.

To digest this observation, let us examine the perturbative series of a physical observable:  $f(\lambda) = \sum f_n \lambda^n$ , where  $\lambda$  is a coupling constant. Since Freeman Dyson's elegant paper [6], it is known that consistency in physical systems forces the function  $f(\lambda)$  to have a singularity, more specifically a branch point, at  $\lambda = 0$ . This leads to the perturbation series to be divergent. Thus, it can not represent the observable fully

as it makes no sense mathematically.

Later studies [7, 8] showed that such a perturbation series diverges factorially, i.e.  $f_n \sim n!$ . While this behaviour indicates a pathology of the perturbation theory, it contains much more information than it shows at first sight. One way to extract the hidden information is taming the factorial divergence using the Borel method which removes the branch point in the  $\lambda$  plane. In this method, the original observable  $f(\lambda)$  is represented by an integral

$$f(\lambda) = \int_{\gamma} db e^{-b} \mathcal{B}[f(\lambda)](b), \quad (1.1)$$

where  $\mathcal{B}[f(\lambda)](s)$  is called the Borel transform of  $f(\lambda)$  and the singularity information is transferred to a singularity of  $\mathcal{B}[f(\lambda)](b)$  in the complex  $b$ -plane, i.e. Borel plane. Then, integration over the singularity leads to an exponentially suppressed complex contribution, i.e.  $\pm i e^{-1/\lambda}$ , which is associated to the non-perturbative sector of the theory.

The Borel method shows first signals of a deeper relationship between perturbative and non-perturbative sectors. This is the subject of resurgence theory which provides a framework to obtain complete and consistent information about the whole quantum spectrum [9, 10]. At the next step, we observe that while curing the divergence pathology, the Borel method leads to another pathology, called a Borel ambiguity, that non-perturbative information obtained from perturbative data is complex and multi-valued. Complex values might be acceptable in some cases. But for example, when they appear in energy eigenvalues of a stable quantum mechanical system, it is a sign of a disaster.

The disaster can be prevented when direct non-perturbative computations via instantons are considered. Based on the separate works of Bogomolny [11] and Zinn-Justin [12], in different settings [13–19], it was precisely shown that the contributions of multi-instanton configurations to the spectrum cancels the imaginary part that arises from the Borel procedure. Then, the resulting expression becomes a real

quantity with no pathology. In fact, this cancellation mechanism can be extended to all non-perturbative orders and the end result after cancellations would contain no pathology [16, 20].

It is also possible to obtain the perturbative data from the non-perturbative one. Suppose that we get the non-perturbative imaginary contribution  $\text{Im}f(\lambda) \sim e^{-1/\lambda}$  from instantons first. Then, via the dispersion relation [21, 22] a term at order  $k$  is related to the imaginary part as

$$f_k = \frac{1}{\pi} \int_0^\infty d\lambda \frac{\text{Im}f(\lambda)}{\lambda^{k+1}}. \quad (1.2)$$

This relation is due to the branch cut, which we assumed to be on positive real axis, associated to the singularity at  $\lambda = 0$ . Although, we will not use it in this thesis, it shows another aspect of the connection between perturbative and non-perturbative sectors arising from the singularity of  $f(\lambda)$ .

Along with the connection between perturbative and non-perturbative sectors, the lesson of the above discussion is that when divergent perturbation series are carefully handled and considered together with the contributions coming from non-perturbative approximations, the resulting expressions lead to a consisted and complete physical picture. However, cancellations between the two sectors can only work for the system with stable vacua or more generally, when an imaginary contribution should not survive in the full expression.

The main problem in such problems is the multivalued nature of the imaginary non-perturbative terms,  $\pm ie^{-1/\lambda}$ , obtained from the Borel method. In physical problems, this is not acceptable as one of the signs violates unitarity or causality of the theory. Therefore, we need to reconsider the Borel method such that only the sign which preserves unitarity/causality appears, i.e. there would be no Borel ambiguity at all. This would be possible if the analytical continuation direction in (1.1) would be pre-determined by construction of the problem.

Long ago in [23, 24], it was shown that it is possible to formulate (1.1) such that the Borel summation  $\mathcal{B}[f(\lambda)]$  corresponds to the propagator of the physical theory in consideration. This suggests that it is possible to compute the propagator directly and its singularities coincide with the Borel plane singularities we discussed. In addition to that formulating the theory in real time determines the possible analytical continuation directions to the propagator by the  $i\varepsilon$  prescription and in this way, the Borel ambiguity problem resolves as it arises from the freedom of the analytical continuation directions in the first place.

### 1.1. About the Thesis

In this thesis, we will first put the arguments of [23, 24] on a more concrete basis and define an unambiguous physical observable. Our derivation is based on the spectral problem where we consider the logarithm of the Fredholm determinant, i.e.

$$\Gamma(u) = \ln \det(u - H), \quad (1.3)$$

as the main spectral function which will call the *quantum action*.<sup>1</sup> In this form, the spectral information is hidden in the logarithmic singularities of  $\Gamma(u)$ . It is possible to extract this information by formulating it in the Schwinger's integral form, i.e.

$$\Gamma(u) = \int_0^\infty dt e^{itu} \text{Tr} e^{iHt}. \quad (1.4)$$

Note that this integral is very similar to the Borel integral (1.1). Then, the singularities of  $\text{Tr} e^{iHt}$  can be used to obtain the non-perturbative part of  $\Gamma(u)$ . On the other hand, Equation (1.4), even without any singularity, is not finite when the integral is computed on the original contour. It can be made finite by setting  $u \rightarrow u + i\varepsilon$  or equivalently rotating  $t$  contour in counter clockwise direction. This is the essence of the resolution of the Borel ambiguity.

---

<sup>1</sup>Note that the naming comes from the usage of the Fredholm determinant in QFT and many-body theories to calculate the effective actions [25] but in addition to that as an achievement of this thesis, we will also show that in one dimensional non-relativistic quantum mechanics,  $\Gamma(u)$  corresponds to the WKB action.

Note that it is known that [1] the poles of an integrand are associated to the branch points of the function represented by that integral. Therefore, probing the poles of the integrand in (1.1) is equivalent to probing branch points of  $\Gamma(u)$ . In this sense, this is very similar to the discussion of the analytical structure of  $f(\lambda)$  above but in this case, the problem is formulated on the  $u$ -plane and it is more direct, as we introduced the logarithmic singularity from the beginning instead of observing it from a divergent perturbation series.

Along with resolving the ambiguity problem, as the expression (1.4) is based on the spectral theory, the analytical properties of  $\Gamma(u)$  can also be used to obtain perturbative data as well. This is indeed the case, as we will show in Chapter 3, in one dimensional quantum mechanics settings, the discontinuity at the branch cut of  $\Gamma(u)$  corresponds to the WKB action. It is well-known that in the WKB setting, the discontinuity appears on the position space and the spectral information arises from closed line integrals, such that

$$\Delta\Gamma \sim \oint dx \sqrt{u - V(x)}, \quad (1.5)$$

which corresponds to the leading order WKB action in the semi-classical expansion and where  $V(x)$  is the classical potential of the quantum mechanical system. Formulating  $\Gamma(u)$  in the time dependent setting as in (1.4), we transfer this information to the  $t$  plane. In addition to that this formulation enables practical calculations for systems in arbitrary dimensions rather than one dimension where the standard WKB method is effective.

In addition to the spectral problem that is based on the definition in (1.3), we will also discuss a scattering problem in Chapter 5. This problem involves renormalons which are artifacts of the renormalization of logarithmically divergent diagrams and present themselves as factorial divergence in perturbation series. Although the sources the divergences of perturbative expansions of the renormalon problem and the spectral problem, which we will discuss briefly in Section 2.1, and the construction of these two problems are different, we will show that the renormalon divergence is also associated

to an integral singularity.

## 1.2. Outline of the Thesis

The main part of this thesis consists of the application of the above ideas to three problems which was published in three separate papers [26–28]. Each of these papers will constitute a chapter in the thesis. We complement these chapters with a background discussion on the role of the singularities in both the perturbative and non-perturbative sectors of quantum physics.

- In Chapter 2, we will present the preliminary discussions. We will start with the type of divergences that appear in physical problems and after a technical review of the divergent expansions, we will discuss the connection between perturbative expansions and non-perturbative contributions using the Borel method. Then, we will present how the Borel summation leads to unambiguous results via the cancellation mechanism of Bogomolny and Zinn-Justin. Finally, we will discuss the preliminary discussion with a formal discussion on the singularities of function expressed via an integral. This will be the basis of the computations the following chapters. We will finish the chapter with a brief discussion on the WKB method and the geometry behind it as the discussions in Chapters 3 and 4 presents the same physical structure from a different and more general point of view.
- As the first application, in Chapter 3, we will present how the semi-classical expansion can be obtained from the Schwinger’s integral (1.4) which was originally published in a research paper with the title “*Recursive Generation of The Semi-Classical Expansionin Arbitrary Dimension*” [26]. We will show that the gap  $\Delta\Gamma(u)$  of the quantum action  $\Gamma(u)$  due to the singularity of  $\text{Tr}U(t)$  at  $t = 0$  leads to the perturbative WKB action in one dimensions and the time-dependent formalism we will provide a generalization to higher dimensions. The main computations will be carried out via a recursion relation that will also be derived in this chapter.

- In Chapter 4, which was originally published in a research paper with the title “*Pair Production in Real Proper Time and Unitarity Without Borel Ambiguity*” [27], we will focus on obtaining the non-perturbative pair production probability without any Borel ambiguity. We will show that although the non-perturbative information is extracted from a singularity of  $\text{Tr}U(t)$ , contrary to the perturbative case we discuss in Chapter 3, it arises from the singularities at finite  $t$ . While, the treatment of this singularity is similar to the integration of the Borel method, using  $i\varepsilon$  prescription we will be able to obtain the non-perturbative part with a fixed sign. We will also explain the connection with the singularities of  $\text{Tr}U(t)$  appear in the time dependent formalism with the WKB cycles. Finally, we will explain the non-existence of the Borel ambiguity from using the Lefschetz thimbles.
- Finally, in Chapter 5, we will focus on a non-relativistic scattering problem that involve the renormalon divergence in the perturbative expansion of  $S$ -matrix. Reducing the many body scattering problem to one dimensional quantum mechanics, we will be able to obtain the renormalons in one particle quantum mechanics in 3 dimensions with a background potential of 2D  $\delta$ -potential perturbed with 1D  $\delta$ -potential that corresponds to a plane in 3D space. In addition to that in a similar way to Chapter 4, we will obtain the non-perturbative information associated to the renormalon divergence without any Borel-like ambiguity. The content we will present in this chapter was originally published in a research paper with the title “*Renormalons in quantum mechanics*” [28].

## 2. PRELIMINARY DISCUSSION

### 2.1. Divergence of Perturbation Series in Physics

In this section, we will briefly discuss the divergent perturbative expansion that we encounter in physical problems. There are two known sources for the divergent behaviour. One source is associated to the number of Feynman diagrams and their proliferation as the order of the perturbative expansion increases [7, 8]. The other one, on the other hand, arises as an artifact of the renormalization procedure and it is associated to the dominant parts of the loop integrals over logarithmic momentum dependent quantities which are results of the renormalization procedure [29–31]. Due to its relation to the renormalization process, this divergence source is called “renormalon”.

Both proliferation of diagrams and renormalons result in the same type of divergences in their corresponding perturbative series, i.e. at higher orders, the series is dominated by a factorial growth. This is a serious problem for the consistency of the theory as the perturbation series is not well-defined. In Section 2.2, we will discuss how this problem is resolved by the Borel summation procedure. This will also enable us to obtain consistent non-perturbative information about the theory by probing exponentially suppressed terms that are ignored in the original perturbative expansion. Before that, in the following, we will elaborate on both type of divergence sources.

Let us first discuss the proliferation of Feynman diagrams. Consider Feynman diagrams at a given order in a perturbation series. While it is possible to get different types of diagrams, most of them are related to each other by a permutation symmetry and their contributions are equal to each other. However, as higher order diagrams are analyzed, the number of diagrams symmetric to each other also increases. Therefore, although the contribution of an individual diagram does not increase on average, the overall contribution at high orders increases due to the number of diagrams. By

counting the number of diagrams by statistical methods [7, 8], it was found that the growth is a factorial one and the term  $f_n$  in the perturbation series at order  $n$  behaves as  $f_n \sim A^{-n}n!$ .

As an example, instead of using statistical methods, we will consider the ordinary integrals that count the number of diagrams contributing to the partition function [32, 33]. This will help us to understand the analytical background of the divergent behaviour. Take the quartic anharmonic oscillator

$$V(x) = \frac{x^2}{2} + \lambda x^4.$$

Then, the large order estimation of the number of diagrams is given by

$$I(\lambda) = \frac{1}{\sqrt{2\pi}} \int_{-\infty}^{\infty} dx e^{-\frac{x^2}{2} - \lambda x^4}. \quad (2.1)$$

Expanding the exponential in  $\lambda$ , we get

$$I(\lambda) = \frac{1}{\sqrt{2\pi}} \sum_{n=0}^{\infty} \frac{(-\lambda)^n}{n!} \int_{-\infty}^{\infty} dx x^{4n} e^{-\frac{x^2}{2}}, \quad (2.2)$$

which can be easily computed in terms of Gamma functions by setting  $\frac{x^2}{2} = t$ :

$$I(\lambda) = \frac{1}{2\pi} \sum_{k=0}^{\infty} \frac{2^{2n+\frac{1}{2}} (-\lambda)^n}{n!} \int_0^{\infty} dt t^{2n-\frac{1}{2}} e^{-t} = \frac{1}{2\pi} \sum_{k=0}^{\infty} \frac{2^{2n+\frac{1}{2}} (-\lambda)^n}{n!} \Gamma\left[n + \frac{1}{2}\right]. \quad (2.3)$$

However, since we are interested in the high order estimations, let us use the saddle point approximation by re-writing (2.2) as

$$I(\lambda) = \frac{1}{\sqrt{2\pi}} \sum_{n=0}^{\infty} \frac{(-\lambda)^n}{n!} \int_{-\infty}^{\infty} dx e^{-ng(x)}, \quad (2.4)$$

where  $g(x) = \frac{x^2}{2n} - 4 \ln x$ . For large  $n$ , the integral is dominated by the saddle point of  $g(x)$  at  $x^2 = 4n$  and at the leading order, we get

$$\begin{aligned} I(\lambda) &= \frac{1}{\sqrt{2\pi}} \sum_{n=0}^{\infty} \frac{(-\lambda)^n}{n!} \sqrt{\pi} e^{-2n+2n \ln 4n} = \frac{1}{2\sqrt{\pi}} \sum_{n=0}^{\infty} \frac{(-16\lambda)^n}{\sqrt{n}} e^{-n+n \ln n} \\ &= \frac{4}{\pi} \sum_{n=0}^{\infty} (-16)^{n-1} (n-1)! \lambda^n, \end{aligned} \quad (2.5)$$

where we used the Stirling approximation  $n! = \sqrt{2\pi n} e^{-n+n \ln n}$ . This result verifies the factorially divergent behaviour of the perturbation series.

Note that in addition to counting the number of Feynman diagrams, (2.1) helps us to understand another critical aspect of the quartic oscillator: For  $\lambda < 0$ , the integral is not well-defined. This is related to the instability of the vacuum at  $x = 0$  for negative  $\lambda$ -values. As Dyson indicated in [6], this means that  $I(\lambda)$  should be problematic on the negative real axis in the  $\lambda$ -plane. Specifically, it can be shown by an analytical continuation in the  $\lambda$  plane that  $I(\lambda)$  has a branch cut along the real negative axis which connects the branch points at  $\lambda = 0$  and  $\lambda = -\infty$ . In the perturbation series (2.5), the branch point at  $\lambda = 0$  leads to the factorial divergence and as a result the lack of mathematical definition of the series itself.

Now, let us focus on the renormalon problem. The main difference with the proliferation of Feynman diagrams is that the divergent behaviour associated to the renormalon arises from a single type of diagram. Here we will sketch how this divergent behaviour arises. More detailed discussions with explicit examples in QED, QCD and  $\phi_4^4$  can be found in [32, 34–37].

Consider a loop diagram with logarithmic momentum dependence  $l(p^2) = \log\left(\frac{p^2}{\mu}\right)$ , where  $\mu$  is an energy scale introduced in the renormalization procedure. Then, put its  $n$  consecutive insertion in a larger loop as in Figure 2.1. The whole diagram is represented by an integral of the form

$$I_n = \int d^D p f(\mathbf{p}) \left( \lambda \ln \frac{p^2}{\mu} \right)^n. \quad (2.6)$$

Let us assume that in  $f(\mathbf{p}) \sim p^\alpha$  in high or low energy limits. Then, we can separate the radial part and

$$I_n = \int d\Omega_{D-1} \int dp p^{A-1} \left( \lambda \ln \frac{p^2}{\mu} \right)^n, \quad A = D + \alpha \quad (2.7)$$

and evaluate the radial part by saddle point approximation. If we set  $y = \ln \frac{p^2}{\mu}$ , the

radial part transforms as

$$dp p^{A-1} \left( \ln \frac{p^2}{\mu} \right)^n \rightarrow \mu^{\frac{A}{2}} dy y^n e^{\frac{A}{2}y}, \quad (2.8)$$

which is dominated by the saddle point  $y = -\frac{2n}{A}$  and the leading order approximation around this point leads to

$$I_n \sim \mu^{\frac{A}{2}} \left( -\frac{2\lambda}{A} \right)^n (n-1)!. \quad (2.9)$$

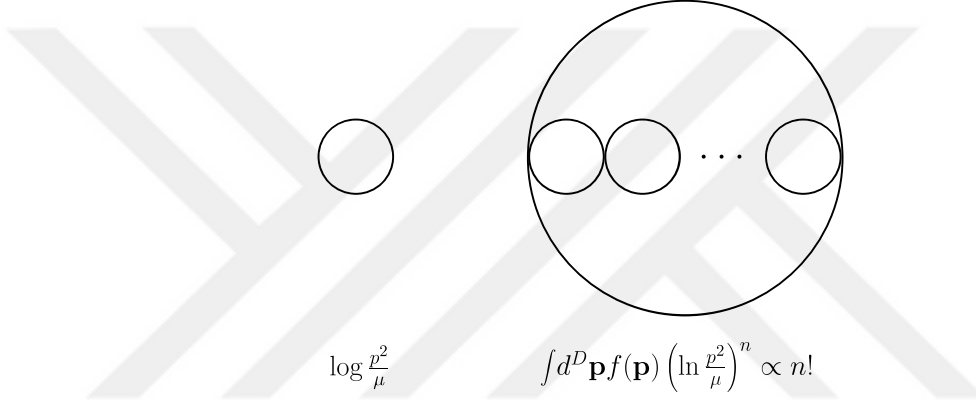


Figure 2.1. Left: A renormalized 1-loop diagram with logarithmic momentum dependence. Right:  $n$  renormalized diagrams inserted in a larger loop.

This is the renormalon divergence. Note that depending on  $A$ , there are two different renormalon types:

- If  $A > 0$ , as  $n \rightarrow \infty$ ,  $y = \ln \frac{p^2}{\mu} \rightarrow -\infty$  and the radial momentum integral in (2.7) is dominated by low energy region and the divergence is associated to the IR renormalons
- If  $A < 0$ , as  $n \rightarrow \infty$ ,  $y = \ln \frac{p^2}{\mu} \rightarrow \infty$  and the divergence is related to the dominant region high energies and it is associated to the UV renormalons.

## 2.2. Divergent Series and Borel Summation

### 2.2.1. An Analysis of Divergent Series:

Let us consider the Taylor expansion of a function  $f(x)$  around  $x = 0$

$$f(x) = \sum_{n=0}^{\infty} f_n x^n \quad ; \quad x \in \mathbb{R}, \quad (2.10)$$

where we assume the series diverges as  $n \rightarrow \infty$ . It is possible to truncate the series at the  $(N + 1)^{\text{th}}$  term and analyze the partially summed series

$$f^{(N)}(x) = \sum_{n=0}^N f_n x^n. \quad (2.11)$$

Since the original series diverges, although the partial summation makes an estimation possible for the original function  $f(x)$ , there is always a difference between  $f(x)$  and its partial sum  $f^{(N)}(x)$

$$\left| f(x) - \sum_{n=0}^N f_n x^n \right| \leq C_{N+1} |x|^{N+1}, \quad (2.12)$$

where  $C_{N+1} > 0$  is some constant that it shows the accuracy of the partial summation. It is possible to minimize  $C_N$  by finding the optimal truncation point and get the best possible estimation from the partial summation but there would always be some part of  $f(x)$  that can not be probed by its Taylor expansion.

Let us consider the physical cases we discussed in Section 2.1. In both cases, the perturbative expansions diverges factorially for large orders. Then, in the following, we will assume  $C_N \sim A^{-N} N!$ . To find the optimal truncation order, we minimize  $C_N |x|^N$ :

$$\frac{\partial}{\partial N} \left( C_N |x|^N \right) = \frac{\partial}{\partial N} \left( e^{(N \log N - N + N \log \left[ \frac{|x|}{A} \right])} \right) = 0,$$

where we used the Stirling approximation  $\log N! \simeq N \log N - N$ . Then, we get the optimal truncation order as

$$N_* = \frac{A}{|x|} \quad (2.13)$$

and the minimum possible deviation from the original function  $f(x)$  as

$$\begin{aligned} C_{N_*} |x|^{N_*} &= \left(\frac{|x|}{A}\right)^{N_*} N_*! = e^{(\log N_*! + N_* \log \frac{|x|}{A})} \\ &\simeq e^{(N_* \log N_* - N_* - N_* \log N_*)} = e^{-\frac{A}{|x|}}. \end{aligned} \quad (2.14)$$

Note that this is the smallest possible error we can achieve with a partial summation. It is always possible to find some function of order  $e^{-\frac{k}{|x|}}$  for  $k > A$  and add to the original function  $f(x)$ . The resulting function would have the same asymptotic expansion with  $f(x)$ . Therefore, the minimum error bound indicates that as one can expect, no divergent expansion can define a unique function.

However, this is not end of the story. In fact, it is possible to reconstruct the function uniquely using the original asymptotic series [38]. First step of this reconstruction, which we will focus on in this thesis, is probing the exponentially suppressed information using the divergent series. The most common way to do this is the Borel summation method. We will discuss this Borel summation method in Section 2.2.3. Before that in the next subsection, we will elaborate the connection between the exponentially suppressed terms and the divergent power series by discussing a specific example, i.e. Euler's equation.

### 2.2.2. The Euler Equation

Euler's equation is a 1<sup>st</sup> order ordinary differential equation:

$$x^2 \frac{df(x)}{dx} = A(f(x) - x). \quad (2.15)$$

Although, it contains a rich structure related to Stoke's phenomenon and Resurgence theory [39], in this and next subsections following the analysis in [40], we will restrict ourselves with a brief discussion on the solution of the Euler's equation and the emergence of exponentially suppressed terms as a part of the full solution, via Borel summation.

First, we are interested in the series solution to (2.15) and its properties. Using the ansatz

$$f(x) = \sum_{k=0}^{\infty} f_k x^k, \quad (2.16)$$

we get

$$\sum_{k=0}^{\infty} k f_k x^{k+1} = A \left( \sum_{k=0}^{\infty} f_k x^k - \lambda \right). \quad (2.17)$$

The first two terms of the series are  $f_0 = 0$  and  $f_1 = 1$  and rest of the series coefficients satisfies the following recursion relation:

$$f_k = A^{-1}(k-1)f_{k-1} \quad ; \quad k \geq 2. \quad (2.18)$$

From this relation, the  $k^{\text{th}}$  term is found as

$$f_k = A^{-(k-1)}(k-1)! \quad , \quad k \geq 1 \quad (2.19)$$

and the expansion of the function  $f(x)$  is found as

$$f(x) = \sum_{k=0}^{\infty} A^{-k} k! x^{k+1}. \quad (2.20)$$

The series diverges factorially for  $k \gg 1$  and as we have shown above, the best possible estimation of  $f(x)$  with this series leads to an error on the order of  $e^{-\frac{A}{x}}$  and the asymptotic series can not be the unique solution as any exponentially suppressed term can be added to the solution.

In fact, this is not a surprise as the solutions of ODEs should depend on an arbitrary integration constant, which is determined by the initial or boundary conditions specific to the problem. In the case of Euler's equation, the arbitrary parameter arises from the associated homogeneous differential equation

$$x^2 \frac{df_h(x)}{dx} = A f_h(x), \quad (2.21)$$

whose solution is

$$f_h(x) = Ce^{-A/x}. \quad (2.22)$$

Then, the full solution is written as

$$f(x) = \sum_{k=0}^{\infty} A^{-k} k! x^{k+1} + Ce^{-A/x}, \quad (2.23)$$

where  $C$  is an arbitrary constant.

Note that both parts of the solution in (2.23) have a common problem: Neither of them is defined at  $x = 0$ . Specifically, the first part is a divergent expansion around  $x = 0$ , which shows that its radius of convergence is zero. The second part, on the other hand, blows up as  $x \rightarrow 0^-$ . This is not surprising as  $x = 0$  is a singularity for the differential equation (2.15). However, the connection between inhomogeneous and homogeneous solutions is much deeper than this and in the next subsection using the Borel summation method, we will show how the homogeneous part arises from the inhomogeneous part represented by the divergent series.

### 2.2.3. Borel Summation

Recall the divergent expansion in (2.20)

$$f(x) = \sum_{k=0}^{\infty} f_k x^{k+1} \quad ; \quad f_k = A^{-k} k!.$$

To tame the divergent behaviour, we will utilize  $k! = \int_0^\infty db b^n e^{-b}$  and by multiplying and dividing the series with  $k!$ , re-write  $f(x)$  as

$$f(x) = \sum_{n=0}^{\infty} \int_0^\infty db e^{-b} \frac{b^k f_k x^{k+1}}{k!} = \sum_{n=0}^{\infty} \int_0^\infty db e^{-b} \left(\frac{b}{A}\right)^k x^{k+1}. \quad (2.24)$$

However, a serious problem arises when we want to exchange the summation and the integration. This is not allowed since the series is divergent. Instead, we define a new

function  $\mathcal{B}[f(x)]$  as

$$\mathcal{B}[f(x)](b) = \sum_{k=0}^{\infty} \left( \frac{b x}{A} \right)^k, \quad (2.25)$$

which is called the Borel transform of the original function  $f(x)$ . Then, we can introduce the inverse Borel transformation

$$\mathcal{B}^{-1}[\mathcal{B}[f(x)]] = \int_0^{\infty} db e^{-b} \mathcal{B}[f(x)](b) \quad (2.26)$$

and return to the original domain. In this way, we obtain the Borel summation of  $f(x)$ , which we denote as  $\mathcal{S}[f(x)]$ :

$$\mathcal{S}[f(x)] = \int_0^{\infty} db e^{-b} x \sum_{k=0}^{\infty} \left( \frac{b x}{A} \right)^k = \int_0^{\infty} db e^{-b} \frac{x}{1 - \frac{b x}{A}}. \quad (2.27)$$

The radius of convergence of the integrand is  $R_{conv} = \frac{A}{x}$ . This means that by using the Borel summation method, we exchanged the singularity at  $x = 0$  of  $f(x)$  with another singularity on the Borel plane at  $b = \frac{A}{x}$  which as we will see contains non-trivial information about  $\mathcal{S}[f(x)]$ .

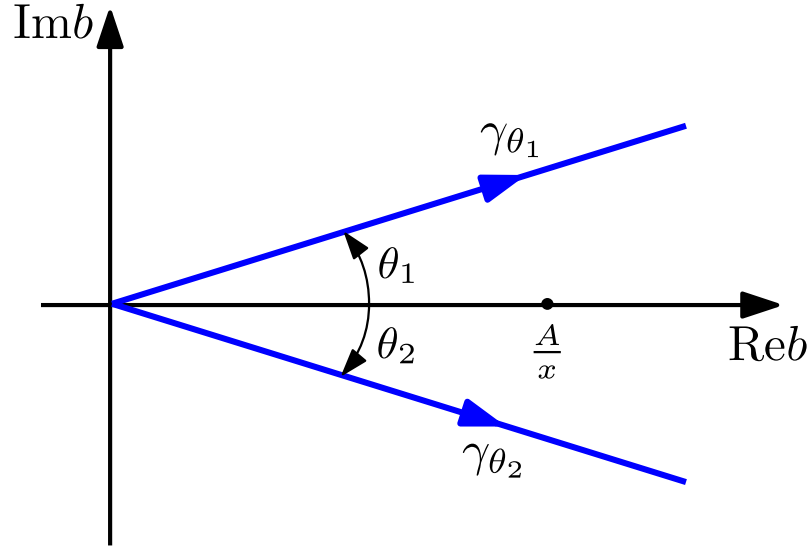


Figure 2.2. Contours for the Borel summation integral.

Let us assume that  $A > 0$ . Then, the singularity  $b = \frac{A}{x}$  lies on the integration path and the integral contour should be analytically continued to the complex plane as in Figure 2.2. We have two choices for analytical continuation: Counter-clockwise

direction or clockwise direction. These are represented by paths  $\gamma_{\theta_1}$  and  $\gamma_{\theta_2}$  in the figure and corresponding integrals are written as

$$\mathcal{S}_{\theta_1}[f(x)] = \int_{\gamma_{\theta_1}} db e^{-b} \frac{x}{1 - \frac{bx}{A}} \quad , \quad \mathcal{S}_{\theta_2}[f(x)] = \int_{\gamma_{\theta_2}} db e^{-b} \frac{x}{1 - \frac{bx}{A}}. \quad (2.28)$$

Both  $\mathcal{S}_{\theta_1}[f(x)]$  and  $\mathcal{S}_{\theta_2}[f(x)]$  are well-defined along their integration contours. However, the limits  $\theta_1 \rightarrow 0$  and  $\theta_2 \rightarrow 0$  leads to complex conjugate results since they encircle the singularity in different directions as shown in Figure 2.3. This leads to a difference between two analytical continuation choices which is given by

$$\Delta\mathcal{S}[f(x)] = \mathcal{S}_{0+}[f(x)] - \mathcal{S}_{0-}[f(x)] = \int_{\gamma_+ - \gamma_-} db e^{-b} \frac{x}{1 - \frac{bx}{A}} = 2\pi i A e^{-\frac{A}{x}}. \quad (2.29)$$

Note that this exponentially suppressed term is a solution to homogeneous Euler's equation in (2.21), i.e.  $\Delta\mathcal{S}[f(x)] \sim f_h(x)$ . This is not surprising since both summations written in (2.28) are solutions to the inhomogeneous Euler's equation. To see this, after re-scaling  $b \rightarrow \frac{Ab}{x}$  in (2.27), take the derivative of  $\mathcal{S}[f(x)]$ :

$$\begin{aligned} \frac{d}{dx}(\mathcal{S}[f(x)]) &= A \int_0^\infty db \frac{d}{dx} \left( \frac{e^{-\frac{Ab}{x}}}{1 - b} \right) \\ &= \frac{A}{x^2} \int_0^\infty db \frac{Ab}{1 - b} e^{-\frac{Ab}{x}} \\ &= A \left[ \frac{A}{x^2} \int_0^\infty db e^{-\frac{Ab}{x}} - \frac{A}{x^2} \int_0^\infty db \frac{e^{-\frac{Ab}{x}}}{1 - b} \right] \\ &= A \left( \frac{1}{x} - \frac{\mathcal{S}[f(x)]}{x} \right), \end{aligned} \quad (2.30)$$

which is indeed re-scaled version of the Euler's equation in (2.15). This shows that  $\mathcal{S}_{0+}[f(x)]$ ,  $\mathcal{S}_{0-}[f(x)]$  and their linear difference  $\Delta\mathcal{S}[f(x)] = \mathcal{S}_{0+}[f(x)] - \mathcal{S}_{0-}[f(x)]$  are also solutions to the Euler's equation.

This analysis shows us that the divergent series solution in (2.20) indeed contains more information than it shows at first sight. In fact, although the divergent series is meaningless on first sight, via Borel summation, it leads to the full solution to the

Euler's equation which can now be written as

$$f(x) = \int_{\tilde{\gamma}_0} db e^{-b} \frac{x}{1 - \frac{bx}{A}} + Ce^{-\frac{A}{x}}, \quad (2.31)$$

where  $\tilde{\gamma}_0$  corresponds to the integration line on the positive real axis without the singular point.

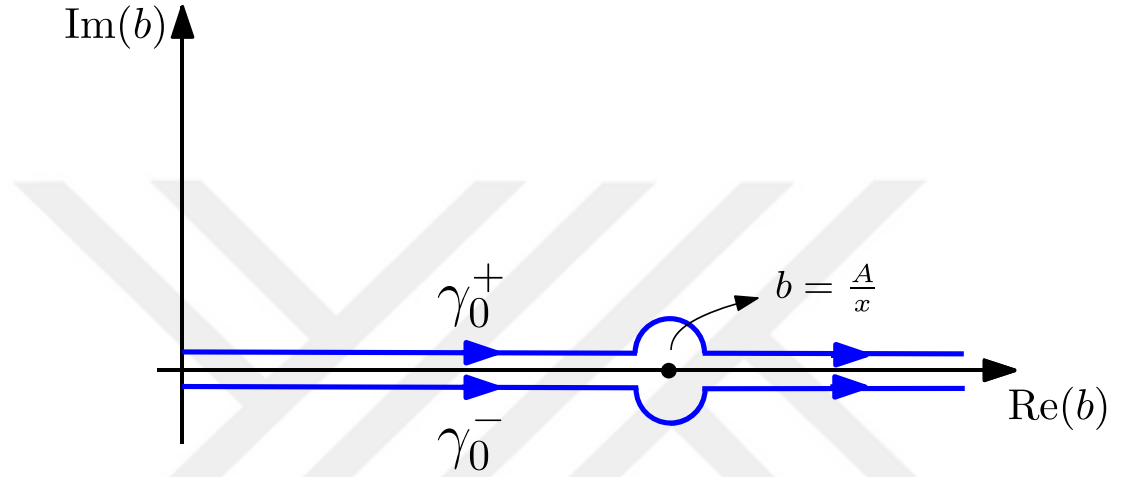


Figure 2.3. The Borel summation integral contours in the limit  $\theta_1 \rightarrow 0$  and  $\theta_2 \rightarrow 0$ .

#### 2.2.4. Borel Ambiguity and Its Resolution

The main lesson of our analysis is that investigation of the asymptotic solution  $f(x) = \sum f_k x^k$  leads to the full solution of the Euler's equation which contains information beyond the polynomial series. The same analysis can be carried to the physical problems we briefly mentioned in Section 2.1 where the perturbative expansion of a physical observable can be utilized to obtain non-perturbative information about the problem by using the Borel summation. This presents an intimate connection between perturbative and non-perturbative physics.

One main problem of the Borel analysis is the freedom of choice in the analytical continuations we made in the inverse Borel transformations in (2.27). As we showed, this leads to a multi-valued exponential contribution to the solution. While this is not a problem in Euler's equation analysis where a convenient initial condition determines the pre-factor of the exponential term, it becomes a crucial problem in physics when

the exponentially suppressed terms carry important physical information.

Having multi-valued exponential factors in non-perturbative sectors is called the Borel ambiguity problem. Let us elaborate it and discuss its solution in a specific quantum mechanical setting. We will consider the double-well potential in one-dimension: (See Figure 2.4.)

$$V(x) = \frac{1}{2}x^2(1+gx)^2. \quad (2.32)$$

Its spectral properties and its resurgent structure is well-studied in [13, 16] and we will briefly explain the resolution of the Borel ambiguity by using the results in those studies.

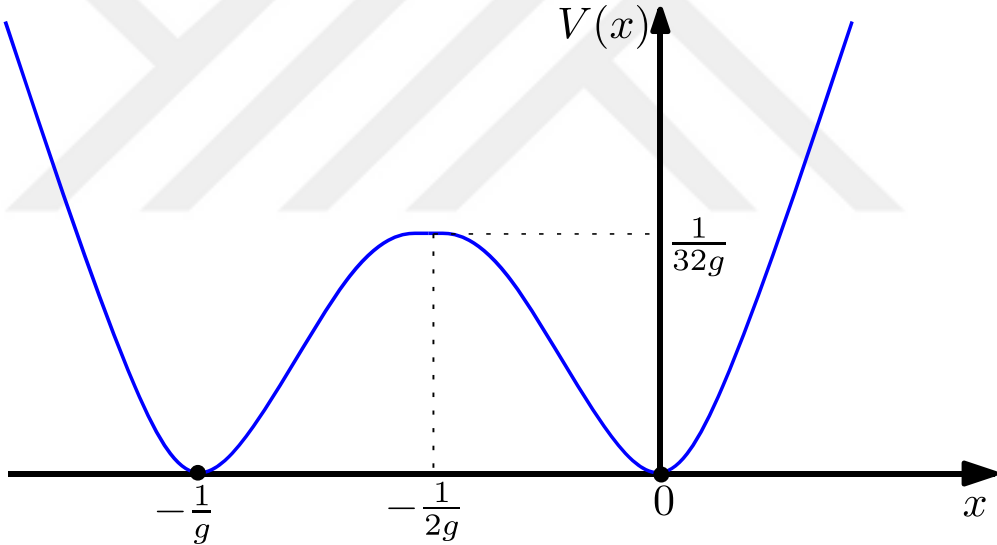


Figure 2.4. Double-well potential.

Energy levels for each well can be computed perturbatively and expressed in an asymptotic expansion in  $g$  as

$$u_N(g) = \sum_{k=0} \varepsilon_k^{(N)} g^{2k}. \quad (2.33)$$

Since both wells are locally equivalent to each other, at all order perturbative energy levels are degenerate. The degeneracy is broken when non-perturbative effects which are induced by tunneling between the wells are considered. This can be computed by the WKB approximation [41] or instantons methods [5] and leads to a non-perturbative

contribution to the spectrum, i.e.  $\Delta u_{\text{gap}}(g) \sim e^{-1/6g^2}$ . Then, naively, we can write the energy eigenvalues for the ground state as

$$u_0(g) = \sum_{k=0} \varepsilon_k^{(0)} g^{2k} - \frac{1}{\sqrt{\pi g^2}} e^{-1/6g^2}. \quad (2.34)$$

Equation (2.34), however, can not be the complete energy for the ground state since, as we expect from the discussion in Section 2.1, the perturbative expansion is a divergent one. For high orders, i.e.  $k \gg 1$ , the expansion diverges as  $\varepsilon_k^{(0)} \sim \frac{1}{\pi} 3^{k+1} k!$ . This is similar to the behaviour we studied in Section 2.2. Then, handling the divergence by Borel summation leads to the ambiguous imaginary contribution to the spectrum as

$$\mathcal{S}[u_0(g)] \sim \pm \frac{i}{\pi g^2} e^{1/3g^2}. \quad (2.35)$$

First of all this leads to a multi-valued function representing the ground state energy eigenvalue  $u_0(g)$ . Moreover, it makes the energy of a stable state complex. None of them is acceptable and should be resolved to get a consistent picture.

Resolution to this problem comes from the two instantons level. At this order, the instanton contribution to the non-perturbative spectrum acquires an imaginary part and it is found as [13, 16]

$$\text{Im}u_0^{(2)} = \mp \frac{1}{\pi g^2} e^{-1/3g^2}. \quad (2.36)$$

Note that this imaginary contribution arises from a combination of instanton anti-instanton solutions which requires analytical continuation in the variable  $g^2$  similar to the one we encounter in the Borel summation and the freedom of choice in the analytical continuation direction leads to the multi-valued result in (2.36). However, it comes with an opposite sign with the one we get from the Borel summation in (2.35). Therefore, if these two contributions are considered together, they would cancel each other and the resulting ground state eigenvalue  $u_0(g^2)$  would be real and unambiguous.

The cancellation of the Borel ambiguity at perturbative level is just a small part of the whole resurgence structure associated to the eigenvalue  $u(g)$  of all levels in the spectrum. In fact, at each instanton order, there is a divergent perturbation

series associated to fluctuations around the instantons and these series leads to a Borel ambiguity as well. The cancellation of these ambiguities comes from the imaginary parts of the higher order instanton contributions and this leads to well-defined unique eigenvalues. In this thesis, we will not discuss this structure.

*Remark:* While this analysis leads to a complete and consistent picture for the spectral problem for stable systems, when there is an instability in the system, the cancellation procedure is not suitable to resolve the ambiguity as the imaginary contributions should survive. This motivates us to investigate the analytical structure of the physical observables from a different point of view. Integral representations of physical functions, which we will focus on throughout this thesis, allow us to investigate this structure in a more direct way and solve the ambiguity problem once and for all.

### 2.3. Physics from Analytic Structure

As we discussed earlier, the main subject of this thesis is extracting physical information out of singularities of a function which is formulated in an integral representation. In the following chapter, we will encounter two different types of integral representations.

First, in Chapters 3 and 4, we will formulate the spectral problem in non-relativistic quantum mechanics and the pair production of scalar particles in a time dependent formalism based on Schwinger's integral

$$\Gamma(u) = \int_0^\infty \frac{dt}{t} e^{itu} \text{Tr}U(t), \quad (2.37)$$

where  $\Gamma(u)$  is the quantum action and  $U(t) = e^{itH}$  is the time-dependent propagator.

As we will see in Chapter 3, this integral is closely related to the semi-classical expansion that we are familiar from the WKB method. To see this connection, let us consider a Hamiltonian in one dimension  $H = \frac{p^2}{2} + V(x)$ . The propagator can be expressed in terms of commutators between kinetic and potential terms via the

Zassenhaus formula which gives

$$U(t) \simeq e^{-\frac{itp^2}{2}} e^{-itV(x)} \quad (2.38)$$

at the leading order. Then, after properly projecting  $\text{Tr}U(t)$  onto the phase space and taking  $p$  and  $t$ -integrals, which we will discuss in Chapter 3, the quantum action becomes

$$\Delta\Gamma(u) = \sqrt{2} \oint dx \sqrt{u - V(x)}, \quad (2.39)$$

This is the well-known Bohr-Sommerfeld integral and it gives the leading order WKB action in the semi-classical expansion. We represented it as  $\Delta\Gamma$  since over a closed loop, only the branch point at  $u = V(x)$  contributes to the integral.

Note that since the integral (2.39) comes from Schwinger's integral in (2.37), the same information should be hidden somewhere in the time-dependent formalism as well. As we will show in Section 2.3.1, the branch point information is hidden in the singularities of the integrand in (2.37), i.e.  $\frac{\text{Tr}U(t)}{t}$ . In Chapter 3, we will show that the quantum action is associated to the perturbative sector that arises from the singularity at  $t = 0$ . In addition to that  $\text{Tr}U(t)$  also contains information about the non-perturbative sector which is hidden in singularities at finite  $t$ . As we will show in Chapter 4, this singularity is in fact equivalent to the Borel singularity that we discussed in Section 2.2.3.

In addition to the integral representation of the quantum action, in Chapter 5, we will formulate the renormalon problem in momentum space and investigate integrals of the form

$$\tau(\mathbf{p}_f, \mathbf{p}_i) = \int_{-\infty}^{\infty} dq F(q; \mathbf{p}_f, \mathbf{p}_i), \quad (2.40)$$

where  $\tau(\mathbf{p}_f, \mathbf{p}_i)$  is the on-shell T-matrix of a scattering process that we will define in Chapter 5. In this case, the non-perturbative information that is carried by the renormalon again arises from a singularity of  $F(q; \mathbf{p}_f, \mathbf{p}_i)$  and it is handled in the same fashion with the Borel singularity.

*Remark:* In all three cases, we will utilize the  $i\varepsilon$  prescription and as a result, the gap arising from the singularities would have no ambiguity. This is possible due to the relationship between the  $i\varepsilon$  prescription and the time flow direction, which is manifest in Schwinger's integral and well-known for the energy dependent description of scattering processes [42].

In the next subsection, following [1], we will discuss the relation between the singularities of integrands and the analytical properties of the function represented by the integral. We will also elaborate on their connection with the  $i\varepsilon$  prescription and the analytical continuation of the Borel summation integral. Due to the connection between the semi-classical expansion and the singularity at  $t = 0$  of  $\frac{\text{Tr}U(t)}{t}$ , we will finish this chapter with a discussion on the WKB method and its geometric background.

### 2.3.1. Integrals and Their Singularities

Let us consider an integral along a finite sized contour  $C : \alpha \rightarrow \beta$  where  $\alpha, \beta$  are fixed end points:

$$f(\lambda) = \int_C dz g(\lambda, z). \quad (2.41)$$

Suppose that  $g(\lambda, z)$  has simple poles at  $z = z_p(\lambda)$ , where  $p = 1, \dots, n$ . As long as the contour  $C$  does not pass through any of these singularities,  $f(\lambda)$  remains an analytical function. On the other hand, as  $\lambda$  varies it is possible one of the poles to reaches the contour  $C$ . Then, an analytical continuation would be needed to keep  $f(\lambda)$  analytic. However, in certain situations, there is no way to escape from the singularities and in these cases,  $f(\lambda)$  would have singularities associated to the poles of  $g(\lambda, z)$  on  $z$ -plane.

In the following, we will investigate end-point singularities, i.e. a singularity of  $g(\lambda, z)$  coincides with one of the end points of integral contour  $C$ . Suppose  $\lambda_*$  is a point such that  $z_1(\lambda_*) = \alpha$  is an end-point singularity. Let us consider a circle path around  $\lambda_*$  of radius  $\varepsilon$ :  $\lambda = \lambda_* + |\varepsilon|e^{i\theta}$ ,  $\theta \in [0, 2\pi]$ . This would correspond to a similar

circle around the end point:

$$z_1(\lambda_* + \varepsilon) \simeq \alpha + |\varepsilon| e^{i\theta} \frac{dz_1}{d\lambda} \Big|_{\lambda=\lambda_*}, \quad (2.42)$$

where we assumed the first derivative of  $z_1$  exists and non-zero at  $\lambda = \lambda_*$ . Then, if we start at a point on the circle in the  $\lambda$ -plane and go along the circle for one complete round, we would do the same for the circle in  $z$ -plane. As illustrated in Figure 2.5, by Cauchy theorem, this would lead to a difference between  $f(\lambda)$  and  $f(\lambda e^{2\pi i})$  which is equal to the contour integral around the singularity at  $z_1$ , i.e. the residue of  $g(\lambda, z)$  at  $z = z_1$ . This indicates a logarithmic singularity of  $f(\lambda)$  at point the  $\lambda = \lambda_*$ .

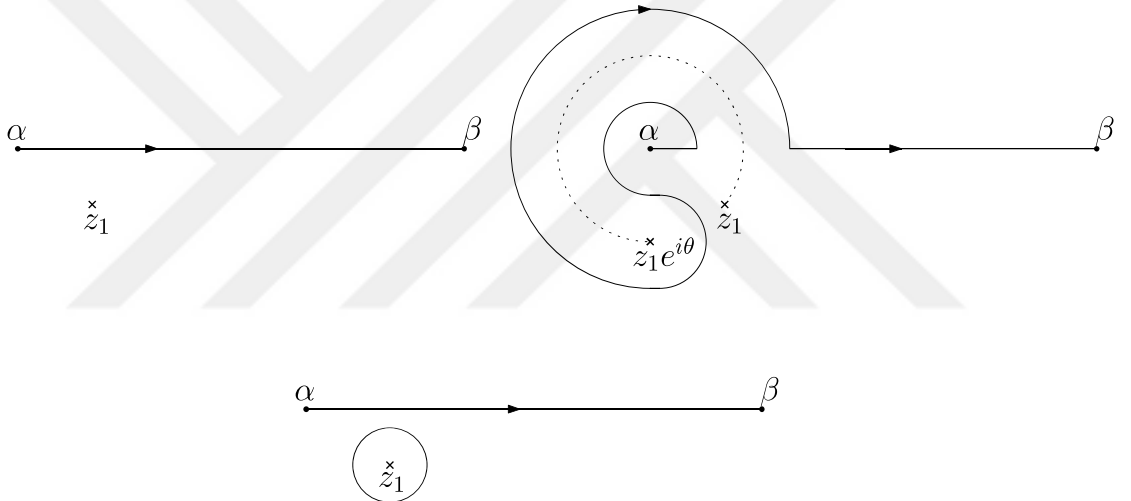


Figure 2.5. Deformation of contour as the singularity at  $z_1$  moves on a circle.

As an example, consider the integral

$$f(\lambda) = \int_0^\infty dz \frac{\phi(\lambda, z)}{\lambda - z} \quad , \quad \lambda \in \mathbb{R}^+ \cup 0. \quad (2.43)$$

It is an elementary example. We know that the pole at  $z = \lambda$  can be easily handled by the residue theorem and as a result, an imaginary part for  $f(\lambda)$  arises. In the context of our discussion, however, now we know that this gap is resulting from a branch cut of  $f(\lambda)$  on  $\lambda$  plane. More specifically, the pole  $z = \lambda$  coincides with the end point  $z = \alpha = 0$  as  $\lambda \rightarrow \lambda_* = 0$ . Therefore, a circle around the pole at  $z = \lambda$  for finite  $\lambda$  corresponds to a circle around  $\lambda = \lambda_* = 0$  and the residue of the integrand corresponds to the gap of  $f(\lambda)$  due to its branch point at  $\lambda = 0$ .

Instead of considering rotations in  $\lambda$  plane, we might utilize  $i\varepsilon$  prescription by defining

$$f^\pm(\lambda) = \lim_{\varepsilon \rightarrow 0} f(\lambda \pm i\varepsilon).$$

Then, the gap arising from encircling the singularity would simply be

$$\Delta f(\lambda) = f^+(\lambda) - f^-(\lambda). \quad (2.44)$$

Equivalently, we might rotate the contour to avoid the singularity at  $z = z_1(\lambda) = \lambda$ . The latter one is what we have done in Borel analysis. Now we see that the imaginary exponential term arising via summation is indeed a result of passing through the branch cut of the original function.

In Chapter 3, we will encounter another type of integral where the end-point singularities are fixed:

$$f(\lambda) = \int_0^\infty \frac{dz}{z} e^{iz\lambda} \phi(z). \quad (2.45)$$

The denominator is already zero at the end-point  $z = 0$ . We can slightly move the singularity of the denominator by defining

$$f(\lambda) = \lim_{\Omega \rightarrow 0} f(\lambda, \Omega) = \lim_{\Omega \rightarrow 0} \int_0^\infty \frac{dz}{z - \Omega} e^{i\lambda z} \phi(z). \quad (2.46)$$

In this way, we return to the problem in (2.43). However, in this form, the relation between the singularity at  $\Omega = 0$  and the function  $f(\lambda)$  is not explicit. On the other hand, for  $\lambda \in \mathbb{R}$ , due to the oscillatory behaviour of the exponential, the integral is not well defined at the other end-point  $z = \infty$  as well. This second problem indicates that  $f(\lambda)$  in (2.46) is not well-defined on the real axis in the  $\lambda$ -plane. The oscillatory behaviour can be handled by the  $i\varepsilon$  prescription and by re-defining  $f(\lambda)$  for  $\lambda > 0$  and  $\lambda < 0$  regions separately as

$$\begin{aligned} f^+(\lambda) &= \lim_{\varepsilon \rightarrow 0} f(\lambda + i\varepsilon) \quad , \quad \lambda > 0, \\ f^-(\lambda) &= \lim_{\varepsilon \rightarrow 0} f(\lambda - i\varepsilon) \quad , \quad \lambda < 0. \end{aligned} \quad (2.47)$$

Then, the integrals for  $f^\pm(\lambda)$  can be written as

$$f^\pm(\lambda) = \lim_{\substack{\varepsilon \rightarrow 0 \\ \Omega \rightarrow 0}} \int_0^\infty \frac{dz}{z - \Omega} e^{\pm iz(\lambda \pm i\varepsilon)} \phi(z), \quad (2.48)$$

where  $\lambda > 0$  in both cases. Equivalently, we can put the analytical continuations information to the contour:

$$f^\pm(\lambda) = \lim_{\substack{\varepsilon \rightarrow 0 \\ \Omega \rightarrow 0}} \int_{\Omega \pm i\varepsilon}^{\infty \pm i\varepsilon} \frac{dz}{z} e^{\pm iz\lambda} \phi(z). \quad (2.49)$$

In this form, it is clear that encircling the singularity at  $z = 0$  is associated to the difference  $\Delta f(\lambda) = f^+(\lambda) - f^-(\lambda)$  which is equal to the residue of  $f(\lambda, \Omega)$  at  $\Omega = 0$  and  $f(\lambda)$  has a branch point at  $\lambda = 0$ .

### 2.3.2. Geometry and WKB Method

The WKB approximation is well-known textbook material widely used to express the semi-classical approximation of the wave-function by the Bohr-Sommerfeld integral, which we introduce in (2.39), and to compute tunneling rates in one dimensional quantum mechanics. A less known but important aspect of the WKB approximation is that it can be made exact by extending the semi-classical series to all orders and investigating the analytical properties of (2.39) and its quantum corrections. It is called the exact WKB method [43–45] and used to obtain the resurgence structure we discussed in Section 2.2. The analytical structure of (2.39) has also a topological basis from which the resurgent structure can be derived in terms of cycles on a torus or  $n$ -tori. We will first discuss this basis and its relation to the resurgence theory briefly. Then discuss the derivation of the all order WKB expansion.

Any quantum theory can be written as a spectral problem written as an eigenvalue equation of an Hamiltonian  $\mathsf{H}$

$$\mathsf{H}(\mathbf{p}, \mathbf{x})\psi = u\psi. \quad (2.50)$$

It is possible to have the Hamiltonian as a general function of two canonical variables  $\mathbf{p}$  and  $\mathbf{x}$ . For example, in Chapter 3 we will consider  $\mathsf{H}(\mathbf{p}, \mathbf{x}) = \mathsf{T}(\mathbf{p}) + \mathsf{V}(\mathbf{x})$ ,

where  $\mathsf{T}$  corresponds to generalized kinetic term, and in Chapter 4 we will study  $H = \frac{1}{2}(p_\mu - eA_\mu(x))^2$ . In this section, we will consider the standard Hamiltonian in one dimension

$$\mathsf{H}(p, x) = \frac{p^2}{2} + V(x). \quad (2.51)$$

We know that the classical Hamiltonian corresponds to the total energy, i.e.  $H = u$ . Equivalently, the momentum can be written as a function of the position

$$p^2(x) = 2(u - V(x)). \quad (2.52)$$

In this form,  $p(x)$  defines a Riemann surface,  $\Sigma$ , which has two sheets due to the branch points given by

$$p(x) = \sqrt{2(u - V(x))} = 0.$$

While the number of branch points determines the topology of  $\Sigma$ , they also play an important role in quantization of the Hamiltonian (2.51). To see how this relation takes place, let us examine the double well potential in (2.32).

Focusing on low energies  $0 < u < \frac{1}{32g}$ , it is easy to see that there are four turning points, given by  $u = V(x)$ , corresponding to the branch points on  $\Sigma$ . There are two branch cuts on each Riemann surface  $\Sigma$ . We know that crossing these cuts means traveling from one Riemann sheet to the other one. Then, we can connect each cut by a tube and by compactifying each Riemann surface, we get a torus. See Figure 2.6 for an illustration.

On the torus, there are two independent cycles. We identify them as  $\alpha$  and  $\beta$  cycles. In our construction, the  $\alpha$  cycle is associated to the branch cuts connecting the singularities on  $\Sigma$ . On the other hand, the  $\beta$  cycles connect different branch cuts. If we return to the standard double-well potential, we identify  $\alpha$  cycle with a closed loop in one of the wells of the potential.  $\beta$  cycle, on the other hand, corresponds to a closed loop under the barrier. These are the closed paths of the Bohr-Sommerfeld integral in (2.39). Then, the above identifications shows that  $\alpha$  cycle is associated to

the perturbative sector of the theory, while the  $\beta$  cycle represents tunneling effects and is linked to the non-perturbative sector.

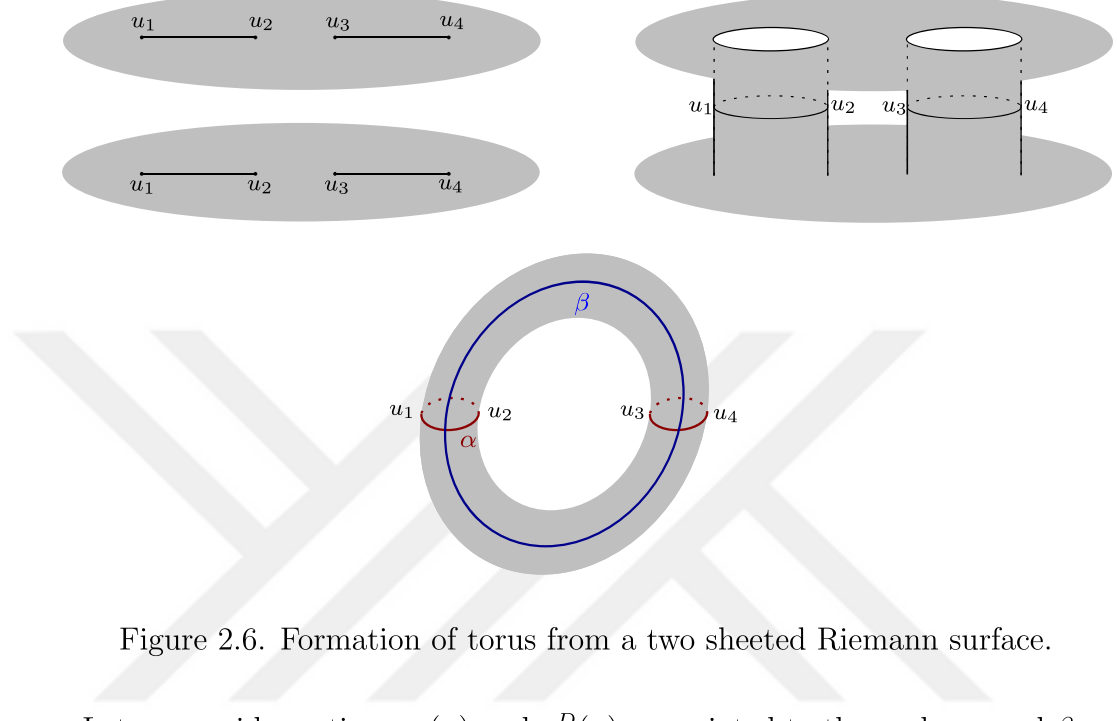


Figure 2.6. Formation of torus from a two sheeted Riemann surface.

Let us consider actions,  $a(u)$  and  $a^D(u)$ , associated to the cycles  $\alpha$  and  $\beta$  respectively and their formal Taylor series of  $\hbar$ :

$$a(u) = \sum_{m=0}^{\infty} a_m \hbar^m \quad , \quad a^D(u) = \sum_{m=0}^{\infty} a_m^D \hbar^m. \quad (2.53)$$

Then, on the perturbative side, the leading order Bohr-Sommerfeld quantization is written as

$$a_0(u) = \sqrt{2} \oint_{\alpha} \sqrt{u - V(x)} = \left( N + \frac{1}{2} \right) \hbar$$

and on the non-perturbative side, the tunneling probability between two wells is given by  $\mathcal{P} \sim e^{-\frac{1}{\hbar} \text{Im} a_0^D(u)}$ .

As we showed in Section 2.2, these two pieces of information should be connected. In fact, the connection goes beyond this, the series in (2.53) are connected to each other term by term. In addition to that terms in each series are also connected among themselves. One way to see this connection is the Picard-Fuchs differential equation [46–50] which are derived by using the geometry of the Riemann surface. For genus

1 potentials, the Picard-Fuchs equation is a second order differential equation and at the classical level, the actions  $a_0(u)$  and  $a_0^D(u)$  correspond to its solution. Then, the solutions  $a_0$  and  $a_0^D$  are connected by the Wronskian condition

$$W(a, a^D) = a_0(u) \frac{da_0^D(u)}{du} - a_0^D(u) \frac{da_0(u)}{du} = 2iS_I\mathcal{T}, \quad (2.54)$$

where  $S_I$  is one instanton action and  $\mathcal{T}$  is the period of the harmonic oscillator at the well [47]. On the other hand, using the same geometry it is also possible to derive differential operators [49, 50],  $\mathcal{D}^{2n}$ , whose action onto  $a_0$  and  $a_0^D$  yield the quantum corrections at order  $\hbar^{2n}$ , i.e.

$$a_{2n} = \mathcal{D}^{2n}a_0 \quad , \quad a_{2n}^D = \mathcal{D}^{2n}a_0^D. \quad (2.55)$$

Note also that in [47], it was also shown that the Wronskian relation generalizes to all orders in the semi-classical expansion and this shows the generalization of the connection between  $a(u)$  and  $a^D(u)$  to all quantum levels.

The Picard-Fuchs equations present a geometric picture for the resurgence relation between perturbative and non-perturbative sectors at all orders in semi-classical expansion which we discussed in Section 2.2. Another way to obtain the same picture is using the holomorphic anomaly equations known from topological string theory [51,52]. In this approach, the anomaly equations provide the free energy, i.e. prepotential in string theory language, as a function of the action  $a(u)$  and the connection between the perturbative and non-perturbative parts are given by the simple relation

$$a^D(u) = \frac{\partial F(a(u))}{\partial a(u)}. \quad (2.56)$$

Note that the topological strings are related to one dimensional quantum mechanics via the Nekrasov-Shatashvili limit [53]. Therefore, (2.56) is also another resurgence relation for the potential  $V(x)$  as well.

*Remark:* Another aspect of the Picard-Fuchs equation and the Holomorphic equation approaches is their recursive nature which is akin to topological recursion [54,55]. It simplifies the computations of quantum corrections to the classical actions  $a_0(u)$  and

$a_0^D(u)$ . In standard quantum mechanics, we can get the same recursive nature from the all orders WKB method. However, all of these methods are restricted to one dimensional problems. As we have implied, one of the main achievements of this thesis is the generalization of the application realm of the recursion relation to arbitrary dimensional problems. In Chapter 3, we will show that using Schwinger's integral, we can indeed find an equivalent recursion relation and generate the quantum corrections without any restriction on the dimension of the theory. For completeness, let us finish this chapter with a brief presentation of the all order semi-classical expansion using the WKB method.

Consider the one dimensional Schrödinger equation in the following form

$$\frac{d^2\psi(x)}{dx^2} = -\frac{p^2(x)}{\hbar^2}\psi(x), \quad (2.57)$$

where we again use  $p^2(x) = 2(u - V(x))$ . The WKB ansatz for this equation is

$$\psi(x) \sim \exp \left\{ \frac{i}{\hbar} \int^x dx' Q(x', \hbar) \right\}, \quad (2.58)$$

where we assume  $Q(x, \hbar)$  is a formal series in  $\hbar$

$$Q(x, \hbar) = \sum_{n=0}^{\infty} Q_n(x) \hbar^n. \quad (2.59)$$

Inserting the ansatz in (2.57), we get the Riccati equation

$$Q^2(x, \hbar) - i\hbar \frac{dQ(x, \hbar)}{dx} = p^2(x), \quad (2.60)$$

which is written in terms of the formal series as

$$\left( \sum_{n=0}^{\infty} Q_n(x) \hbar^n \right)^2 - i\hbar \sum_{n=0}^{\infty} Q'(x) \hbar^n = p^2(x). \quad (2.61)$$

Then, at order  $\hbar^0$ , we get

$$Q_0^{\pm}(x) = \pm p(x). \quad (2.62)$$

Higher order terms are given by the recursive expression

$$\sum_{k=0}^n Q_k(x) Q_{n-k}(x) - i Q'_{n-1}(x) = 0 \quad , \quad n \geq 1 \quad (2.63)$$

or equivalently

$$2Q_0(x)Q_n(x) = i Q'_{n-1}(x) - \sum_{k=0}^{n-1} Q_k(x) Q_{n-k}(x) \quad , \quad n \geq 1. \quad (2.64)$$

Here we used

$$\left( \sum_{n=0}^{\infty} Q_n(x) \hbar^n \right)^2 = \sum_{n=0}^{\infty} \left( \sum_{k=0}^n Q_k(x) Q_{n-k}(x) \right) \hbar^n \quad (2.65)$$

to obtain the recursive expression. This is the recursion relation we mentioned above.

Note that there are two solutions for the leading order in (2.62). Since higher orders are determined from this term, the same is true for higher orders and the Riccati equation has two independent solutions:

$$Q^{\pm}(x, \hbar) = \sum_{n=0}^{\infty} Q_n^{\pm}(x) \hbar^n. \quad (2.66)$$

However, for odd terms, i.e.  $n = 2N + 1$ , the  $\pm$  signs cancel each other and these terms are the same in both solutions. Then, we can separate the formal series into two parts:

$$Q(x, \hbar) = \sum_{n=0}^{\infty} Q_{2n+1}(x) \hbar^{2n+1} \pm \sum_{n=0}^{\infty} Q_{2n}(x) \hbar^{2n} \equiv Q_{\text{odd}}(x, \hbar) \pm Q_{\text{even}}(x, \hbar). \quad (2.67)$$

If we put these solutions into the Riccati equation, we get

$$\left[ Q_{\text{odd}}(x, \hbar) + Q_{\text{even}}(x, \hbar) \right]^2 + i \hbar \frac{d}{dx} \left[ Q_{\text{odd}}(x, \hbar) + Q_{\text{even}}(x, \hbar) \right] = p^2(x), \quad (2.68)$$

$$\left[ Q_{\text{odd}}(x, \hbar) - Q_{\text{even}}(x, \hbar) \right]^2 + i \hbar \frac{d}{dx} \left[ Q_{\text{odd}}(x, \hbar) - Q_{\text{even}}(x, \hbar) \right] = p^2(x). \quad (2.69)$$

These equations lead to

$$2Q_{\text{odd}}(x, \hbar)Q_{\text{even}}(x, \hbar) = -i \hbar \frac{dQ_{\text{even}}(x, \hbar)}{dx} \quad (2.70)$$

and consequently

$$Q_{\text{odd}}(x, \hbar) = -\frac{i\hbar}{2} \frac{d}{dx} \log Q_{\text{even}}(x, \hbar). \quad (2.71)$$

As a result, we can re-write the WKB ansatz (2.58) as

$$\psi^\pm(x) = \frac{1}{\sqrt{Q_{\text{even}}}} \exp \left[ \pm \frac{i}{\hbar} \int^x dx' Q_{\text{even}}(x', \hbar) \right]. \quad (2.72)$$

When the integral in the exponent is taken along closed loops, it corresponds to the quantum action we discussed above, i.e.  $a(u)$  and  $a^D(u)$  depending on the integration contour:

$$a(u) = \oint_\alpha dx Q_{\text{even}}(x, \hbar) \quad , \quad a^D(u) = \oint_\beta dx Q_{\text{even}}(x, \hbar). \quad (2.73)$$

For future reference, we also present the well-known first two terms in the  $\hbar$  expansion:

$$a_0(u) = \sqrt{2} \oint dx \sqrt{u - V(x)}, \quad (2.74)$$

$$a_2(u) = -i \frac{\sqrt{2}}{2^6} \oint dx \frac{(V'(x))^2}{(u - V)^{5/2}}. \quad (2.75)$$

### 3. THE SEMI-CLASSICAL EXPANSION IN ARBITRARY DIMENSION

In this chapter, starting from the definition of the quantum action as the logarithm of the Fredholm determinant, i.e.

$$\Gamma(u) = \log \det(u - H), \quad (3.1)$$

we will discuss how the semi-classical expansion of the quantum action  $\Gamma$  can be obtained recursively using Schwinger's integral

$$\Gamma^\pm(u) = - \int_0^\infty \frac{dt}{t} e^{\pm itu} \text{Tr } U^\pm(t). \quad (3.2)$$

The perturbative semi-classical expansion is obtained from the pole of its integrand  $\frac{\text{Tr } U(t)}{t}$  at  $t = 0$ . As we explained in Section 2.3 it is associated to the logarithmic branch point of  $\Gamma(u)$ , whose appearance is also clear from the logarithm in (3.1), and equivalent to the branch points that appear in the WKB method. In this chapter, by obtaining the recursion relation for the semi-classical expansion, we will be able to provide a generalization of the WKB method and its geometric counter parts that we discussed in Section 2.3.2.

The content of this chapter was originally published by the author of this thesis as a research paper with the title “*Recursive Generation of The Semi-Classical Expansion in Arbitrary Dimension*” [26]. The rest of this chapter is identical to that paper with appropriate modifications.

Before start the discussion on the recursive expansion, let us outline the content of this chapter. In Section 3.1, we start with its relation to spectral functions and derive an integral representation of the so-called WKB action. Then, in Section 3.2, which is the main section of this chapter, we discuss the perturbative expansion of the propagator by utilizing a small time expansion and derive the recursion relation we were looking for. Note that at first, the time dependent formulation might ap-

pear to have a disadvantage for practical purposes despite its applicability to higher dimensional problems. However, the construction we describe in Section 3.2, the main computational task reduces to the integration of ordinary integrals and basic complex analysis. In Section 3.3, we will apply our method to anharmonic oscillators in arbitrary dimensions. The numerical results for this part are presented in Appendix C. Finally, in Section 3.5, we finish the chapter with a discussion of our analysis.

### 3.1. Spectral Problem

In this section, we will briefly review the spectral problem of a Hermitian operator  $\mathsf{H}$  acting on a Hilbert space. From elementary linear algebra, we know that the spectrum of  $\mathsf{H}$  is given by the zeroes of the Fredholm determinant, i.e.,

$$D(u) = \det(u - \mathsf{H}) = 0, \quad (3.3)$$

where  $u$  represents the elements of the spectrum. Instead of dealing with  $D(u)$  directly, we focus on another spectral function, which is the *quantum action*,

$$\Gamma(u) = \ln \det(u - \mathsf{H}) = \text{Tr} \ln(u - \mathsf{H}). \quad (3.4)$$

Now, the branch point of this new function carries the spectral information.

One way to handle the singularity is introducing the resolvent  $G(u) = (u - \mathsf{H})^{-1}$  as

$$\Gamma(u) = \int_{u_0}^u dz \text{Tr} G(z), \quad (3.5)$$

where  $u_0$  is an arbitrary regular point of  $G(z)$  on the complex  $z$  plane. Note that the simple poles of  $G(z)$ , where the (discrete) spectrum appears, correspond to the branch points of  $\Gamma(u)$  as demanded by construction [1]. The information around the branch point can be obtained by employing the  $i\varepsilon$  prescription [13] and defining a gap for the action  $\Gamma(u)$  as

$$\Delta\Gamma(u) = \Gamma^+(u) - \Gamma^-(u), \quad (3.6)$$

where we defined the actions in different branches as

$$\Gamma^\pm(u) = \lim_{\varepsilon \rightarrow 0} \Gamma(u \pm i\varepsilon) = \lim_{\varepsilon \rightarrow 0} \left\{ \int_{0 \pm i\varepsilon}^{u \pm i\varepsilon} dz \operatorname{Tr} G(z) \right\}. \quad (3.7)$$

It is well-known that the resolvent approach connects the classical dynamics and the quantum spectrum of  $\mathsf{H}$  [56, 57]. However, in perturbative calculations, it may become impractical. For this reason, it is more convenient to introduce its Fourier integral representation

$$G(u) = \pm i \int_0^\infty dt e^{\pm i(u - \mathsf{H})t}, \quad (3.8)$$

where  $t$  corresponds to a flow-time parameter conjugate to the eigenvalue  $u$ .

Near the branch cut,  $\Gamma^\pm(u)$  becomes

$$\Gamma^\pm(u) = - \lim_{\varepsilon \rightarrow 0} \int_0^\infty \frac{dt}{t} e^{\pm it(u \pm i\varepsilon)} \operatorname{Tr} U^\pm(t), \quad (3.9)$$

where  $U^\pm(t) = e^{\mp i\mathsf{H}t}$  is the propagator<sup>2</sup> which governs the flow generated by  $\mathsf{H}$ . It is also possible to incorporate the analytical continuations into integration contours,

$$\Gamma^\pm(u) = - \lim_{\varepsilon \rightarrow 0} \int_{0 \pm i\varepsilon}^{\infty \pm i\varepsilon} \frac{dt}{t} e^{\pm itu} \operatorname{Tr} U^\pm(t). \quad (3.10)$$

In this form, the spectral information arises from the singularities on the complex  $t$ -plane, which are intimately related to periods of classical orbits [58]. Note that the integrand in (3.10) is already singular at  $t = 0$ , which corresponds to stationary classical motion. In Section 3.3, for quantum anharmonic oscillators, we will explain how the spectral information for a perturbative sector, which is related to the stationary classical motion, emerges from this singularity. First we will continue our discussion with the perturbative expansion of  $\operatorname{Tr} U^\pm$  and its recursive structure.

### 3.2. Expansion in $D$ Dimensions

Before describing our recursive scheme for the perturbative expansion of  $\operatorname{Tr} U^\pm(t)$ , let's first investigate its general perturbative structure for a Hermitian operator  $\mathsf{H}$  given

---

<sup>2</sup>For simplicity in future calculations, the  $\frac{1}{\hbar}$  factor in the exponential is canceled by scaling  $t \rightarrow \hbar t$ .

in the following form:

$$\mathsf{H}(\mathbf{p}, \mathbf{x}) = \mathsf{T}(\mathbf{p}) + \mathsf{V}(\mathbf{x}), \quad (3.11)$$

where  $\mathsf{T}$  and  $\mathsf{V}$  are operator valued functions of appropriately chosen canonical variables  $\mathbf{x}$  and  $\mathbf{p}$  such that they form a  $2D$  dimensional phase space. From the quantum mechanical point of view,  $\mathsf{H}$  can be considered as a generalized Hamiltonian. Moreover, from ordinary QM, we know that projecting  $\mathsf{H}$  onto  $\mathbf{x}$ -space, the operator  $\mathbf{p}$  starts acting as a derivative operator and vice versa. From this fact, one can easily deduce

$$[\mathbf{p}, \mathsf{V}(\mathbf{x})] = -i\hbar \nabla_{\mathbf{x}} \mathsf{V}(\mathbf{x}) \quad , \quad [\mathbf{x}, \mathsf{T}(\mathbf{p})] = i\hbar \nabla_{\mathbf{p}} \mathsf{T}(\mathbf{p}), \quad (3.12)$$

and the well-known commutation relation between the canonical variables,

$$[x^i, p^j] = i\hbar \delta^{ij}. \quad (3.13)$$

The general structure of the perturbative expansion of  $U^\pm$  can be examined by using the Zassenhauss formula,

$$U^\pm(t) = e^{\mp i\mathsf{T}(\mathbf{p})t} e^{\mp it\mathsf{V}(\mathbf{x})} e^{\pm \frac{t^2}{4} [\mathsf{T}(\mathbf{p}), \mathsf{V}(\mathbf{x})]} e^{\pm \frac{it^3}{3!} (2[\mathsf{V}(\mathbf{x}), [\mathsf{T}(\mathbf{p}), \mathsf{V}(\mathbf{x})]] + [\mathsf{T}(\mathbf{p}), [\mathsf{T}(\mathbf{p}), \mathsf{V}(\mathbf{x})]])} \dots \quad (3.14)$$

Together with (3.12), it is easy to see that the sequence of exponents in (3.14) correspond to a *derivative* expansion. Besides this, expanding these exponentials, we can get another expansion which we call *coupling* expansion. This simple observation shows that a perturbative analysis of  $U^\pm(t)$  with an operator  $\mathsf{H}$  as in (3.11) should be treated as a double expansion.

Despite the simplicity of the discussion above, the Zassenhauss formula is not a convenient way for practical calculations. Instead, we take a step back and re-write the propagator as a time ordered exponential,

$$U^\pm(t) = \mathcal{T} \exp \left\{ \mp i \int_0^t dt' \mathsf{H}(\mathbf{p}, \mathbf{x}) \right\}, \quad (3.15)$$

which simplifies to an ordinary one when  $\mathsf{H}$  is  $t$  independent. Note that (3.15) is the

solution of

$$\pm i \frac{dU^\pm(t)}{dt} = \mathsf{H}(\mathbf{p}, \mathbf{x}) U^\pm(t). \quad (3.16)$$

One way to compute (3.15) is by introducing a Fourier transformation between the canonical variables and eliminate one of them [59–61]. In the following, we will present a perturbative expansion for  $\text{Tr}U^\pm$  inspired by this approach. However, instead of eliminating one of the variables, we will work on the phase space and integrate out  $\mathbf{x}$  and  $\mathbf{p}$  after computing the perturbative expansion. This approach was initiated in [62, 63] however, in these papers, the recursive structure behind the expansion of the time-ordered exponential (3.15) and its relation to the semi-classical expansion were not mentioned.

Let us start by separating the  $\mathsf{T}(\mathbf{p})$  part as

$$U^\pm(t) = e^{\mp it\mathsf{T}(\mathbf{p})} \tilde{U}^\pm(t) \quad (3.17)$$

and re-write (3.16) as

$$\pm i \frac{d\tilde{U}^\pm(t)}{dt} = \mathsf{V}_I^\pm \tilde{U}^\pm(t), \quad (3.18)$$

where we introduced the interaction picture potential,

$$\mathsf{V}_I^\pm = e^{\mp it\mathsf{T}(\mathbf{p})} \mathsf{V}(\mathbf{x}) e^{\pm it\mathsf{T}(\mathbf{p})}.$$

With these definitions,  $U^\pm(t)$  is expressed as

$$\begin{aligned} U^\pm(t) &= e^{\mp it\mathsf{T}(\mathbf{p})} \mathcal{T} \exp \left\{ \mp i \int_0^t dt' \mathsf{V}_I^\pm \right\} \\ &= e^{\mp it\mathsf{T}(\mathbf{p})} \sum_{n=0} \frac{(\mp i)^n}{n!} \int_0^t \prod_{i=1}^n dt_i \mathcal{T} \left\{ \mathsf{V}_I^\pm(t_1) \dots \mathsf{V}_I^\pm(t_n) \right\}. \end{aligned} \quad (3.19)$$

The next step is projecting the operator valued functions onto a  $2D$  dimensional phase space using <sup>3</sup>

$$\mathsf{V}(\mathbf{x})|\mathbf{x}\rangle = V(\mathbf{x})|\mathbf{x}\rangle \quad , \quad \mathsf{T}(\mathbf{p})|\mathbf{p}\rangle = T(\mathbf{p})|\mathbf{p}\rangle \quad (3.20)$$

---

<sup>3</sup>See Appendix A for conventions.

and re-writing

$$\text{Tr} U^\pm(t) = \int \frac{d^D x d^D p}{(2\pi\hbar)^D} e^{\mp iT(\mathbf{p})t} \sum_{n=0} \frac{(\mp i)^n}{n!} \int_0^t \prod_{i=1}^n dt_i \langle \mathbf{x} | \mathbf{p} \rangle \langle \mathbf{p} | \mathcal{T} [V_I^\pm(t_1) \dots V_I^\pm(t_n)] | \mathbf{x} \rangle. \quad (3.21)$$

This allows us to exchange the commutators with a derivative expansion. In order to do this, we insert an identity operator for each  $V_I(t_i)$ ,

$$\begin{aligned} \langle \mathbf{x} | \mathbf{p} \rangle \langle \mathbf{p} | V_I^\pm(t_i) &= \langle \mathbf{x} | \mathbf{p} \rangle e^{\pm iT(\mathbf{p})t_i} \int d^D x' \langle \mathbf{p} | \mathbf{x}' \rangle \langle \mathbf{x}' | V e^{\mp iT(\mathbf{p})t_i} \\ &= e^{\pm iT(\mathbf{p})t_i} \int \frac{d^D x'}{(2\pi\hbar)^D} e^{-\frac{i\mathbf{p}\cdot(\mathbf{x}'-\mathbf{x})}{\hbar}} V(\mathbf{x}') \langle \mathbf{x}' | e^{\pm iT(\mathbf{p})t_i}. \end{aligned} \quad (3.22)$$

At this point, instead inserting a second identity operator for  $e^{\pm iT(\mathbf{p})t_i}$ , we expand  $V(\mathbf{x}')$  around  $\mathbf{x}' = \mathbf{x}$ ,

$$V(\mathbf{x}') = \sum_{k=0} \frac{1}{k!} \left( (\mathbf{x}' - \mathbf{x}) \cdot \nabla_{\mathbf{x}} \right)^k V(\mathbf{x}). \quad (3.23)$$

This enables us to take  $x'$  integral using integration by parts. Then, removing the part we introduced as identity element, we get

$$\langle \mathbf{x} | \mathbf{p} \rangle \langle \mathbf{p} | V_I(t_i) = \sum_{k=0} \hbar^k W_k^\pm \langle \mathbf{x} | \mathbf{p} \rangle \langle \mathbf{p} |, \quad (3.24)$$

where

$$W_k^\pm = \frac{V^{(k)}(\mathbf{x})}{k!} \mathbf{b}_\pm^k(\mathbf{p}, \nabla_{\mathbf{p}}, t_i) \quad , \quad \mathbf{b}_\pm(\mathbf{p}, \nabla_{\mathbf{p}}, t_i) = i\nabla_{\mathbf{p}} \pm \nabla_{\mathbf{p}} T(\mathbf{p}) t_i \mp \nabla_{\mathbf{p}} T(\mathbf{p}) t. \quad (3.25)$$

Finally, we can express  $\text{Tr} U^\pm$  as a time-ordered exponential,

$$\text{Tr} U^\pm(t) = \int \frac{d^D x}{(2\pi\hbar)^D} \left\langle \mathcal{T} \exp \left\{ \mp i \int_0^t dt' \sum_{k=0} \hbar^k W_k^\pm \right\} \right\rangle_\pm, \quad (3.26)$$

where

$$\langle \dots \rangle_\pm = \int d^D p \dots e^{\mp iT(\mathbf{p})t}.$$

### 3.2.1. Recursion Relation

Equation (3.26) is still impractical for perturbative calculations. In addition to that, depending on the functions  $V(\mathbf{x})$  and  $T(\mathbf{p})$ , the volume integrals might lead to infinities which have no physical implications and they are handled by a normalization technique. In the following, we propose a method that can be used for practical calculations and only infinities we encounter will be related to the physical spectrum. We will extract this physical information without a need to normalize.

We start by making use of the time-ordered exponential in (3.26). It enables us to re-write (3.16) as

$$\pm i \frac{d\tilde{U}^\pm(t)}{dt} = \sum_{k=0} \hbar^k W_k^\pm \tilde{U}^\pm(t). \quad (3.27)$$

Let us write  $\tilde{U}$  in an  $\hbar$  expansion as well

$$\tilde{U}^\pm(t) = \sum_l \tilde{U}_l^\pm(t) \hbar^l.$$

Then, matching orders in (3.27), we get

$$\pm i \frac{d\tilde{U}_m^\pm(t)}{dt} = \sum_{l=0}^m W_l^\pm \tilde{U}_{m-l}^\pm(t). \quad (3.28)$$

At order  $m = 0$ , the solution is

$$\tilde{U}_0^\pm(t) = \mathcal{T} \exp \left\{ \mp i \int_0^t dt' W_0^\pm(t') \right\} = e^{\mp i V t}. \quad (3.29)$$

For  $m \geq 1$ , after multiplying (3.28) with  $(\tilde{U}_0^\pm)^{-1}$ , we get

$$\tilde{U}_m^\pm(t) = \mp i \tilde{U}_0^\pm(t) \int_0^t dt' (\tilde{U}_0^\pm)^{-1}(t') R_m^\pm(t'), \quad (3.30)$$

where

$$R_m^\pm(t) = \sum_{l=1}^m W_l^\pm(t) \tilde{U}_{m-l}^\pm(t).$$

Note that each  $\tilde{U}_m^\pm(t)$  is written in terms of  $\tilde{U}_{l \leq m}^\pm(t)$ . This makes the recursive behaviour

of the perturbative expansion evident. To utilize this recursive behaviour, we express  $\tilde{U}_m$  in terms of  $\tilde{U}_0$  and  $W_l$  only as

$$\tilde{U}_m(t) = \tilde{U}_0^\pm(t) \sum_{k=1} \tilde{U}_{m,k}(t), \quad (3.31)$$

where

$$\tilde{U}_{m,k}^\pm(t) = \sum_{\substack{\alpha_1, \dots, \alpha_k=1 \\ (\alpha_1 + \dots + \alpha_k = m)}}^m (\mp i)^k \int_0^t dt_1 \int_0^{t_1} dt_2 \dots \int_0^{t_{k-1}} dt_k W_{\alpha_1}^\pm(t_1) \dots W_{\alpha_k}^\pm(t_k). \quad (3.32)$$

In (3.32), we have used  $(\tilde{U}_0^\pm)^{-1} W_\alpha^\pm \tilde{U}_0^\pm = W_\alpha^\pm$ , which was possible since  $U_0^\pm = e^{\mp itV}$  is  $\mathbf{p}$  independent. Finally, let us define the sum of products as

$$Q_{m,k}^\pm = \sum_{\substack{\alpha_1, \dots, \alpha_k=1 \\ (\alpha_1 + \dots + \alpha_k = m)}}^m W_{\alpha_1}^\pm(t_1) \dots W_{\alpha_k}^\pm(t_k). \quad (3.33)$$

For each  $m$  and  $k$ ,  $Q_{m,k}^\pm$  can be written as a product of two lower order terms. For example, let us separate  $W_{\alpha_1}$  from the rest. Then, we get

$$\begin{aligned} Q_{m,k}^\pm &= \sum_{\alpha_1} W_{\alpha_1}^\pm Q_{m-\alpha_1, k-1}^\pm \\ &= W_1^\pm Q_{m-1, k-1}^\pm + W_2^\pm(t_1) Q_{m-2, k-1}^\pm + \dots + W_{m-(k-1)}^\pm(t_1) Q_{k-1, k-1}^\pm \\ &= \sum_{l=1}^{m-k+1} Q_{l,1}^\pm Q_{m-l, k-1}^\pm, \end{aligned} \quad (3.34)$$

where we set  $Q_{\alpha,0} = \delta_{\alpha,0}$ . This is the recursion relation we were looking for. Using this recursion relation, we can explicitly express (3.32) as

$$\tilde{U}_{m,k}(t) = \sum_{l=1}^{m-k+1} \int_0^t dt_1 W_l(t_1) \tilde{U}_{m-l, k-1}(t_1) \quad (3.35)$$

$$= \sum_{l=1}^{m-k+1} \frac{V^{(l)}(\mathbf{x})}{l!} \int_0^t dt_1 \mathbf{b}^l(\mathbf{p}, \nabla \mathbf{p}, t_1) \tilde{U}_{m-l, k-1}(t_1). \quad (3.36)$$

Assuming  $\tilde{U}_{m-l, k-1}$  is already computed, for each  $\tilde{U}_{m,k}$ , we only need to compute one  $l^{\text{th}}$  order differentiation and one  $t_k$  integral. This is a crucial point to speed up practical calculations.

Combining all of these, we write the actions in an  $\hbar$  expansion,

$$\Gamma^\pm(u) = -\lim_{\varepsilon \rightarrow 0} \sum_{m=0} \hbar^m \int_{0 \pm i\varepsilon}^{\infty \pm i\varepsilon} \frac{dt}{t} e^{\pm iut} \int \frac{d^D x}{(2\pi\hbar)^D} e^{\mp iV(\mathbf{x})t} \left\langle \sum_{k=1}^m \tilde{U}_{m,k}^\pm(t) \right\rangle_\pm. \quad (3.37)$$

Note that in  $\tilde{U}_{m,k}$ ,  $k$  represents the number of potentials, i.e. the order of coupling expansion, while  $m$  represents the total number of derivatives acting on these potentials. In our arrangement, at any order  $k \leq m$ . Higher order terms in the coupling expansion comes from the expansion of  $\tilde{U}_0^\pm = e^{\pm itV}$ , if the  $x$  integral could not be taken directly.

In addition to generating additional terms for the coupling expansion,  $\tilde{U}_0^\pm = e^{\pm itV}$  in (3.37) also enables us to obtain finite results for the  $x$  integration as long as we compute it around a minimum of  $V(\mathbf{x})$ . For example, in Section 3.3, we will compute the expansion for quantum anharmonic oscillators around their harmonic minima. In those cases, the  $x$  integrals will be Gaussian and with a proper analytical continuation of in complex  $t$  plane, they lead to finite results. However, this would not be possible if we use the time-ordered exponential in (3.26) directly. Note also that due to the separation in (3.17), the  $p$  integrals do not need a further treatment to prevent non-physical infinities.

At this point let us states some remarks about the above discussion:

- Instead of the definition in (3.17), we can split the original propagator as

$$U^\pm(t) = e^{\mp iV(\mathbf{x})t} \tilde{U}^\pm(t). \quad (3.38)$$

This is an equivalent definition and the only difference would be the roles of  $\mathbf{T}(\mathbf{p})$  and  $\mathbf{V}(\mathbf{x})$  in the double expansion. Following the same procedure, we get the following recursion relation

$$P_{n,k}^\pm(t) = \sum_{l=1}^{m-k+1} \int_0^t dt_1 R_l(t_1) P_{n-l,k-1}(t_k), \quad (3.39)$$

where

$$P_{n,k}^\pm(t) = \sum_{\substack{\alpha_1, \dots, \alpha_k=1 \\ (\alpha_1+\dots+\alpha_k=n)}}^n (\mp i)^k \int_0^t dt_1 \int_0^{t_1} dt_2 \cdots \int_0^{t_{k-1}} dt_k R_{\alpha_1}^\pm(t_1) \cdots R_{\alpha_k}^\pm(t_k) \quad (3.40)$$

and

$$R_k^\pm = \frac{T^{(k)}(\mathbf{p})}{k!} \mathbf{c}_\pm^k(\mathbf{x}, \nabla_{\mathbf{x}}, t_i) \quad , \quad \mathbf{c}_\pm(\mathbf{x}, \nabla_{\mathbf{x}}, t_i) = i\nabla_{\mathbf{x}} \pm \nabla_{\mathbf{x}} V(\mathbf{x}) t_i \mp \nabla_{\mathbf{x}} V(\mathbf{x}) t. \quad (3.41)$$

In this case, the actions  $\Gamma^\pm$  becomes

$$\Gamma^\pm(u) = -\lim_{\varepsilon \rightarrow 0} \sum_{n=0} \hbar^n \int_{0 \pm i\varepsilon}^{\infty \pm i\varepsilon} \frac{dt}{t} e^{\pm iut} \int \frac{d^D p}{(2\pi\hbar)^D} e^{\mp iT(\mathbf{p})t} \left\langle \sum_{k=1}^n P_{n,k}^\pm(t) \right\rangle_\pm, \quad (3.42)$$

where

$$\langle \dots \rangle_\pm = \int d^D x \dots e^{\mp iV(\mathbf{x})t}.$$

- In both of (3.37) and (3.42), the order  $\hbar$  counts the number of derivatives. But the difference is in the first one, it is the number of derivatives on  $V(\mathbf{x})$ , while in the latter, it is the one on  $T(\mathbf{p})$ . This difference indicates that (3.37) and (3.42) are different expressions of same object. However, as long as we do not truncate one of these expansions, results coming from both approaches would be equal.
- The recursion relation (3.34) is in the same form with the well-known WKB recursion relation [64]. However, as stated before, since we consider the contributions of branch points through the  $t$  integral, we will take  $x$  and  $p$  integrals directly and this will be our ticket to go to higher dimensions. For completeness, we will also show the equivalence between our method and the standard WKB in one dimension in Section 3.4.
- Finally, note that the recursive behaviour is an intrinsic property of the iterated integrals, which stem from the time-ordered exponential, and it is independent of the functions  $T(\mathbf{p})$  and  $V(\mathbf{x})$ . This indicates the topological nature of the derivative expansions, and it is totally consistent with the conjectured equivalence of topological recursion and WKB expansion [54, 55].

### 3.3. An Example: Anharmonic Oscillators in Quantum Mechanics

Up to this point, we have constructed a recursive expansion formula for the quantum action  $\Gamma$  and expressed each term by a number of integrals. In this section, as an illustrative example, we will demonstrate how the spectral information of the  $D$  dimensional quantum anharmonic oscillator is obtained.

Let us start with setting

$$T(\mathbf{p}) = \frac{\mathbf{p}^2}{2} \quad (3.43)$$

and

$$V(\mathbf{x}) = \frac{\mathbf{x}^2}{2} + \lambda v(\mathbf{x}), \quad (3.44)$$

where  $v(\mathbf{x})$  is a higher degree polynomial. Then, the quantum actions in (3.37) are written as

$$\Gamma^\pm(u) = -\lim_{\varepsilon \rightarrow 0} \sum_{m=0} \hbar^m \int_{0 \pm i\varepsilon}^{\infty \pm i\varepsilon} \frac{dt}{t} e^{\pm iut} \int \frac{d^D x d^D p}{(2\pi\hbar)^D} e^{\mp i(\frac{\mathbf{x}^2}{2} + \lambda v(\mathbf{x}))t} \sum_{k=1}^m \tilde{U}_{m,k}^\pm(t) e^{\mp \frac{i\mathbf{p}^2 t}{2}}.$$

We carried out the computations in three separate stages:

(i) *Iterated Integrals:* We first need to compute the iterated time integrals using the recursion relation in (4.28).

- In these computations, the operator,

$$\mathbf{b}_\pm(\mathbf{p}, \nabla_{\mathbf{p}}, t_i) = i\nabla_{\mathbf{p}} \pm \mathbf{p} t_i \mp \mathbf{p} t$$

serves as a generator of polynomials in  $p$  by acting on both the polynomials generated in the lower orders and  $e^{\mp \frac{i\mathbf{p}^2 t}{2}}$ . We carried out this procedure by using the `Nest` function in *Mathematica*.

- Note that the  $\mathbf{x}$  dependent functions are not affected by this procedure. Their multiplication leads to the polynomials in  $\mathbf{x}$ .
- The  $t_i$  terms in  $\mathbf{b}_\pm$  also form polynomials. They can easily be integrated at each order. Note that they will also contribute to the next order in the

iteration.

(ii) *Phase Space Integrals:* At this point, each term in the expansion is written as a polynomial of  $\mathbf{p}$ ,  $\mathbf{x}$  and  $t$ .

- Note that  $e^{\mp \frac{i\mathbf{p}^2 t}{2}}$  is already in Gaussian form and  $e^{\mp iV(\mathbf{x})t}$  can be made Gaussian by expanding it for small  $\lambda$ . Then, we can integrate out  $\mathbf{x}$  and  $\mathbf{p}$  using the standard Gaussian integrals,

$$\begin{aligned} I_{2n} &= \int d^D z e^{\mp \frac{it}{2} \sum_{k=1}^D z_k^2} z_1^{2n_1} \dots z_D^{2n_D} \\ &= \prod_{k=1}^D \int dz_k e^{\mp \frac{it}{2} z_k^2} z_k^{2n_k} = \left( \frac{1}{\pm 2it} \right)^n \prod_{k=1}^D \frac{(2n_k)!}{n_k!} \sqrt{\frac{2\pi}{\pm it}}, \end{aligned} \quad (3.45)$$

where we set  $n_1 + \dots + n_D = n$  and in order to prevent divergences in the  $z_k$  integrals, the analytical continuation of  $t$  in appropriate directions is assumed.

- For example, at the leading order in the derivative expansion, we get

$$\begin{aligned} \Gamma_{m=0}^{\pm}(u, \lambda) &= -\lim_{\varepsilon \rightarrow 0} \int_{0 \pm i\varepsilon}^{\infty \pm i\varepsilon} \frac{dt}{t} e^{\pm iut} \left( \frac{2\pi}{\pm it} \right)^{\frac{D}{2}} \int \frac{d^D x}{(2\pi\hbar)^D} e^{\mp \frac{i\mathbf{x}^2 t}{2}} \sum_{k=0} \frac{(\mp i\lambda t v(\mathbf{x}))^k}{k!} \\ &= -\lim_{\varepsilon \rightarrow 0} \int_{0 \pm i\varepsilon}^{\infty \pm i\varepsilon} \frac{dt}{t} \frac{e^{\pm iut}}{(\pm it\hbar)^D} \sum_{n=0} \frac{A_{2n}^{(0)}(\lambda)}{(\pm it)^n}, \end{aligned} \quad (3.46)$$

where  $A_{2n}^{(0)}(\lambda)$  is a polynomial of  $\lambda$  originating from the Gaussian integral of the  $\mathbf{x}^{2n}$  term of  $v^k(\mathbf{x})$ .

- For the higher order terms, additional contributions to both  $\mathbf{x}$  and  $\mathbf{p}$  polynomials come from the recursive procedure in stage 1. This makes the general expression more complicated but it is still easy to handle by a computer.
- Observe that higher order poles at  $t = 0$  appear in (3.46). They are critical for us since in our setting they are associated with the spectrum of  $\mathsf{H}$ .

(iii) *From Singularities to Spectrum:* The singularity at  $t = 0$  is usually handled by zeta function regularization [65]. However, instead we will show that the basic contour integration techniques together with the  $i\varepsilon$  prescription we mentioned in Section 3.1 are sufficient.

- To explain how we handle these singularities, let us continue with (3.46). We start with introducing a cutoff  $\Omega$  at the lower limit of the  $t$  integral.

This allows us to express (3.46) as

$$\Gamma_{m=0}^{\pm}(u, \lambda) = -\hbar^{-D} \sum_{n=0} A_{2n}^{(0)}(\lambda) (-u)^{D+n} \lim_{\substack{\varepsilon \rightarrow 0 \\ \Omega \rightarrow 0}} \frac{E_{D+n+1}(\Omega \pm i\varepsilon)}{(\Omega \pm i\varepsilon)^{D+n}}, \quad (3.47)$$

where we used the generalized exponential integral [66],

$$E_{\alpha}(z) = z^{\alpha-1} \int_z^{\infty} dt \frac{e^{-t}}{t^{\alpha}}. \quad (3.48)$$

- For  $\alpha \in \mathbb{N}$ , it can be expressed as

$$E_{\alpha}(z) = \frac{(-z)^{\alpha-1}}{(\alpha-1)!} E_1(z) + \frac{e^{-z}}{(\alpha-1)!} \sum_{k=0}^{\alpha-2} (\alpha-k-2)! (-z)^k. \quad (3.49)$$

The second part of (3.49) is regular at  $z = 0$ , while the first part has a branch cut due to the branch points of  $E_1(z)$  at  $z = 0$  and  $z = \infty$ . This branch cut leads to

$$E_1(ze^{2m\pi i}) - E_1(z) = -2m\pi i \quad ; \quad m \in \mathbb{Z}. \quad (3.50)$$

Note that to use (3.50) in (3.47), we interpret the analytical continuation as

$$\Omega - i\varepsilon = (\Omega + i\varepsilon)e^{2\pi i}.$$

Then, at the leading order we have

$$\Delta\Gamma_0(u, \lambda) = \frac{2\pi i}{\hbar^D} \sum_{n=0} \frac{A_{2n}^{(0)}(\lambda) u^{D+n}}{(D+n)!}. \quad (3.51)$$

- Same technique can be applied to the higher orders and  $\Delta\Gamma(u)$  can be expressed as

$$\Delta\Gamma(u, \lambda, \hbar) = \sum_{m=0}^{\infty} \Delta\Gamma_{2m}(u, \lambda) \hbar^{2m}, \quad (3.52)$$

where each  $\Delta\Gamma_{2m}(u, \lambda)$  corresponds to a series in  $u$  and  $\lambda$ . In Appendix C, we will provide numerical results for several anharmonic oscillators in  $D = 1, 2, 3$  dimensions.

At this point let us make a comment on *quantization conditions*. Setting  $\lambda = 1$  for convenience, (3.52) allows us to express  $\Delta\Gamma$  as a series in  $u$  and  $\hbar$ . However, as

we reviewed in Section 3.1, the original spectral quantity is  $u$  itself, so it is natural to investigate a method for obtaining a perturbative series for  $u$  starting from  $\Delta\Gamma$ . In one dimension, this can be achieved by imposing the Bohr-Sommerfeld quantization condition for (an)harmonic oscillators. In our formulation, it is expressed as

$$\Delta\Gamma(u, \hbar) = 2\pi i \left( N + \frac{1}{2} \right). \quad (3.53)$$

For a simple harmonic oscillator in one dimension, we have

$$\Delta\Gamma(u, \hbar) = \frac{2\pi i u}{\hbar}, \quad (3.54)$$

and it is obvious that (3.53) and (3.54) lead to correct eigenvalues, i.e.  $u = \hbar \left( N + \frac{1}{2} \right)$ . For anharmonic cases, we will have a series in  $u$  for each  $\Delta\Gamma_{2m}$  in (3.52). In these cases, the perturbative expansion of  $u$  is achieved by inverting the series in (3.52) [48, 67, 68]. On the other hand, it appears that a meaningful generalization of the Bohr-Sommerfeld quantization condition to higher dimensions remains lacking and further investigation is needed.

### 3.4. WKB Expansion = Derivative Expansion

Here, for completeness, we compute the first two non-zero terms in the expansions of the one dimensional non-relativistic quantum mechanics, i.e.,  $T(p) = \frac{p^2}{2}$ , for a general potential  $V(x)$ . This will show the equivalence between the standard WKB approximation and the derivative expansion in our formalism. In addition to that we will also observe how the “*physical*” singularities transfer from the  $t$  integral to the  $x$  integral.

We already derived the leading order WKB integral from the Schwinger’s integral in Section 2.3. Here we present its complete derivation. For  $m = 0$  and  $D = 1$ , (3.37) simplifies to

$$\Gamma_0^\pm(u) = - \lim_{\varepsilon \rightarrow 0} \int_0^\infty \frac{dt}{t} \int \frac{dx dp}{2\pi\hbar} e^{\mp \frac{ip^2 t}{2}} e^{\pm i(u \pm i\varepsilon - V)t}. \quad (3.55)$$

Performing the  $p$  integral, rotating the  $t$  integral contour by  $e^{\pm i\pi/2}$  and re-scaling

$$t \rightarrow \frac{t}{u \pm i\varepsilon - V(x)},$$

we get

$$\Gamma_0^\pm(u) = \frac{e^{\mp i\pi/2}}{\hbar} \int_0^\infty \frac{dt e^{-t}}{\sqrt{2\pi t^3}} \int dx \sqrt{u \pm i\varepsilon - V(x)}. \quad (3.56)$$

Note that the  $t$  integral is still divergent at the lower boundary. Remark that the branch cut information is now carried to points giving  $u = V(x)$  in  $x$  space. Handling the divergence at  $t = 0$  by zeta-regularization, we get

$$\Delta\Gamma(u) = \Gamma^+(u) - \Gamma^-(u) = \frac{i\sqrt{2}}{\hbar} \sum_i \oint_{\alpha_i} dx \sqrt{u - V(x)}, \quad (3.57)$$

where the each contour  $\alpha_i$  is taken around the singularities at  $u = V(x)$ , i.e the turning points. Finally, combining with the quantization condition (3.53), we get

$$\sqrt{2} \oint dx \sqrt{u - V(x)} = 2\pi \left( N + \frac{1}{2} \right) \hbar, \quad (3.58)$$

which matches the Bohr-Sommerfeld formula (2.74).

At the next to the leading order, for  $m = 1$ , the action is given as

$$\Gamma_{m=1}^\pm(u) = -\lim_{\varepsilon \rightarrow 0} \hbar \int_0^\infty \frac{dt}{t} e^{\pm it(u \pm i\varepsilon)} \int \frac{dx}{2\pi\hbar} e^{\mp iVt} \int_0^t dt' \left\langle W_1(t') \right\rangle_\pm, \quad (3.59)$$

where  $\left\langle W_1 \right\rangle_\pm = \left\langle V'(x) b_\pm(p) \right\rangle_\pm = 0$ . Thus, at order  $\hbar$  there is no contribution to the action.

Similarly, for  $m = 2$ , we have

$$\begin{aligned} \hbar\Gamma_{m=2}^\pm(u) &= -\lim_{\varepsilon \rightarrow 0} \hbar^2 \int_0^\infty \frac{dt}{t} e^{\pm it(u \pm i\varepsilon)} \int dx e^{\mp iVt} \\ &\quad \left\{ \int_0^t dt_1 \frac{V''(x)}{2} \left\langle b_\pm(t_1) b_\pm(t_1) \right\rangle_\pm \mp \int_0^t dt_1 \int_0^{t_1} dt_2 (V'(x))^2 \left\langle b_\pm(t_1) b_\pm(t_2) \right\rangle_\pm \right\}. \end{aligned}$$

Following the same arguments as for the leading order, we get

$$\begin{aligned}\hbar\Delta\Gamma_{m=2} &= -\frac{i\hbar^2}{\sqrt{2}} \sum_i \oint_{\alpha_i} dx \left\{ \frac{V''(x)}{24(u-V)^{3/2}} + \frac{(V'(x))^2}{32(u-V)^{5/2}} \right\} \\ &= -i\hbar^2 \frac{\sqrt{2}}{2^6} \sum_i \oint_{\alpha_i} \frac{(V'(x))^2}{(u-V)^{5/2}},\end{aligned}$$

which is the first quantum correction to the WKB approximation in (2.75).

### 3.5. Discussion

In this chapter, we investigated the recursive nature of the derivative expansion of the quantum action and showed how to implement it in practical calculations for quantum anharmonic oscillators in arbitrary dimensions. In quantum mechanics, the semi-classical expansion, which is represented by a derivative expansion in our language, can also be obtained via WKB methods in one dimension, or path integrals in arbitrary dimensions. However, our method has advantages over both methods since perturbative calculations using path integral becomes cumbersome very quickly and the WKB method is only applicable to effectively one dimensional problems.

Besides this practical advantage, the method we used separates the spectral information into two distinct parts. The first part, which is identified as the recursion relation and iterated integrals, is universal. It is the same for all quantum mechanical systems. Moreover, despite some differences in the details, we expect the same structure to be present in many-body systems and effective quantum field theories as well. This reveals a general relation between the classical action and its quantum corrections at different orders in a wide range of quantum theories. As we mentioned in Section 2.3.2, this relation has been well studied for one dimensional quantum mechanical models via Picard-Fuchs differential equations and the holomorphic anomaly equation [46–52]. Thus, the method that discussed in this chapter can also be interpreted as an extension of those methods to higher dimensions and possibly to more complicated theories.

On the other hand, the second part, which is identified as the phase-space integrals, depends on the particular system chosen, and therefore it carries information specific to that system. One important piece of information is the divergent large order behaviour of the semi-classical expansion. Our systematic construction allows an efficient computation of high orders and allows us to examine its hidden non-perturbative structure.

As we have described, the perturbative spectrum gets contribution from the singular part of the small  $t$  expansion in (3.37). However, each order in the derivative expansion in (3.37) contains finite contributions as well. Note that their order by order integration leads to a divergent series. Although, this was not important in our construction one could, before taking  $t$  integral, obtain a function by summing the finite part and it would be interesting to examine its contribution to the non-perturbative sector of the spectrum through  $t$  integration. We will apply these ideas in Chapter 4 to obtain the non-perturbative pair production probability from the recursive expansion we discussed here.

Finally, let us finish with some apparent downsides of the method we proposed. The first is the lack of expansions related to non-perturbative sector. In WKB related approaches, these expansions are obtained by integrating along classically non-allowed paths, but we get the spectral information from the singularity at  $t = 0$  plane and so no non-perturbative term emerges in our calculations. However, as the resurgence theory indicates there should be intimate connection between perturbative and non-perturbative sectors. For genus one potentials this is described by Matone's relation [47, 69, 70]. Adapting this to our formalism could be useful to understand the emergence of non-perturbative terms and it can be used to verify the connection between perturbative and non-perturbative sectors in more complicated theories.

## 4. PAIR PRODUCTION WITHOUT BOREL AMBIGUITY

In this chapter, we will use the recursive approximation scheme that we developed in Chapter 3 to obtain the non-perturbative pair production probability of general electromagnetic background potentials in arbitrary dimensions. The main difference with Chapter 3 is that in this case, we will probe the singularities of  $\text{Tr}U(t)$  at finite  $t$  instead of the one at  $t = 0$ . While the way we extract the non-perturbative information is similar to the Borel summation method of Section 2.2.3, in this chapter, using real time formalism and the  $i\varepsilon$  prescription, we will be able to bypass the ambiguity problem and obtain an unambiguous non-perturbative pair production probability which does not cancel through an additional non-perturbative contribution.

In addition to this perturbation theory based approach, to get more insight about the calculations we pursued in this chapter and the previous one, we will also discuss its relation to the WKB method and Lefschetz thimbles in the periodic background electromagnetic field. The comparison with the WKB method enables us to associate the singularities of  $\text{Tr}U(t)$  with the WKB cycles and this reveals a version of electromagnetic duality in terms of the singularities of  $\text{Tr}U(t)$ . On the other hand, the Lefschetz thimble approach will demonstrate how the unambiguous pair production arises from the path integral perspective.

The content of this chapter was originally published by the author of this thesis as a research paper with the title “*Pair Production in Real Proper Time and Unitarity Without Borel Ambiguity*” [27]. The rest of this chapter is identical to that paper with appropriate modifications.

### 4.1. Background Discussion

Particle pair production is one of the fundamental predictions of relativistic quantum theories. Early on, it was noticed that this can be explained by modifications in

the effective Lagrangian of constant electromagnetic fields [71]. Later, in [59], using proper time formalism, Schwinger systematically showed that in the presence of constant electromagnetic backgrounds, the effective Lagrangian (or action) develops an imaginary part which indicates the vacuum instability so that particle creation. Since then, the particle production in background electromagnetic fields has been investigated thoroughly for different types of background potentials using different methods.

From a mathematical perspective, a consequence of the vacuum instability, so that the particle creation, presents itself in the perturbation theory [6]: In QED, an expansion in the fine structure constant  $\alpha$  should be divergent, as the theory is ill-defined for negative values of  $\alpha$ . As we discussed in Section 2.2, the divergence can be handled by the Borel summation method which also probes the non-perturbative information about the system.

For the pair production problems, this method was used in [72] for a solvable background electromagnetic field to obtain the pair production probability from the imaginary part of the 1 loop QED effective action. However, as we know from Section 2.2.4 in details, the standard Borel summation method possesses a pathology: The imaginary contribution is multi-valued. Although it has a resolution for problems with stable vacua by the cancellation mechanism of Bogomolny and Zinn-Justin, when the vacua of a physical system is not stable one needs to found another solution since the imaginary contribution should survive. In letter cases, the main problem is the multi-valued pair production probability since one of them violates the unitarity of the theory.

To see how this violation presents itself in the effective action, let us review vacuum-vacuum amplitude, i.e.  $\mathcal{A} = \langle 0|0 \rangle$ . In a time dependent setting, this amplitude is expressed as

$$\mathcal{A} = \langle 0_+|U(\infty, -\infty)|0_- \rangle, \quad (4.1)$$

where  $|0_\pm\rangle$  are the vacua at infinite past and future while  $U$  is the unitary time prop-

agator connecting these two states. In general, the amplitude is a pure phase, i.e.,

$$\mathcal{A} = e^{i\Gamma}, \quad (4.2)$$

where  $\Gamma$  is the effective action of the theory. As long as  $\Gamma \in \mathbb{R}$ , the transition probability  $|\mathcal{A}|^2 = 1$  and the vacuum is a stable one, i.e. there is no creation of particles. However, when  $\Gamma \in \mathbb{C}$ , the transition probability becomes

$$|\mathcal{A}|^2 = e^{-2\text{Im}\Gamma} \leq 1. \quad (4.3)$$

Obviously, whenever  $\text{Im}\Gamma \neq 0$ , the vacuum is not stable and there is a probability of particle creation which is defined as

$$\mathcal{P} = 1 - |\mathcal{A}|^2 \sim 2\text{Im}\Gamma. \quad (4.4)$$

Note that since the theory is unitary,  $\text{Im}\Gamma$  should not be negative. At first, this seems to be a trivial statement. However, for consistency and completeness, the  $\text{Im}\Gamma > 0$  condition should be implicit in methods we use, which should also cover the stable cases on an equal footing.

In the context of the pair production problem, the unitarity problem was first noticed in [23] and it was shown that the consistent treatment can be achieved with the Schwinger proper time integral but only when the proper time is chosen to be real. This approach was motivated from two observations:

- (i) Schwinger's proper time integral at 1 loop order and the Borel integral have the same form.
- (ii) When the proper time is chosen real, possible analytical continuation directions of the integral are defined by construction.

In general, the divergent series for the perturbative effective action is found first, then the Borel procedure is applied to tame the divergence and probe the singularity which leads to the non-perturbative information, i.e the pair production probability in our case. Instead of following this standard path, the first point suggests that it

is possible to probe these singularities before taking the proper time integral. While the two approaches are equivalent, in this way, the crucial analytical continuation information would be kept.

The predefined analytical continuation, on the other hand, stems from utilization of the  $i\varepsilon$  prescription. In addition to [23], its relation with the resolution of the Borel ambiguity was also discussed in [24, 28]. Let us summarize the idea briefly: It is known that propagator(resolvent)  $G^\pm(u) = (u - H)^{-1}$  of a quantum theory is not well defined on the real  $u$  line [42]. Instead, it is defined by an analytical continuation on the upper or lower half of the complex plane by redefining  $G^\pm(u) = \lim_{\varepsilon \rightarrow 0} (u \pm i\varepsilon - H)^{-1}$ . Then, any observable computed using these redefined propagators have a certain predefined analytical continuation which prevents any ambiguity in directions of the limit  $\varepsilon \rightarrow 0$ . The analytical continuation information is also transferred the integral contour of the 1 loop effective action when the proper time is taken real instead of imaginary.

In this chapter, we will first reformulate this real time approach by providing an unambiguous definition of the pair production probability which is coherent with the time dependent scattering amplitude description we discussed above. This reformulation is based on the well-known fact that  $i\varepsilon$  prescription which is associated to the forward/backward time flow directions in the scattering process and puts the ideas in [23], where only one time direction for the electric case was discussed, on a more rigorous basis. After discussing this reformulation in Section 4.2, we will present its application to uniform electric and magnetic backgrounds in Section 4.2.1 and show that how the emerging imaginary contributions are consistent with the unitarity condition and properties of their associated vacua.

In Section 4.3, we will extend our discussion to arbitrary background gauge potentials in arbitrary dimensions and using the Pade summation of the perturbative expansion of the propagator, we will extract the leading order non-perturbative pair production probabilities for general space dependent and time dependent electric fields under very general assumptions. These results will be a generalization of the ones

found for specific background potentials using exact solutions [72, 73] or direct non-perturbative methods [74–79]. In order to get the perturbative expansion, we will use a perturbative scheme developed in [26] for non-relativistic quantum mechanics and adapt it to arbitrary background gauge potentials, which are suitable for pair production problems. The perturbative scheme we will use is analogous to the small time expansion of heat kernels [60, 61, 80] and string inspired methods [81–83], but it organizes the expansion via a recursion relation.

Along with extracting the non-perturbative pair production probability, the discussion in Section 4.3 indicates that the perturbative expansion of the propagator can be separated in two parts. As shown in [26], one part corresponds to the perturbative semi-classical series which can be obtained by WKB approximation. Application of this method to the pair production problems in QED shows us that this series is originated from the same source with the UV divergences, which are handled by the renormalization methods in this context. On the other hand, the pair production probability emerges from the second part which is an originally convergent expansion. Its direct summation with the Pade approximation leads to an unambiguous imaginary part which represents the pair production rate. We will further investigate the nature of these singularities and associated perturbative/non-perturbative information in Section 4.4.1 by expressing the actions in WKB formalism.

Finally, in Section 4.4, we will connect the real time approach to two semi-classical approaches to the pair production problem by investigating periodic background potential. One approach is the WKB method, which treats the pair production problem as a tunnelling problem [84–91]. As we stated, connecting the time dependent perturbative scheme to the WKB method in Section 4.4.1 will help us to understand the real nature of the perturbative calculations in Section 4.3 by indicating that the vacua of electric and magnetic cases correspond to peaks and valleys of the background potential. This observation will also enable us to associate the two types of expansion governing the effective action, which we discuss in Section 4.3, with the perturbative and non-perturbative information represented by WKB cycles and show us that there

is a duality between electric and magnetic cases which can be understood from the geometric properties of the potential.

The other approach we will focus on in Section 4.4 is path integrals, which identify the pair production probability with the action of the classical equation of motion governed by the Hamiltonian of the system. In pair production problems, the most common path integral approach is the worldline instanton method [74–79, 92–94]. It has been shown [95, 96] that the worldline instanton method is equivalent to the semi-classical construction of Gutzwiller [97, 98], which has also been linked to Lefschetz thimbles recently [99]. While our construction can be adapted to any of these techniques, in Section 4.4.2, we will use the real time Lefschetz thimble description, which was shown to be an effective way to define semi-classical path integrals in various contexts [100–103] including the pair production problem [104]. With the help of the recursive construction in Section 4.3, we will only deal with an ordinary integral, which corresponds to the exact leading order limit of the full effective action; therefore, it carries the full information at this order. In this way, using complex steepest descent paths, which correspond to the classical paths at the leading order, we will demonstrate the Borel ambiguity resolution from a geometric point of view.

## 4.2. Pair Production Problem and Resolution of Ambiguity

In this chapter, we will only consider the pair production of bosonic matter as the fermionic matter production can be handled equivalently and only constant prefactors would differ in their results. For bosonic matter fields in the presence of an electromagnetic background, the effective action at 1 loop order is expressed as

$$\Gamma(m^2) = \frac{i}{2} \ln \det(m^2 - \mathsf{H}), \quad (4.5)$$

where  $m$  is the mass of bosonic matter particles and

$$\mathsf{H} = \frac{1}{2}(p_\mu - eA_\mu)^2 \quad (4.6)$$

is the Hamiltonian operator governing the motion of the bosonic particles. Note that in this paper, we use  $g_{\mu\nu} = \text{diag}(- + + \dots)$  metric convention.

In a time-independent setting, the 1-loop effective action (4.5) can be expressed as

$$\Gamma^\pm(m^2) = \int_{m_0^2}^{m^2} dz \text{Tr} G^\pm(z), \quad (4.7)$$

where  $G^\pm(z) = (z \pm i\varepsilon - \mathsf{H})^{-1}$  is the Green's operator, which should be defined via the  $i\varepsilon$  prescription and  $\Gamma^\pm(m^2)$  are defined as limits  $\lim_{\varepsilon \rightarrow 0} \Gamma(m^2 \pm i\varepsilon)$ .  $G^\pm(z)$  is not continuous in  $\varepsilon \rightarrow 0$  limit. We define a gap function which represents the discontinuity

$$\Delta\Gamma = \Gamma^+(m^2) - \Gamma^-(m^2) \quad (4.8)$$

as our physical quantity and its imaginary part,  $\text{Im}\Delta\Gamma(m^2)$ , becomes the pair production probability.

If we go to the time-dependent setting, the action in different branches is written as

$$\Gamma^\pm(m^2) = -i \int_0^\infty \frac{dt}{t} e^{\pm im^2 t} \text{Tr} e^{\mp i\mathsf{H}t}, \quad (4.9)$$

where we assumed the  $\varepsilon \rightarrow 0$  limit is already taken in respective branches. Note that it is also possible to analytically continue  $t$  instead of  $m^2$ . This is a much more convenient approach in the time-dependent case and we will adapt it throughout the paper to extract the imaginary contributions by rotating the contour in appropriate directions, i.e. upper half-plane for  $\Gamma^+$  and lower half-plane for  $\Gamma^-$ .

The gap  $\Delta\Gamma(m^2)$  originates from a branch cut of  $\Gamma(m^2)$  on the complex  $m^2$  plane, which is associated to simple poles of the integrand in (4.9) [1]. There is already a pole at  $t = 0$ , which corresponds to the UV divergence in quantum fields theories and through the renormalization procedure, they lead to the energy scale dependence of physical quantities. In non-relativistic quantum mechanics [26], the author showed that  $t = 0$  also acts as a source for the semi-classical expansion which is intimately

related to the perturbative spectrum of the theory. On the other hand, the integrand has other possible singularities at  $t \neq 0$  which will be our focus in this paper.

Note that the time evolution operator in (4.9) indicates that  $\Gamma^\pm$  correspond to effective actions for two different time evolutions, i.e, forward time evolution for  $\Gamma^+$  and backward time evolution for  $\Gamma^-$ . The latter can simply be seen by setting  $t \rightarrow -t$  and re-writing it as

$$\Gamma^-(m^2) = i \int_{-\infty}^0 \frac{dt}{t} e^{im^2 t} \text{Tr} e^{-iHt}. \quad (4.10)$$

Now, the action is described by forward time evolution between  $t = -\infty$  and  $t = 0$ . Moreover, in this form the gap equation in (4.8) becomes

$$\Delta\Gamma(m^2) = -i \int_{-\infty}^{\infty} \frac{dt}{t} e^{im^2 t} \text{Tr} e^{-iHt}, \quad (4.11)$$

which defines an action of transition between infinite past and future. Therefore, (4.11) justifies the definition of the pair production probability as in (4.8) in an unambiguous way. Note that since the integration contour should be rotated in different directions for  $t > 0$  and  $t < 0$ , throughout the paper we will use the integrals defined in (4.9) together with the definition (4.8).

#### 4.2.1. Ambiguity and Its Resolution in Uniform Electromagnetic Background

Before considering general electromagnetic backgrounds, we are going to discuss how the unambiguous pair production rate emerges from the exact effective action in both uniform electric and magnetic backgrounds and precisely show that the real proper time approach leads to unambiguous results, which are consistent with the unitarity condition.

Before addressing the problem in real time, for completeness, let us first look at the imaginary time case and show how the ambiguity arises. The 1 loop effective action

in Euclidean proper time for the bosonic fields in an electromagnetic background is

$$\Gamma(m) = \frac{1}{8\pi^2} \int_0^\infty \frac{ds}{s^3} \frac{e^{-sm^2}(se\mathcal{E})(seB)}{\sin(se\mathcal{E}) \sinh(seB)}. \quad (4.12)$$

Note that in the literature, sometimes the prefactor appears as  $\frac{1}{16\pi^2}$ . The difference is due to  $\frac{1}{2}$  factor in the Hamiltonian (4.6).

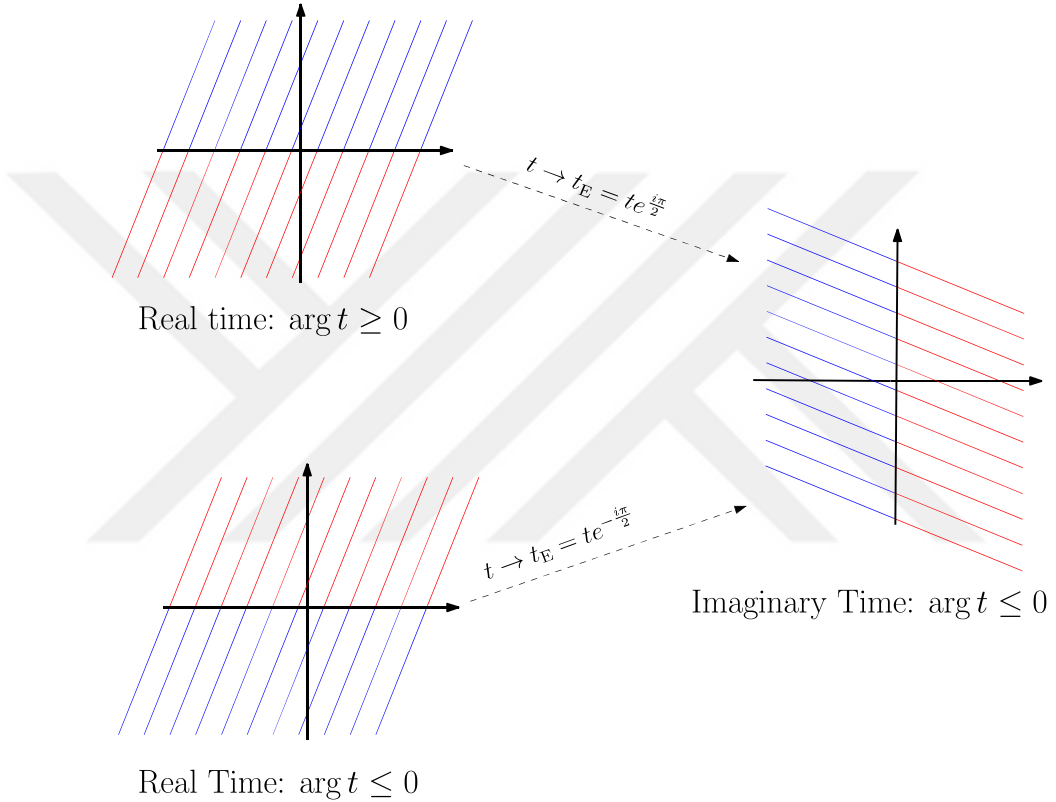


Figure 4.1. Complex  $t$  planes. (Left) Real time cases. (Right) Imaginary time case.

Similar to the real time case that we described above, one can always deform the mass term as  $m^2 \rightarrow m^2 \pm \varepsilon$  and allow complexification of the proper time while keeping the integral finite. However, this is not equivalent to the  $i\varepsilon$  deformation in the real time description and important information, which will allow us to keep unitarity, is lost. The main reason behind this is that when we start with the Euclidean time, the allowed/forbidden regions for forward and backward time evolutions are merged. This is illustrated in Figure 4.1. Therefore, the distinction between forward and backward time evolutions vanishes and the expression (4.12) represents the effective action for both cases. This also prevents from defining the gap  $\Delta\Gamma$  unambiguously as in (4.8).

This shows the origin of the ambiguity in the Euclidean case and why its resolution needs a real time approach.

Let us review the standard picture for the pair production to emphasize its problem. In (4.12), the poles related to the background electric field lie on the real axis at  $t = \pm \frac{n\pi}{e\mathcal{E}}$  while the poles corresponding to magnetic background are on the imaginary axis  $t = \pm i \frac{n\pi}{eB}$ , where  $n \in \mathbb{N}^+$  for both cases. It is possible to compute the imaginary contributions using standard contour integration. Common lore is that the electric poles lead to emergence of  $\text{Im}\Gamma$  while the magnetic ones are not relevant since they do not lie on the integration contour in (4.12).

Consider the contribution of the first electric pole. There are two possible ways to analytically continue which leads to two distinct integration paths, i.e.  $J_0^+$  and  $J_0^-$  as in Figure 4.2. There is no guideline for choosing any of these paths and this leads to complex conjugate results:

$$\text{Im}\Gamma \sim \mp e^{-\frac{m^2\pi}{e\mathcal{E}}}. \quad (4.13)$$

We know that the pair production probability is defined by  $\mathcal{P} \sim 2\text{Im}\Gamma$  and can only be positive. Therefore, we can just choose the result with  $+$  sign in (4.13). However, this is an ad-hoc approach and does not hide the fact that the result is ambiguous. This is equivalent to the Borel ambiguity and as we mentioned it can be overcome by real proper time approach which provides us an ambiguous definition of the pair production probability as we described above.

Let us now return to the real proper time case. The effective action is

$$\Gamma^\pm(m) = \frac{1}{8\pi^2} \int_0^\infty \frac{dt}{t^3} \frac{e^{\pm itm^2}(te\mathcal{E})(teB)}{\sinh(te\mathcal{E}) \sin(teB)}. \quad (4.14)$$

Note that the location of the poles related to electric and magnetic fields exchanged and for both  $\Gamma^\pm$  the possible analytical continuation directions are determined by definition. In the following, for simplicity of discussion, we are going to continue with pure electric field and pure magnetic field backgrounds.

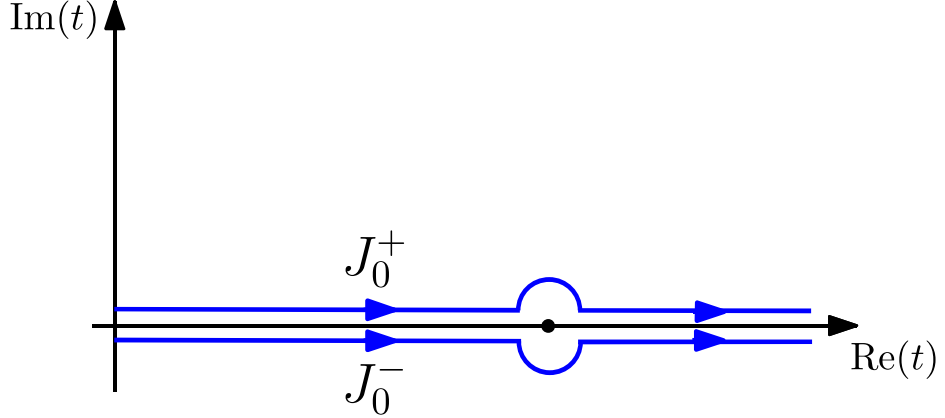


Figure 4.2. Possible paths to probe the singularity on the real axis. This picture describes for the electric poles in the Euclidean case and the magnetic poles in the real time case.

To get the uniform electric background case, let us take  $B \rightarrow 0$  limit. Then, the effective action (4.14) becomes

$$\Gamma^\pm(m) = \frac{1}{8\pi^2} \int_0^\infty \frac{dt}{t^3} \frac{e^{\pm itm^2}(te\mathcal{E})}{\sinh(te\mathcal{E})} \quad (4.15)$$

and the integrand has poles at

$$t_E = \pm \frac{in_E\pi}{e\mathcal{E}} \quad , \quad n_E \in \mathbb{N}^+.$$

While all the poles can be treated collectively, the pair production rate of first particle and anti-particle pair is only linked to the first order non-perturbative term [105, 106]. Therefore, only this part needs to satisfy the unitarity condition without any ambiguity and we will consider the first poles at  $t_E = \pm \frac{i\pi}{e\mathcal{E}}$  in our analysis.

For both  $\Gamma^+$  and  $\Gamma^-$ , both poles at  $\pm \frac{i\pi}{e\mathcal{E}}$  exist in the complex  $t$  plane. However, since the analytical continuation of  $t$  is allowed only in one direction by construction,  $\Gamma^+$  and  $\Gamma^-$  can only get contributions from one of the poles, i.e.,  $+\frac{i\pi}{e\mathcal{E}}$  or  $-\frac{i\pi}{e\mathcal{E}}$  respectively.

First, we consider  $\Gamma^+(m)$ . To get the contribution from the pole at  $\frac{i\pi}{e\mathcal{E}}$ , we simply rotate the contour as in the left of Figure 4.3 and using  $\int_{J_0} + \int_{-J_{\pi/2}} = 0$ , we re-write

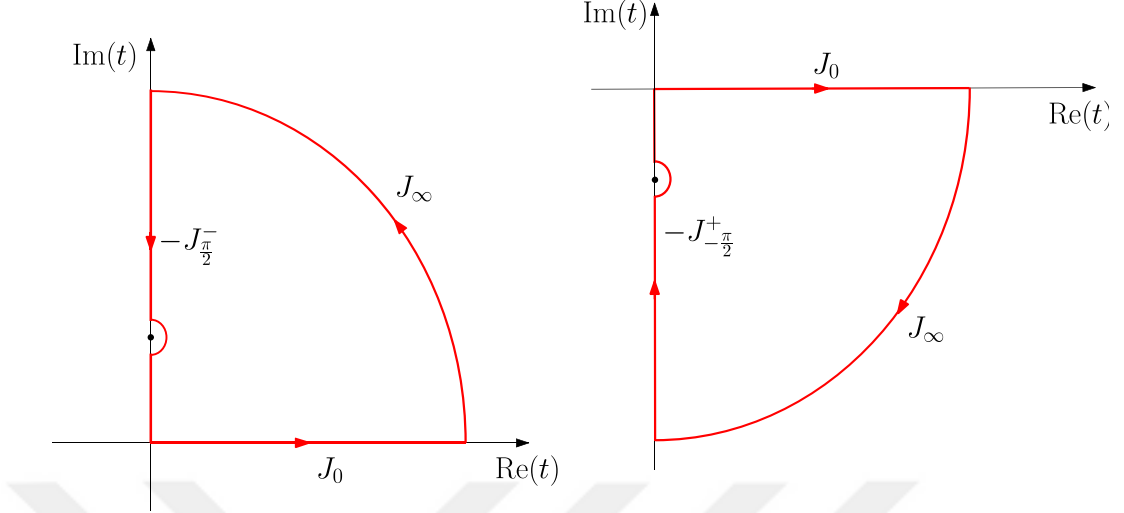


Figure 4.3. Contours for the real time integrals in Electric case. Left: Contours for  $\Gamma^+$ . Right: Contours for  $\Gamma^-$ .

the effective action as

$$\Gamma^+(m^2) = -\frac{eE}{8\pi^2} \int_{J_{\frac{\pi}{2}}^-} \frac{dt}{t^2} \frac{e^{-tm^2}}{\sin(te\mathcal{E})}, \quad (4.16)$$

where  $J_{\pi/2}^-$  corresponds to the contour along the positive imaginary axis with a pre-defined analytical continuation direction. Then, the contour integral in (4.16) leads to the imaginary contribution

$$\text{Im}\Gamma^+(m^2) = +\frac{(e\mathcal{E})^2}{8\pi^2} e^{-\frac{\pi m^2}{e\mathcal{E}}}. \quad (4.17)$$

In the same way, we can extract the imaginary part of  $\Gamma^-(m^2)$  from the pole at  $-\frac{i\pi}{e\mathcal{E}}$ . This time, we rotate the contour as in the right of Figure 4.3 and re-write the effective action as

$$\Gamma^-(m^2) = -\frac{e\mathcal{E}}{8\pi^2} \int_{J_{-\frac{\pi}{2}}^+} \frac{dt}{t^2} \frac{e^{-tm^2}}{\sin(te\mathcal{E})}. \quad (4.18)$$

This is the same integral with only difference is that the direction of the contour  $J_{-\frac{\pi}{2}}^+$  is now along the negative real axis. Then, we get the imaginary part of  $\Gamma^-$  as

$$\text{Im}\Gamma^-(m^2) = -\frac{(e\mathcal{E})^2}{8\pi^2} e^{-\frac{\pi m^2}{e\mathcal{E}}}. \quad (4.19)$$

Combining these two results, we get the imaginary part of the gap

$$\Delta\Gamma(m^2) = \Gamma^+(m^2) - \Gamma^-(m^2),$$

so that the pair production rate as

$$\mathcal{P} = \text{Im}\Delta\Gamma(m^2) = \frac{(e\mathcal{E})^2}{4\pi^2} e^{-\frac{\pi m^2}{e\mathcal{E}}}, \quad (4.20)$$

which recovers the standard pair production probability  $\mathcal{P} \sim e^{-2\text{Im}W}$  with an unambiguous sign. Note that along with the individual results for  $\text{Im}\Gamma^\pm$ , the unambiguous definition of  $\Delta\Gamma$  is also a primary factor for the unambiguous end result. Without this definition, the ambiguity would be persistent in the real time case in the same way with the Euclidean case.

Note that the rotations of the initial contours in both cases are equivalent to respective proper Wick rotations and the resulting integrals are the same with the ones written in the imaginary proper time (4.12). However, since we started with the real time, contrary to the imaginary proper time case, the analytical continuation directions around the poles are pre-determined, so there *can not* be any ambiguity in the signs of the imaginary parts of  $\Gamma^\pm(m^2)$  arising from them. Moreover, with these proper Wick rotations, we can match the Euclidean time contours in Figure 4.2 with the real time contours in Figure 4.3 as  $J_0^- \longleftrightarrow J_{\frac{\pi}{2}}^-$  and  $J_0^+ \longleftrightarrow J_{-\frac{\pi}{2}}^+$ .

Now we will focus on the uniform magnetic case. Although it does not yield pair production, it is important to see how the unambiguous definition of  $\Delta\Gamma$  fits in this case. In  $E \rightarrow 0$  limit, (4.14) reduces to

$$\Gamma^\pm(m^2) = \frac{1}{8\pi^2} \int_0^\infty \frac{dt}{t^3} \frac{e^{\pm itm^2}(teB)}{\sin(teB)}. \quad (4.21)$$

Now the poles are on the real axis and the treatment is similar to the standard Borel integral. However, again as in the electric background case, the restriction on the analytical continuation directions for both  $\Gamma^+$  and  $\Gamma^-$  prevents ambiguous results. Taking the integrals using the appropriate contours as pictured in Figure 4.2, we find

the gap  $\Delta\Gamma(m) = \Gamma^+(m) - \Gamma^-(m)$  due to the pole at  $t_B = \frac{\pi}{eB}$  as

$$\Delta\Gamma = \frac{eB}{8\pi^2} \left[ (-i\pi) \frac{(eB)}{\pi^2} e^{\frac{i\pi m^2}{eB}} - (+i\pi) \frac{eB}{\pi^2} e^{-\frac{i\pi m^2}{eB}} \right] = i \frac{(eB)^2}{4\pi^3} \cos\left(\frac{\pi m^2}{eB}\right). \quad (4.22)$$

The gap is again imaginary with a sign that keeps the theory unitary but now it represents an oscillatory contribution. This is fine as the oscillatory behaviour indicates that the stable vacuum is alive and there are successive particle creations and annihilations as expected from any relativistic quantum theory but effectively this process leads to no pair creation at the end of the scattering process. Therefore, there is no need for the cancellation of this contribution by Bogomolny Zinn-Justin mechanism.

### 4.3. Unambiguous Pair Production from Perturbative Expansions

In physics, exact solutions are very rare. Therefore, while the discussion in Section 4.2.1 explicitly show how the pair production rate in the presence of a uniform electromagnetic field emerges in a way that the unitarity is preserved, it is also important to show how the same information can be achieved when an exact solution is not possible.

In absence of an exact solution, perturbative techniques allow us to compute the coefficients in a perturbation series, which form generically divergent series. The non-perturbative information is encoded in this divergent series and can be extracted using Borel-Pade techniques [73, 107–109]. However, the Borel-Pade summation leads to the same ambiguity that we discussed in the Euclidean case in the previous section and whenever there is a persistent instability of the vacuum. As in the uniform case, to get an unambiguous result, we will use the real time approach and probe the poles of the propagator directly, i.e. we need to sum the perturbative expansion of the propagator  $U(t) = \text{Tr}e^{\pm itH}$  in (4.9) before taking the proper time integral.

For this reason, we are going to adapt the recursive perturbative scheme introduced in [26] which is based on the construction in [62, 63] to problems with background gauge potentials. In [26], it was shown that the non-commutativity of phase-space vari-

ables acts as a source for a derivative expansion which is identified as the semi-classical expansion. In the present context, the non-commutativity again produces a derivative expansion which corresponds to the deviation from the uniform field <sup>4</sup>. At each order of the derivative expansion, there is also another expansion which depends on the electromagnetic field strength and using this one the non-perturbative pair production probability at each order in the derivative expansion can be obtained. Note that this approach has already been applied to an exactly solvable case in [72]. The perturbative scheme we will present in this section provides a generalization of this result to arbitrary strongly coupled background potentials in arbitrary dimensions.

In this section, we will investigate pure electric fields. The Hamiltonian is written in general as

$$H = -\frac{1}{2}(p_0 - eA_0(\mathbf{x}))^2 + \frac{1}{2}(\mathbf{p} - e\mathbf{A}(x_0))^2 \equiv -\frac{1}{2}\pi_0^2(p_0, \mathbf{x}) + \frac{1}{2}\boldsymbol{\pi}^2(\mathbf{p}, x_0). \quad (4.23)$$

We assume that the gauge potential has the following form

$$A_\mu(x_0, \mathbf{x}) = -\frac{\mathcal{E}}{\omega} (H_0(\omega \mathbf{x}), \mathbf{H}(\omega x_0)), \quad (4.24)$$

so that the electric field is  $\mathbf{E} = \mathcal{E} \left( \frac{d\mathbf{H}(x_0)}{dx_0} + \nabla H_0(\omega \mathbf{x}) \right)$ . Since we are mainly interested in the locally uniform fields, we assume that both  $H_0(\omega \mathbf{x})$  and  $\mathbf{H}(\omega x_0)$  are slowly varying functions of  $\mathbf{x}$  and  $x_0$  respectively. For the same reason, we also assume that  $m^2 \gg e\mathcal{E} \gg \omega$  throughout this section. This will guide us in our calculations.

The effective action for the Hamiltonian in (4.23) is written as

$$\Gamma^\pm(m^2) = -i \int_0^\infty \frac{dt}{t} e^{\pm im^2 t} \int \frac{dp_0 d\mathbf{p}}{(2\pi)^4} \langle p_0, \mathbf{p} | e^{\mp it(-\frac{1}{2}\pi_0^2(p_0, \mathbf{x}) + \frac{1}{2}\boldsymbol{\pi}^2(\mathbf{p}, x_0))} | \mathbf{p}, p_0 \rangle. \quad (4.25)$$

Note that since  $\pi_0$  and  $\boldsymbol{\pi}$  do not commute with each other, the propagator does not factorize trivially. To get the perturbative expansion, we can either redefine the prop-

---

<sup>4</sup>Although, the derivative expansion we will consider in this paper is not the semi-classical expansion as in [26], these two expansions are related to each other with a redefinition of expansion parameters. See e.g. [110].

agator  $U(t) = \text{Tr} e^{\mp itH}$  as

$$U(t) = e^{\pm \frac{it\pi_0^2}{2}} \tilde{U}(t) \quad \text{or} \quad U(t) = e^{\mp \frac{it\pi^2}{2}} \tilde{U}(t). \quad (4.26)$$

As shown in [26], both choices are equivalent. Solving the time dependent Schrodinger equation for redefined propagators and following the steps in [26], we reach a recursive expansion for  $\tilde{U}(t)$  for each case and express the effective action in terms of this recursive expansion.

Let us consider pure time dependent and pure space dependent electric fields. For the time dependent case, where  $A_0(\mathbf{x}) = 0$  and  $\pi_0 = p_0$ , the perturbative expansion is written as

$$\Gamma_{\text{time}}^{\pm}(u) = -i \sum_{m=0}^{\infty} \int_0^{\infty} \frac{dt}{t} e^{\pm im^2 t} \int \frac{dp_0 dx_0 d^3 p}{(2\pi)^4} e^{\mp \frac{i\pi^2 t}{2}} \sum_{k=1}^m \tilde{U}_{m,k}^{\pm}(t) e^{\mp \frac{ip_0^2 t}{2}}, \quad (4.27)$$

where  $\tilde{U}^{\pm}$  is given by the recursion relation

$$\tilde{U}_{m,k}^{\pm}(t) = \sum_{l=1}^{m-k+1} \frac{\hbar^l}{l!} \frac{\partial^l \boldsymbol{\pi}^2}{\partial x_0^l} \int_0^t dt_1 \mathbf{b}_{\pm}^l(p_0, \partial_{p_0}, t_1) \tilde{U}_{m-l,k-1}^{\pm}(t_1), \quad (4.28)$$

with the initial value  $\tilde{U}_{0,0}^{\pm} = 1$  and the operator valued function

$$\mathbf{b}_{\pm}(p_0, \partial_{p_0}, t_i) = i\partial_{p_0} \pm p_0 t_i \mp p_0 t. \quad (4.29)$$

Note that equations (4.27) - (4.29) indicate that the problem is effectively a one dimensional one regardless the details of the background gauge field.

If the background field, on the other hand, is space dependent, then the problem might be a multi-dimensional one. In this case,  $\mathbf{A}(x_0) = 0$ ,  $\boldsymbol{\pi} = \mathbf{p}$  and the perturbative expansion becomes

$$\Gamma_{\text{space}}^{\pm}(u) = -i \sum_{m=0}^{\infty} \int_0^{\infty} \frac{dt}{t} e^{\pm im^2 t} \int \frac{dp_0 d^3 p d^D \mathbf{x}}{(2\pi)^4} e^{\mp \frac{i\pi_0 t}{2}} \sum_{k=1}^m \tilde{U}_{m,k}^{\pm}(t) e^{\mp \frac{i\mathbf{p}^2 t}{2}}, \quad (4.30)$$

where  $\tilde{U}^\pm$  is

$$\tilde{U}_{m,k}^\pm(t) = \sum_{l=1}^{m-k+1} \frac{\hbar^l}{l!} \nabla^l \pi_0^2 \int_0^t dt_1 \mathbf{b}_\pm^l(\mathbf{p}, \nabla_{\mathbf{p}}, t_1) \tilde{U}_{m-l, k-1}^\pm(t_1), \quad (4.31)$$

with  $\tilde{U}_{0,0}^\pm = 1$  and

$$\mathbf{b}_\pm(\mathbf{p}, \nabla_{\mathbf{p}}, t_i) = i \nabla_{\mathbf{p}} \pm \mathbf{p} t_i \mp \mathbf{p} t. \quad (4.32)$$

Note that the dimension  $D$  of the space integral depends on the dimensionality of  $A_0(\mathbf{x})$ . Even though it does not change the general structure of pair production probability, it plays a role in prefactors. We will elaborate this, when we discuss the space dependent fields.

Equations (4.28) and (4.31) shows that the expansion is a semi-classical one. However, in this section, we set  $\hbar = 1$ , since the only expansion parameters we are interested in are  $\omega$  and  $e\mathcal{E}$ . When the pair production problem is considered as a semi-classical approximation after redefining parameters  $\hbar, \omega, e\mathcal{E}$ , the pair production probability is given by the classical action, i.e.  $\hbar^0$  term in (4.27) and (4.30) [110]. We will use this information Section 4.4, when we compare our method to the semi-classical approaches.

Using the recursive formula, we can now compute the perturbative expansion of the integrand  $\frac{\text{Tr} e^{\mp itH}}{t}$  in powers of  $\omega$  and  $g = e\mathcal{E}$ . This is a double expansion which is formally expressed as

$$\frac{\text{Tr} e^{\mp itH}}{t} = \sum_{m,n} \alpha_{m,n}(t) \omega^{2m} g^{2n}. \quad (4.33)$$

The poles of the integrand at  $t \neq 0$  are related to the summation of this double series. This poses a problem of summation order. The order of summation should be chosen according to the dominance of the expansion variables  $\omega$  and  $g$ . Since  $m \gg g \gg \omega$  while summing the series in (4.33), we keep the order of  $\omega$  constant and sum over the  $g$  expansion.

In the following, we will analyze general time dependent and space dependent cases in 4 dimensional space-time dimensions and compute the leading order non-perturbative pair production probability, which is obtained from the series at  $O(\omega^0)$ , while postponing the analysis of corrections to this leading order for the future.

#### 4.3.1. Time Dependent Electric Fields:

We first consider time dependent electric fields for

$$\mathbf{A}(x_0) = \frac{\mathcal{E}}{\omega} \mathbf{H}(\omega x_0). \quad (4.34)$$

As we stated above, this is effectively a one-dimensional problem. Although this has already been treated by the exact WKB method [91], here using the recursion relation and the Pade summation of perturbative expansion of the propagator, we will obtain unambiguous version of the pair production probability.

Using the recursion formula (4.28), we compute the expansion at order  $O(\omega^0)$  up to  $x_0$  integral:

$$\sum_{n=0} \alpha_{0,n} g^{2n} = \frac{1}{4\pi^2 i t^3} \left[ 1 - \frac{(gt\mathbf{H}')^2}{24} + \frac{7(gt\mathbf{H}')^4}{5760} - \frac{31(gt\mathbf{H}')^6}{967680} + \frac{127(gt\mathbf{H}')^8}{154828800} + \dots \right], \quad (4.35)$$

where  $\mathbf{H}' = \frac{d\mathbf{H}(\omega x_0)}{dx_0}$ . In (4.27), before integrating over  $\mathbf{p}$ , we rescaled the momentum as  $\mathbf{p} \rightarrow \mathbf{p} + \mathbf{A}(x_0)$  and in this way, all momentum integrals become Gaussian. Note that due to the sign change in Lorentzian metric, prefactor of the Gaussian integrals comes up as  $\frac{1}{(\sqrt{2\pi i t})^3 \sqrt{-2\pi i t}} = \frac{1}{4\pi^2 i t^2}$  rather than standard prefactor of 4 dimensional Gaussian integrals  $\left(\frac{1}{\sqrt{2\pi i t^2}}\right)^4 = -\frac{1}{4\pi^2 t^2}$ . Overall imaginary factor is important as it contributes to the effective action directly.

Note that first two terms in the expansion are singular at  $t = 0$ . They correspond to the UV divergent terms and can be treated by renormalization. On the other hand, from the spectral theory point of view, this singularity contains the information about

the perturbative part of the quantized spectrum [26]. In this context, the gap,  $\Delta\Gamma$ , associated to the singularity at  $t = 0$  corresponds to the perturbative part of the quantum action, which is also known as the WKB action. The perturbative expansion of the action can be obtained by order by order integration of the terms which are singular at  $t = 0$ . In one dimensional problems, it is known that imposing the Bohr-Sommerfeld quantization condition to this expansion would lead to the perturbative spectrum of the theory [13, 16].

On the other hand, the series consists of the non-singular terms in (4.35) is associated to singularities at  $t \neq 0$  upon their summation. Note that this series is a convergent one. It becomes divergent if we take the proper time integral directly. This is in fact the divergence predicted by Dyson in [6] and it would need to be treated by the Borel procedure. Instead, similar to the uniform case in Section 4.2.1, it is possible to probe the singularity structure represented by this series directly by using the Pade summation before taking the proper time integral.

Apparently, the nature of these poles are quite different, one at  $t = 0$  is associated to the perturbative information, while the other at  $t \neq 0$  contains non-perturbative information. We will elaborate this separation and investigate their nature in Section 4.4.1. Now we turn back to our discussion on the extracting pair production probability for arbitrary background potentials.

It is possible to ignore them in Pade approximation when probing the poles at finite  $t$ , however, we observe that they play a role in the constant part of the prefactor of the effective action. Although it does not have a physical implication, we prefer to keep them in the calculations for completeness. Then, we write the effective action at order  $O(\omega^0)$  as

$$\Gamma_{\omega^0}^{\pm} = - \int_{\mathbb{R}} dx_0 \int_0^{\infty} \frac{dt e^{\pm im^2 t}}{4\pi^2 t^3} \sum_{n=0} \alpha_{0,n} (gt\mathbf{H})^{2n}. \quad (4.36)$$

Pade summation of term up to  $O(g^{26})$  leads non-zero singularities at

$$g\mathbf{H}'t_\star = \pm\pi \{1.0000i, 2.0000i, 2.9994i\}. \quad (4.37)$$

As we indicated in the previous section, only the first pole is linked to the pair production probability. Therefore, we express the effective action as

$$\Gamma_{\omega^0}^\pm \simeq - \int_{\mathbb{R}} dx_0 \int_0^\infty \frac{dt e^{\pm im^2 t}}{4\pi^2 t^3} \frac{1}{(i\pi)^2 - (g\mathbf{H}'t)^2}. \quad (4.38)$$

As in the uniform case, we compute the imaginary parts by rotating the initial contour for  $t$  integral in appropriate directions as in Figure 4.3. Then, we find the imaginary part as

$$\text{Im}\Gamma_{\omega^0}^\pm(m^2) = \pm \int_{\mathbb{R}} dx_0 \frac{(g\mathbf{H}'(\omega x_0))^2}{8\pi^3} e^{-\frac{m^2\pi}{g\mathbf{H}'(\omega x_0)}}. \quad (4.39)$$

This form of the effective action at the leading order of the derivative expansion is already known as local field approximation [111, 112] and can be evaluated for specific cases for  $\mathbf{H}'$  (See e.g. [72]). Instead, we handle the integral by saddle point approximation, which is possible since  $m \gg g$  and  $\mathbf{H}(\omega x_0)$  is chosen to be slowly varying. For this reason, we make the following general assumptions for  $\mathbf{H}$  around the saddle point:

$$i) \mathbf{H}'(\omega x_0^*) = \mathbf{h}_0 \quad , \quad ii) \mathbf{H}''(\omega x_0^*) = 0 \quad , \quad iii) \mathbf{H}'''(\omega x_0^*) = -\mathbf{h}_2\omega^2, \quad \mathbf{h}_2 \neq 0, \quad (4.40)$$

where second assumption simply follows from the saddle point approximation while first one states that electric field  $\mathbf{E}$  is constant, i.e. independent of  $\omega$ , at the saddle point  $x_0^*$  so the field is locally uniform as we assumed at the beginning. Finally, third assumption indicates deviation from the uniform case while assuring the saddle point  $x_0^*$  is non-degenerate and  $\mathbf{h}_2$  is a constant differs for different backgrounds. With these assumptions, we get the leading order pair production probability as

$$\Delta\Gamma_{\omega^0}(m^2) \simeq \frac{\sqrt{2} (|\mathbf{h}_0|g)^{5/2}}{4\pi^3 m |\mathbf{h}_2|^{1/2} \omega} e^{-\frac{m^2\pi}{|\mathbf{h}_0|g}}, \quad (4.41)$$

where  $\mathbf{h}_0$  and  $\mathbf{h}_2$  can be determined for specific background fields.

### 4.3.2. Space Dependent Electric Fields:

Now, we will consider space-dependent pure electric backgrounds for

$$A_0(\mathbf{x}) = \frac{\mathcal{E}}{\omega} H_0(\omega \mathbf{x}). \quad (4.42)$$

Since the effective dimensionality of this case depends on the details of the function  $H_0$ , its treatment with WKB methods is not always tractable. Therefore, the (proper) time dependent method we present here is much more convenient for applications.

Using the recursive relations (4.28), we get the coupling expansion at order  $O(\omega^0)$  as

$$\sum_{n=0} \alpha_{0,n} g^{2n} = \frac{1}{4\pi^2 i t^3} \left[ 1 - \frac{(gt \nabla H_0)^2}{24} + \frac{7(gt \nabla H_0)^4}{5760} - \frac{31(gt \nabla H_0)^6}{967680} + \dots \right]. \quad (4.43)$$

This is the same expansion in (4.35) up to space dependence via  $\nabla H_0$  terms. Then, the singularities of the integrand in (4.30) is the same as in the time dependent case and we get the imaginary parts of  $\Gamma_{\omega^0}^{\pm}$  as

$$\text{Im}\Gamma_{\omega^0}^{\pm}(m^2) = \pm \int_{\mathbb{R}^D} d^D x \frac{(g \nabla H_0(\mathbf{x}))^2}{8\pi^3} e^{-\frac{m^2 \pi}{g \nabla H_0}}. \quad (4.44)$$

We make assumptions similar to (4.40):

$$i) \nabla H_0(\omega \mathbf{x}^*) = h_0, \quad ii) \nabla^2 H_0(\omega \mathbf{x}^*) = 0, \quad iii) \nabla^3 H_0(\omega \mathbf{x}^*) = -h_2 w^2, \quad h_2 \neq 0. \quad (4.45)$$

The dimensionality play a role in the saddle point approximation as it determines the dimension of the space integral. In general, the saddle point approximation of (4.44) for  $m \gg g$  and slowly varying  $H_0(\omega \mathbf{x})$  leads to

$$\Delta\Gamma_{\omega^0} \simeq \frac{(gh_0)^2}{8\pi^3} \left( \frac{2\pi gh_0}{m^2 \omega^2 \pi h_2} \right)^{D/2} e^{-\frac{m^2 \pi}{gh_0}}, \quad (4.46)$$

where  $D = 1, 2, 3$  depends on the function  $H_0(\omega \mathbf{x})$ . Note that when  $D = 1$ , we recover (4.41).

#### 4.4. Connection to Semi-Classics

The strong field pair production is a non-perturbative effect and it has been studied by more direct non-perturbative methods, such as WKB and worldline instantons. These methods are semi-classical in nature and relate the pair production process to the underlying classical dynamics of the quantum mechanical system. Here we will explain the connection between these non-perturbative pictures and the real time approach we are using. In this way, we will explain the following:

- A duality between magnetic and electric cases in terms of perturbative and non-perturbative WKB cycles.
- The resolution of the ambiguity problem from a path integral point of view.

For concreteness, in this section, we focus on a specific problem and choose the alternating electric and magnetic fields in  $x_3$  direction, i.e.

$$A_\mu = \left( 0, 0, 0, -\frac{\mathcal{E}}{\omega} \sin(\omega x_0) \right) \quad (4.47)$$

for the electric case and

$$A_\mu = \left( 0, 0, -\frac{\mathcal{E}}{\omega} \sin(\omega x_1), 0 \right) \quad (4.48)$$

for the magnetic case. In addition we keep  $p_0$  for the electric case and  $p_1$  for the magnetic case and set the other components of momenta to zero as they only play a role in the prefactor. Then, the corresponding Hamiltonians are written as

$$H_E = -\frac{p_0^2}{2} + \frac{g_E^2}{2\omega^2} \sin^2(\omega x_0) \quad , \quad g_E = e\mathcal{E} \quad (4.49)$$

for the electric case and

$$H_B = \frac{p_1^2}{2} + \frac{g_B^2}{2\omega^2} \sin^2(\omega x_1) \quad , \quad g_B = e\mathcal{B} \quad (4.50)$$

for the magnetic case. The semi-classical aspects of this system are well studied in both worldline formalism [74,75] and WKB formalism [85,110]. In fact, in these settings, the exponent of the pair production probability is just the classical action of the system,

i.e.  $S_0 \sim \frac{m^2\pi}{eE}$ . In the following, for simplicity, we will set  $g = \sqrt{2}$  and  $\omega = 1$ , as they don't play a role in the following discussion.

Recall from (4.27), (4.30) and (4.28), (4.31) that the classical actions for electric and magnetic backgrounds are respectively

$$\begin{aligned}\Gamma_E^\pm &= -i \int_0^\infty \frac{dt}{t} e^{\pm im^2 t} \int \frac{dx_0 dp_0}{2\pi} e^{\mp it \sin^2(x_0)} e^{\pm \frac{ip_0^2 t}{2}} \\ &= -i \int_0^\infty \frac{dt}{t\sqrt{\mp 2\pi it}} e^{\pm im^2 t} \int_{\mathbb{R}} dx_0 e^{\mp it \sin^2(x_0)}\end{aligned}\quad (4.51)$$

and

$$\begin{aligned}\Gamma_B^\pm &= -i \int_0^\infty \frac{dt}{t} e^{\pm im^2 t} \int \frac{dx_1 dp_1}{2\pi} e^{\mp it \sin^2(x_1)} e^{\mp \frac{ip_1^2 t}{2}} \\ &= -i \int_0^\infty \frac{dt}{t\sqrt{\pm 2\pi it}} e^{\pm im^2 t} \int_{\mathbb{R}} dx_1 e^{\mp it \sin^2(x_1)}.\end{aligned}\quad (4.52)$$

These integrals will be the basis of the following discussion on WKB and path integral approaches.

#### 4.4.1. Duality from WKB Cycles:

In order to see the equivalence to the standard WKB integrals, we first take the  $t$  integral after rotating its contour by  $\pm\frac{\pi}{2}$ . Then, we find

$$\Delta\Gamma_B(m^2) = \sqrt{2} \oint dx_1 \sqrt{m^2 - \sin^2(x_1)} \quad (4.53)$$

and

$$\Delta\Gamma_E(m^2) = i\sqrt{2} \oint dx_0 \sqrt{m^2 - \sin^2(x_0)}. \quad (4.54)$$

In these expressions, the main difference between the electric and magnetic cases is the imaginary prefactor. In fact, (4.53) and (4.54) can be thought as action and dual action of the same theory which are intimately related [47, 49–52]. To see the duality clearly, let us take the imaginary factor in (4.54) into the square root term and express

it as

$$\begin{aligned}\Delta\Gamma_E(m^2) &= \sqrt{2} \oint dx_0 \sqrt{-m^2 + \sin^2(x_0)} \\ &= \sqrt{2} \oint dx_0 \sqrt{\tilde{m}^2 - \cos^2(x_0)},\end{aligned}\quad (4.55)$$

where  $\tilde{m}^2 = 1 - m^2$ . Because of the phase difference between  $\sin^2(x)$  and  $\cos^2(x)$ , the perturbative and non-perturbative WKB cycles in electric and magnetic cases exchange.

This observation suggests us that the actions  $\Delta\Gamma_B$  and  $\Delta\Gamma_E$  can be expressed as WKB actions of different cycles of the potential  $V(x) = \sin^2(x)$ . We will denote these actions as  $a(u)$  and  $a_D(u)$  with the following definitions:

$$a(u) = \sqrt{2} \oint_\alpha dx \sqrt{u - \sin^2(x)}, \quad (4.56)$$

$$a_D(u) = \sqrt{2} \oint_\beta dx \sqrt{u - \sin^2(x)}, \quad (4.57)$$

where integration cycles  $\alpha$  and  $\beta$  corresponds to WKB cycles at the valley and barrier of the potential respectively. In this way, we have reached the tunneling interpretation of the pair production problems. Now, the pair production probability is related to the imaginary part of the dual action as  $\mathcal{P} \sim \exp \left[ -\frac{1}{g} \text{Im} a_D(u) \right] = \exp \left[ -\frac{1}{\sqrt{2}} \text{Im} a_D(u) \right]$ .

Using the identity [113]

$$\int_0^{\arcsin \sqrt{x}} d\theta \frac{\cos((2n-1)\theta)}{\sqrt{x - \sin^2 \theta}} = \frac{\pi}{2} {}_2F_1\left(1-n, n; 1, x\right), \quad (4.58)$$

and integrated it once, we compute  $a(u)$  and  $a_D(u)$  as

$$a(u) = 4\sqrt{2} \left\{ \mathbb{E}(u) + (u-1)\mathbb{K}(u) \right\} = \pi\sqrt{2} u {}_2F_1\left(\frac{1}{2}, \frac{1}{2}; 2, u\right) \quad (4.59)$$

and

$$a_D(u) = i 4\sqrt{2} \left\{ \mathbb{E}(1-u) - m^2 \mathbb{K}(1-u) \right\} = i\pi\sqrt{2} (1-u) {}_2F_1\left(\frac{1}{2}, \frac{1}{2}; 2, 1-u\right), \quad (4.60)$$

where  $\mathbb{K}$  and  $\mathbb{E}$  are complete elliptic integrals and to obtain the action in terms of

hypergeometric function we have used the following identities [66]:

$$\mathbb{K}(k^2) = \frac{\pi}{2} {}_2F_1\left(\frac{1}{2}, \frac{1}{2}; 1; k^2\right) , \quad \mathbb{E}(k^2) = \frac{\pi}{2} {}_2F_1\left(-\frac{1}{2}, \frac{1}{2}; 1; k^2\right) \quad (4.61)$$

and

$$k^2(c-b) {}_2F_1(a, b; c+1; k^2) = c {}_2F_1(a-1, b; c; k^2) + c(z-1) {}_2F_1(a, b; c; k^2). \quad (4.62)$$

Note that up to the imaginary prefactor, the actions in (4.59) and (4.60) are related to each other by modular transformation  $m^2 \rightarrow 1 - m^2$  and this is indeed how a perturbative WKB action is transformed to its dual, which is associated to the non-perturbative information, for genus 1 potentials [47].

To understand how this perturbative/non-perturbative information is related to the time dependent formalism and the singularities of the propagator, let us expand  $a(u)$  for  $u \ll 1$ :

$$\frac{1}{\pi\sqrt{2}} a(u \ll 1) = u + \frac{u}{8} + \frac{3u}{64} + \frac{25u}{1024} + \frac{245u}{16384} + \dots \quad (4.63)$$

This is the action of the cycles corresponding to the wells of the potential  $V(x) = \sin^2(x)$  [13, 16, 67]. If we were stuck with the time dependent formalism, we would find the same expansion<sup>5</sup> by probing the singularity at  $t = 0$  in (4.52) and following the guidelines in [26].

On the other hand, in order to relate the electric action to the pair production probability for strongly coupled electric fields, we expand  $a_D(u)$  around  $u = 1$ :

$$\frac{1}{i\pi\sqrt{2}} a_D(u \sim 1) = -(u-1) + \frac{1}{8}(u-1)^2 - \frac{3}{64}(u-1)^3 + \frac{25}{1024}(u-1)^4 + \dots \quad (4.64)$$

Then, with the identification  $m^2 = 1 - u$ , we get the pair production probability as

$$\mathcal{P} \sim \exp[-m^2\pi],$$

which matches with the result in (4.41) for  $g = \sqrt{2}$ . This is what we get from the

---

<sup>5</sup>Note that same expansion with alternating signs would have been obtained from (4.51). This would corresponds to the perturbative action for the region under the barrier.

non-zero singularity of the propagator in Section 4.3 and our analysis identifies this non-perturbative singularity with the dual action at the peak of the barrier.

In summary, these results shows that the observation that  $\Delta\Gamma_B/\Delta\Gamma_E$  correspond to the valley/peak of the potential. This shows a duality between electric and magnetic cases. Another way to understand this duality is making the observation that the electric potential corresponds to the inverted magnetic potential with an unimportant scaling. The connection between inverting the potential and the duality was investigated in [51] using the connection between one dimensional quantum mechanics and holomorphic anomaly equations, where the authors showed that the analysis for the dual case is done around the top of the inverted potential. In our setting, the source of this inversion, and therefore the duality, is the Minkowskian metric. Moreover, this observation shows that the perturbative analysis in Section 4.3 was done around the dual (non-perturbative) vacuum which corresponds to the top of the inverted potential.

Note that this is known for the uniform case as the uniform electric field background corresponds to the inverted harmonic oscillator. However, our description indicates that this is also valid for more general background potentials. Although, we used simple  $\cos^2(x) = 1 - \sin^2(x)$  relationship in (4.55) and re-scaled  $m^2 \rightarrow 1 - m^2$ , these transformations have a geometric origin related to the duality between the two action and similar transformations can be used for other potentials to relate WKB action and its dual. A detailed discussion can be found in [52]. We will use this information in our analysis of the path integral perspective.

#### 4.4.2. Non-cancellation from Lefschetz Thimbles:

Now, turning back to the integrals in (4.51) and (4.52), we will show how the imaginary contributions for electric and magnetic cases arises from path integral perspective. Note that in (4.51) and (4.52), the space integrals are one dimensional not infinite dimensional. This is not introduced for any simplification; instead, they correspond to the exact leading order in the derivative expansion of the theory.

The space integral is the same for both magnetic and electric cases:

$$I^\pm = \int_{\mathbb{R}} dx e^{\mp it \sin^2(x)}, \quad (4.65)$$

where we set  $g = \omega = 1$  as they don't play a role in the following discussion. Note that this integral form was investigated in [17] in a finite region and the cancellation of the Borel ambiguity was explained. Their analysis corresponds to the imaginary proper time version of our discussion. We will follow similar arguments for (4.65) but also use the lessons of previous sections which will lead us to the resolution of the ambiguity. Then, at the end of the section, we will compare these two analyses.

The critical point is on the initial contour, the integral in (4.65) is not convergent due to the oscillating behaviour of its exponent. To prevent this problem, we should express this path integral in terms of paths which behaves as  $e^{-t \sin^2(x)}$  as  $|x| \rightarrow \infty$ . Among all possible such paths, we will choose the steepest descent ones since they have the most dominant contributions. In the following, we will label these paths with  $\mathcal{J}$  and we will label the other paths, which don't converge exponentially as  $|x| \rightarrow \infty$ , with  $\mathcal{K}$ . These are called the Lefschetz thimbles and they are closely related to the Morse theory. We will not discuss their construction since we are only interested in their roles in cancellation mechanism in the pair production problems. For details on the subject see [114, 115].

Due to the periodic nature of the potential, we can focus only on the region  $[-\frac{\pi}{2}, \frac{\pi}{2}]$  and investigate contribution of the paths passing through the extremum point  $x = 0$ , which represents stable/unstable vacuum of theory, to the integral (4.65) for different values of  $\arg t$ . Remember that for electric and magnetic cases, the singularities on the complex proper time plane appear in different regions and we needed to deform the proper time integral accordingly. We will use this information here as our guide to investigate the behaviour of the spatial integral on complex  $x$  plane and in this way, we will describe the resolution of the ambiguity in path integral perspective.

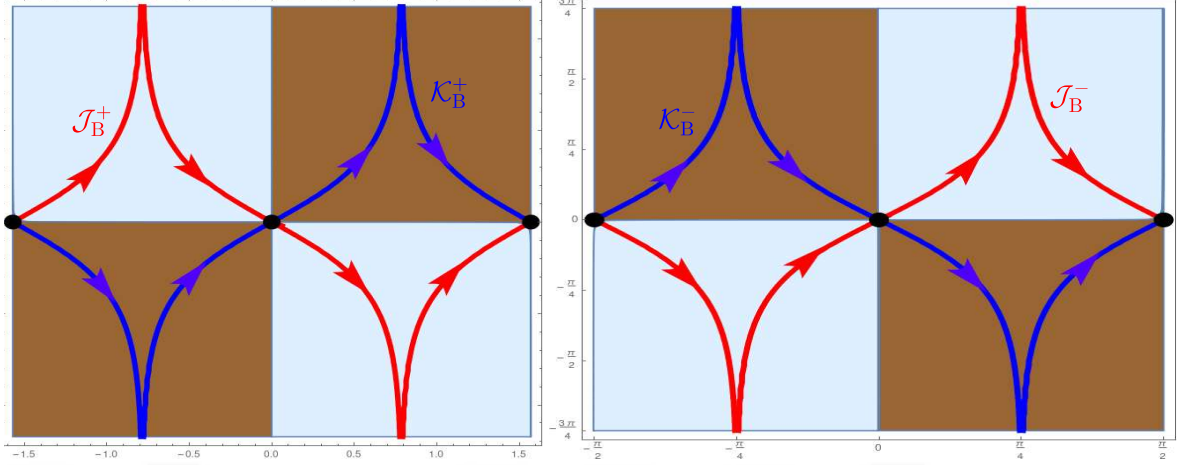


Figure 4.4. Lefschetz thimbles for the magnetic case.

Let us start with the magnetic field background. We know that in this case, the non-perturbative information arises from  $\arg t = 0^\pm$  for  $\Gamma^\pm(m^2)$ . Since the integrands have oscillating behaviours in both cases, the real part of the exponent should be constant along the integration path:

$$\text{Re } \sin^2(x) = \text{const.} \quad (4.66)$$

The imaginary parts should behave differently along these paths due to the sign difference in the exponent. Therefore, as  $|x| \rightarrow \infty$ , the conditions

$$\text{Im } [t \sin^2(x)] < 0 \quad (4.67)$$

for  $\arg t = 0^+$  and

$$\text{Im } [t \sin^2(x)] > 0 \quad (4.68)$$

for  $\arg t = 0^-$  should be satisfied. Corresponding regions and associated contours  $\mathcal{J}_B^\pm$  and  $\mathcal{K}_B^\pm$  are shown in Figure 4.4. Despite the allowed paths are different for two cases, their tails directing to imaginary infinities cancel each other. Therefore, both of the are well defined and the remaining parts are just the original integral (4.65). Moreover, the gap  $\Delta\Gamma_B = \Gamma_B^+ - \Gamma_B^-$  corresponds to the perturbative WKB cycle. All of these are consistent with the expected oscillatory behaviour.

Now, we turn to the electric field background and focus on the behaviour of the integrals around  $\arg t = \pm \frac{\pi}{2}$ . Around these regions, the spatial integral becomes

$$\mathcal{I}^\pm = \int_{\mathbb{R}} dx e^{t \sin^2(x)}, \quad (4.69)$$

which can be interpreted as inverted potential case.

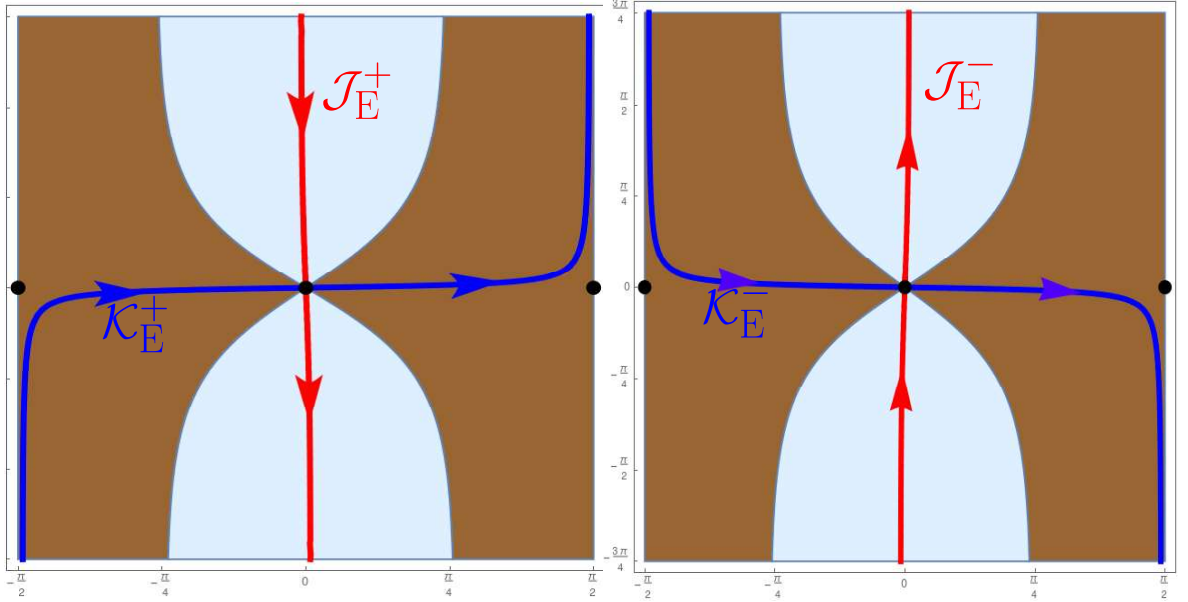


Figure 4.5. Lefschetz thimbles for the electric case.

The integrand in (4.69) is real. Then, in this case, the imaginary part should be constant along the integration contour, i.e.  $\text{Im } \sin^2(x) = \text{const}$ . In both cases, as  $|x| \rightarrow \infty$ , the integration paths should pass through regions corresponding to

$$\text{Re } [t \sin^2(x)] < 0. \quad (4.70)$$

The integration paths  $\mathcal{J}_E^\pm$  and  $\mathcal{K}_E^\pm$  are shown in Figure 4.5. Contrary to the magnetic case, here the allowed regions are the same and the Lefschetz thimbles pass through the same regions in opposite directions. Therefore, their contribution to  $\Delta\Gamma = \Gamma_E^+ - \Gamma_E^-$  is a constructive one rather than a destructive one as we observed in Sections 4.2.1 and 4.3. This explains the ambiguity resolution from a geometric perspective.

These two examples are illustrations of how real time approach resolves the Borel ambiguity from path integral point of view. Note that the electric case is very similar

to the one in [17], where

$$\int dt e^{-t_E \sin^2(x)} \quad (4.71)$$

was considered. Main difference between two analysis is that the roles of regions in complex space exchanged. This is because the electric case corresponds to the inverted potential version, i.e.  $V \sim -\sin^2(x)$ , as we discussed in WKB approach. In [17], paths represented by  $\mathcal{K}_E^\pm$  in Figure 4.5 are the Lefschetz thimbles corresponding to analytical continuations from  $\arg t_E$  and the integral is convergent along these paths. Note that their behaviour around infinities are very different. This is due to a jump at  $\arg t_E = 0$ , which is called the Stokes phenomenon and it is the source of the Borel ambiguity.

In our case, on the other hand, both  $\mathcal{J}_E^+$  and  $\mathcal{J}_E^-$  approach to imaginary axis as  $\arg t \rightarrow \pm \frac{\pi}{2}^\mp$ , which corresponds to  $\arg t_E = 0$  for the Euclidean case as we discussed in Section 4.2.1. They flow towards opposite directions. This is analogous to the Stokes phenomenon but due to the prescription we used throughout the paper, their contribution to  $\Delta\Gamma$  is not ambiguous.

## 4.5. Discussion

In this chapter, we have analyzed how the non-perturbative pair production probability in background electric fields can be obtained from the poles of the time evolution propagator. For this reason, we have put the real time approach discussed in [23] in a rigorous basis by providing a definition of pair production probability from the analytical properties of the effective and adapted the perturbative scheme introduced in [26] to pair production problems. While this approach enabled us to compute the pair production probability for arbitrary background potentials in arbitrary dimensions, a careful investigation of the perturbative scheme helps us to connect our analysis to the semi-classical approaches such as WKB methods and Lefschetz thimbles.

On the one hand, by analyzing the emergence of pair production problem from Lefschetz thimbles perspective, we have put the resolution of ambiguity in a more

geometric basis. Our analysis supports the idea that the Lefschetz thimble approach mimics the standard Borel summation method [17]. On the other hand, comparison to WKB methods allowed us to associate the perturbative series we computed in Section 4.3 and perturbative/non-perturbative information extracted from it with the WKB cycles. A similar investigation of spectral problems in quantum mechanics with both stable and unstable ground states in the light of the lessons we learned here would be an interesting problem.

In addition to this, the analysis we pursued in this chapter indicates future directions that can be addressed using the time dependent formalism: One of these directions is the investigation of possible interpretation of resurgence theory as connecting singularities. The resurgence theory investigates the intimate connection between the perturbative and non-perturbative sectors of a quantum theory. Although it is well understood in one dimensional quantum mechanics, in multidimensional problems our knowledge is still primitive. In our setting, which treats problems in different dimensions in the same way, the perturbative non-perturbative connection demonstrates itself as the connection between the expansion around  $t = 0$  and the singularities at  $t \neq 0$ . To understand this let us review our findings: As we implied in Section 4.3, the propagator has a singularity at  $t = 0$  and its connection to the perturbative sector of the theory was shown in [26]. More precisely, as we showed in a specific example in Section 4.4.1 in the semi-classical context, it yields the perturbative part of the action, which carries information of the perturbative WKB cycles. These cycles are linked to the non-perturbative ones via underlying topology which also determines the resurgence relations [47, 49, 50]. Therefore, it is natural to suggest that these geometric relations can be related to the analytical structure of the propagator. In other words, the perturbative non-perturbative connection can be interpreted as a connection between the singularities at  $t = 0$  and  $t \neq 0$ . This was briefly discussed in [58] but a detailed description of this connection appears to be still lacking. An explanation of the resurgence relations in this approach would be very valuable for investigations of multidimensional problems.

Another interesting future direction is the investigation of the possible connection between renormatization procedure and WKB actions. The pair production problem is a relativistic one. However, as often done in the literature for 1 loop order, we made our analysis by reducing it to a non-relativistic quantum mechanical one. Despite this reduction, the UV divergence of the full theory still exists and they need to be handled by renormalization techniques. In Schwinger integral, this divergence arises from the singularity at  $t = 0$ . On the other hand, as we stated above,  $t = 0$  is also a source for the perturbative part of the WKB actions. This suggests a connection between these two phenomena which, to our knowledge, has not been discussed in the literature. In addition to that the idea of connecting the singularities also suggests that the other singularities, which are associated to the non-perturbative sector of the theory, might also play a role in renormalization scheme, possibly in the renormalization group context.

## 5. RENORMALONS IN QUANTUM MECHANICS

In this chapter, we will discuss the renormalon problem in non-relativistic quantum mechanics. Since renormalization is often associated with QFT, the renormalon divergence is mostly considered in QFT settings. However, the 2D  $\delta$ -potential contains Feynman diagrams with logarithmic momentum dependence [116]. Still this model does not exhibit a renormalon divergence. On the other hand, considering a non-relativistic scattering problem in a background potential that consists of 2D  $\delta$ -potential and an additional part, we will show that the  $S$ -matrix has a divergent perturbative expansion associated to the renormalon. Through the Borel summation, this divergent behaviour leads to an ambiguous non-perturbative contribution to the  $S$ -matrix. In a similar fashion with Chapter 4, we will show that by identifying the renormalon divergence with a singularity of  $S$ -matrix in the momentum plane and using the  $i\varepsilon$  prescription, the ambiguity disappears.

The content of this chapter was originally published by the author of this thesis in a collaboration with Dieter Van den Bleeken as a research paper with the title *“Renormalons in quantum mechanics”* [28]. The rest of this chapter is identical to that paper with appropriate modifications.

### 5.1. Background Discussion

In QFT, there is no restriction on the loop diagrams. Therefore, it is not hard to get a renormalon diagram that we discussed in Section 2.1. Then, from scattering perspective, diagrams like the one on the left of Figure 5.1 can appear in 2 particle scattering, but this is not the case in QM as such a diagram would violate particle number conservation. But from this limitation it is at the same time clear that it can be evaded by considering the 4 particle scattering as in the right of Figure 5.1 so that particle number is indeed conserved. This illustrates that quantum mechanics has all the ingredients for renormalons, at least if one chooses a potential that gets renormalized

and that is interactive enough to allow for non-trivial multi-particle scattering.

One can further simplify the setup considering all particles to have the same mass and interpreting the coordinates of the additional particles as extra spatial dimensions associated to a single particle. This brings us then to a model where, instead of multi-particle scattering, a single particle scatters of a background potential that has a part, say the 2D  $\delta$ -potential, that gets renormalized and an additional part that couples it to a third direction. That this idea is correct and that such models do really have a non-vanishing renormalon divergence in their perturbative S-matrix is what we will show in Sections 5.3 and 5.4. It could be very interesting to look for renormalons in other QM observables of similar models but we leave this for future work.

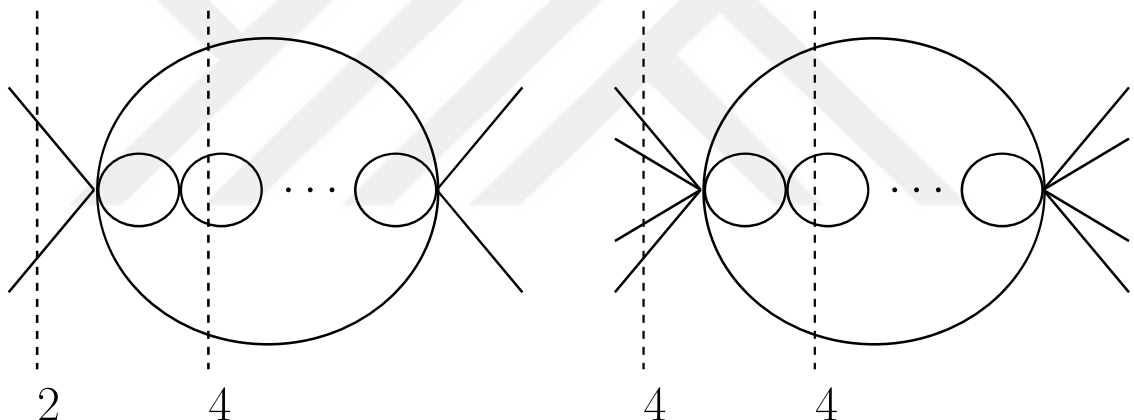


Figure 5.1. Left: Renormalon type diagrams in 2-particle scattering violate particle number conservation. Right: In 4-particle scattering particle number can be conserved.

Due to the simplicity of our model we are able to rigorously show, by explicit calculation, the existence of a renormalon divergence of the perturbative series of its S-matrix. This is important, as for 4d field theories it has so far been impossible to exclude a cancellation between various renormalon diagrams. Interestingly we will see that in our model indeed some cancellations take place, but a total non-zero contribution remains. This reflects itself in a growth  $\propto (n-3)!$  in the order  $n$  of perturbation theory, rather than the naively expected  $\propto (n-1)!$ . Additionally we use the formal tools of quantum mechanical scattering theory to compare the diverging perturbative series to

the exact non-perturbative result. This reveals that Borel summation, using the correct prescription to evade poles, does indeed reconstruct the correct answer including the non-perturbative contribution. The nature of this non-perturbative effect, for example a possible semi-classical realization, would be interesting to further investigate in the future.

Let us outline the content of this chapter. In Section 5.2 we recall the quantum mechanics of the 2D  $\delta$ -potential and its renormalization, which is well-established but maybe not as well-known. We then continue in Section 5.3 by presenting the computation of a simple renormalon diagram in quantum mechanics. We focus on a simple example based on coupling the 2D  $\delta$ -potential to a 1D  $\delta$  potential supported along a third direction.

The main results of our paper are in Section 5.4. We consider there a potential of the form  $V = \lambda_0\delta(x)\delta(y) + \kappa V_*$ . The physical quantity we study is  $\frac{1}{2}\frac{\partial^2}{\partial\kappa^2}S(\mathbf{p}_f, \mathbf{p}_i; \lambda, \kappa)|_{\kappa=0}$  i.e. the S-matrix exact in the renormalized coupling  $\lambda$  and second order in  $\kappa$ . We'll discuss under which conditions on  $V_*$  we expect renormalons to appear and work out in detail the case  $V_* = \delta(\cos\theta z - \sin\theta y)$ . The angle  $\theta$  allows us to interpolate between the case  $\theta = 0$ , where the model factorizes and the renormalon contributions are forced to cancel out among themselves, and the case  $0 < \theta < \frac{\pi}{2}$  where non-trivial interaction takes place and a non-zero renormalon contribution remains once all diagrams at a given order are summed. We compute the leading growth of the series coefficients due to the total renormalon contribution and discuss how this leads to a pole on the real axis in the Borel plane, resulting in a summation ambiguity. Alternatively one can sum the diagrams before performing the outer-loop momentum integral, which reproduces the same ambiguity. We point out that in this second summation procedure the ambiguity is naturally resolved by re-introducing the Feynman  $i\epsilon$  prescription. This illustrates that in this case the summation ambiguity originates from the limits  $\epsilon \rightarrow 0$  and  $n \rightarrow \infty$  not commuting. The link between renormalons and the  $i\epsilon$  prescription was already suggested in some of the earliest studies on renormalons [24]. In the Borel plane this corresponds to a deformation of the integration contour *below* the renormalon pole. In

Section 5.5 we use the operator formalism and exact knowledge of the Green's operator/resolvent of the 2D  $\delta$ -potential to rederive the perturbative result without expanding in the coupling  $\lambda$ . This calculation confirms the absence of further non-perturbative effects that could potentially have cancelled the non-perturbative contribution to the imaginary part due to the summation prescription. The exact calculation also makes the role of the  $i\epsilon$  prescription fully transparent.

## 5.2. Quantum Mechanics with a 2D $\delta$ -potential

In this section we review some aspects of quantum mechanics with a 2D  $\delta$ -potential, see e.g. [116] for a more complete discussion. As we will discuss this model requires renormalization, has a non-trivial, but 1-loop exact,  $\beta$ -function and a renormalization invariant energy scale  $\Lambda = \mu e^{\frac{4\pi}{\lambda}}$  which is the energy of a non-perturbative bound state  $E_b = -\Lambda$ . What makes this model extra appealing is that the perturbative renormalization matches perfectly with a non-perturbative definition through the method of self-adjoint extension [117], as we will shortly recall at the end of this section. Since in the next sections we will couple this model to an additional third direction we will from the beginning discuss it in a 3 dimensional context but, at least in this section, the third direction trivially factorizes. More precisely, we will consider  $S_{3D}(\mathbf{p}_f, \mathbf{p}_i) = 2\pi\delta(q_f - q_i)S_{2D}(\mathbf{v}_f, \mathbf{v}_i)$ . The reader interested only in a review of the 2D  $\delta$  interaction can simply ignore all prefactors  $2\pi\delta(q_f - q_i)$  in this section.

The starting point is the Hamiltonian <sup>6</sup>

$$H = p^2 + \lambda_0 V_*(\mathbf{x}) \quad V_*(\mathbf{x}) = \delta(x)\delta(y). \quad (5.1)$$

We will proceed in a rather pedestrian way with the presentation reflecting a QFT treatment. Our aim is to compute the S-matrix of the model (5.1), describing the scattering of the particle off the background potential  $V_*$ . It is standard practice to

---

<sup>6</sup>See Appendix A for our position and momentum space notation and conventions.

rewrite

$$S(\mathbf{p}_f, \mathbf{p}_i) = \delta^3(\mathbf{p}_f - \mathbf{p}_i) - 2\pi i \delta(p_f^2 - p_i^2) \tau(\mathbf{p}_f, \mathbf{p}_i). \quad (5.2)$$

The perturbative series for the on-shell  $T$ -matrix  $\tau(\mathbf{p}_f, \mathbf{p}_i)$  is the familiar Born-series and it is fully determined by the Fourier transform of the potential:

$$\hat{V}_*(\mathbf{p}) = 2\pi \delta(q). \quad (5.3)$$

At  $n^{\text{th}}$  order in  $\lambda_0$  there is a single diagram made of  $n$  vertices connected by  $n - 1$  propagators with the Feynmann rules

$$\star : \lambda_0 \hat{V}_*(\mathbf{p}_{k-1} - \mathbf{p}_k) \quad - : \int \frac{d^3 \mathbf{p}_k}{(2\pi)^3} \frac{1}{p_f^2 + i\epsilon - p_k^2}. \quad (5.4)$$

More precisely we have ( $\mathbf{p}_0 = \mathbf{p}_f, \mathbf{p}_n = \mathbf{p}_i$ )

$$\star - \star - \dots - \star = \tau^{(n)}(\mathbf{p}_f, \mathbf{p}_i) = \lambda_0^n \int \left( \prod_{k=1}^{n-1} \frac{d^3 \mathbf{p}_k}{(2\pi)^3 (p_f^2 + i\epsilon - p_k^2)} \right) \left( \prod_{k=1}^n \hat{V}_*(\mathbf{p}_{k-1} - \mathbf{p}_k) \right). \quad (5.5)$$

The first order is the so-called Born-approximation, which in this case evaluates to

$$\star = \tau^{(1)}(\mathbf{p}_f, \mathbf{p}_i) = 2\pi \lambda_0 \delta(q_f - q_i). \quad (5.6)$$

### 5.2.1. One Loop

The need for renormalization in this model manifests itself at the next order, which is the 1-loop order, where a UV-divergent momentum integral appears:

$$\star - \star = \tau^{(2)}(\mathbf{p}_f, \mathbf{p}_i) = 2\pi \delta(q_f - q_i) \frac{\lambda_0^2}{4\pi} \int_0^\infty \frac{dv^2}{v_f^2 + i\epsilon - v^2}. \quad (5.7)$$

One deals with this divergent integral in textbook fashion. First we regularize by introducing a UV momentum cutoff  $\Omega$ :

$$I_\Omega(z) = \frac{1}{4\pi} \int_0^\Omega \frac{dv^2}{z - v^2} = \frac{1}{4\pi} \log z - \frac{1}{4\pi} \log (e^{i\pi}(\Omega - z)). \quad (5.8)$$

To proceed we replace the bare coupling  $\lambda_0$  by a physical coupling  $\lambda$  at some fixed energy scale  $\mu$  through  $\lambda_0 = \lambda + \lambda^2 \Delta \left( \frac{\Omega}{\mu} \right) + \mathcal{O}(\lambda^3)$ . Observing that

$$\lambda_0 + \lambda_0^2 I_\Omega(z) + \mathcal{O}(\lambda_0^3) = \lambda + \lambda^2 \left( \Delta \left( \frac{\Omega}{\mu} \right) + \frac{1}{4\pi} (\log z - \log(z - \Omega)) \right) + \mathcal{O}(\lambda^3) \quad (5.9)$$

tells us to choose

$$\Delta(z) = \frac{1}{4\pi} \log z, \quad (5.10)$$

so that

$$\lim_{\Omega \rightarrow \infty} (\lambda_0 + \lambda_0^2 I_\Omega(z) + \mathcal{O}(\lambda_0^2)) = \lambda + \lambda^2 l(z) + \mathcal{O}(\lambda^3), \quad (5.11)$$

where for future convenience we introduced the function

$$l(z) = \frac{1}{4\pi} \log \frac{e^{i\pi} z}{\mu}. \quad (5.12)$$

Note that of course we could add an arbitrary (complex) constant to  $\Delta$ , however from (5.18) it follows that  $\Delta \rightarrow \Delta + c$  can be absorbed by  $\lambda \rightarrow \frac{\lambda}{1-c\lambda}$ . The choice we make has the advantage that real  $\lambda$  corresponds to a unitary S-matrix. This directly follows from (5.13) and the fact that a unitary S-matrix requires the first order on-shell T-matrix to satisfy  $\tau^{(1)}(\mathbf{p}_f, \mathbf{p}_i) = \tau^{(1)}(\mathbf{p}_i, \mathbf{p}_f)^*$ . Of course this requirement only fixed  $c$  to be real, but non-zero real  $c$  amounts only to a rescaling of the momentum scale  $\mu$ , which is arbitrary in any case.

The outcome of this renormalization procedure is to replace (5.6, 5.7) by

$$\star = \tau^{(1)}(\mathbf{p}_f, \mathbf{p}_i) = 2\pi\lambda \delta(q_f - q_i), \quad (5.13)$$

$$\star - \star = \tau^{(2)}(\mathbf{p}_f, \mathbf{p}_i) = 2\pi \delta(q_f - q_i) \lambda^2 l(u_f^2). \quad (5.14)$$

Imposing the result to be independent of the arbitrary scale  $\mu$  leads to the 1-loop  $\beta$ -function

$$\beta(\lambda) = \frac{\lambda^2}{4\pi} + \mathcal{O}(\lambda^3). \quad (5.15)$$

### 5.2.2. All Order

This theory is so simple that the higher orders are easily analysed and can be directly summed. Indeed, note that

$$\star - \dots - \star = \tau^{(n)}(\mathbf{p}_f, \mathbf{p}_i) = 2\pi\delta(q_f - q_i) \lambda_0^n \left( \frac{1}{4\pi} \int_0^\infty \frac{dv^2}{v_f^2 + i\epsilon - v^2} \right)^{n-1}. \quad (5.16)$$

This suggests that higher order renormalization simply amounts to repeating the 1-loop procedure via

$$\lambda_0 \rightarrow \lambda \quad , \quad \frac{1}{4\pi} \int_0^\infty \frac{dv^2}{z - v^2} \rightarrow l(z). \quad (5.17)$$

It can be verified that this is indeed equivalent to the all order definition of the physical coupling

$$\lambda_0 = \sum_{n=1}^{\infty} \left[ \Delta \left( \frac{\Omega}{\mu} \right) \right]^{n-1} \lambda^n = \frac{\lambda}{1 - \Delta \left( \frac{\Omega}{\mu} \right) \lambda}. \quad (5.18)$$

In summary, after renormalization one finds

$$\star - \dots - \star = \tau^{(n)}(\mathbf{p}_f, \mathbf{p}_i) = 2\pi \delta(q_f - q_i) \lambda^n l(v_f^2)^{n-1}. \quad (5.19)$$

So all order perturbation theory takes the simple form of a geometric series and the total answer is thus

$$\tau(\mathbf{p}_f, \mathbf{p}_i) = \sum_{n=1}^{\infty} \tau^{(n)}(\mathbf{p}_f, \mathbf{p}_i) = 2\pi \delta(q_f - q_i) t_*(u_f^2) = \frac{2\pi \delta(q_f - q_i) \lambda}{1 - \frac{\lambda}{4\pi} (\log \frac{v_f^2}{\mu} + i\pi)}, \quad (5.20)$$

where for later convenience we separately define

$$\tau_*(z) = \sum_{n=0}^{\infty} l(z)^{n-1} \lambda^n = \frac{\lambda}{1 - \frac{\lambda}{4\pi} \log \frac{e^{i\pi} z}{\mu}}. \quad (5.21)$$

Let us now interpret the results of the calculation performed above. Via the all order definition of the physical coupling (5.18) one can compute the all order  $\beta$ -function

$$\beta(\lambda) = \frac{\lambda^2}{4\pi}. \quad (5.22)$$

It is interesting to note that this coincides with (5.15), implying the  $\beta$ -function is one-loop exact. From (5.22) one computes the running coupling

$$\bar{\lambda}(p^2) = \frac{\lambda}{1 - \frac{\lambda}{4\pi} \log \frac{p^2}{\mu}} = \frac{4\pi}{\log \frac{\Lambda}{p^2}}, \quad (5.23)$$

which reveals a renormalization invariant scale

$$\Lambda = \mu e^{\frac{4\pi}{\lambda}}. \quad (5.24)$$

In accord with renormalization theory the dependence of (5.20) on the energy scale goes purely through the running coupling:

$$\tau(\mathbf{p}_f, \mathbf{p}_i) = 2\pi\delta(q_f - q_i) \frac{\bar{\lambda}(v_f^2)}{1 - \frac{i}{4}\bar{\lambda}(v_f^2)}. \quad (5.25)$$

Interestingly this theory is both UV and IR free without being trivial. Although the running coupling (5.23) has a Landau pole at energy  $\Lambda$ , the S-matrix (5.2, 5.25) remains perfectly finite at this energy. It does have a pole however at *negative* energy  $E_b = -\Lambda$ , showing that the proper physical interpretation of  $\Lambda$  is that of the energy of a non-perturbative bound state. Interestingly, and contrary to the 1D  $\delta$ -potential, the bound state exists both for positive and negative  $\lambda$ . Let us stress, as this is important for the correct interpretation of the following sections, that the model is well defined if and only if  $\lambda$  is real, or equivalently for all positive real values of  $\Lambda$ .

Surprisingly one is able to extract non-perturbative information of the model, the bound state energy, through a purely perturbative calculation enhanced with renormalization. Note that so far the perturbative series considered was perfectly convergent so the non-perturbative boundstate is not connected to any divergence. In the next sections we will see that it can be linked to the divergence of the perturbative S-matrix once we couple the particle to an additional potential.

### 5.2.3. Exact Solution

Although the non-perturbative bound state emerged out of the perturbative treatment above one might wonder if the S-matrix could not get additional non-perturbative contributions that are missed perturbatively. Due to the simplicity of the 2D  $\delta$ -model one can actually solve it exactly which not only confirms the renormalized perturbative calculations above but additionally shows that that answer is complete. The advantage of QM compared to QFT is that we have an explicit non-perturbative definition provided by the Schrödinger equation with a self-adjoint Hamiltonian. Although they will not be applied in the remainder of the paper, we shortly mention the results obtained by treating the model through the method of self-adjoint extensions as they are quite beautiful and put the work in this and the following sections on firmer footing. For further details including a more precise mathematical treatment see [117].

The idea is to replace (5.1), which is a Hamiltonian defined on all of  $\mathbb{R}^3$ , by the free Hamiltonian on  $\mathbb{R}^3 \setminus \mathbb{R}$ , the line being removed is the origin of the  $xy$ -plane, supplemented by a boundary condition at  $x = y = 0$ . The condition that the 'free' Hamiltonian  $H = p^2$  be self-adjoint with respect to this boundary condition strongly restricts the options, so much so that all possibilities can be classified. Although a priori this could lead to point-interactions which are not described by a  $\delta$ -potential, as indeed in general it does this is not the case in this setting. To be precise let us decompose the wavefunction as  $(x = r \cos \phi, y = r \sin \phi)$

$$\psi(x, y, z) = \int_{-\infty}^{\infty} \frac{dq}{2\pi} \sum_{m=-\infty}^{\infty} \psi_m(r, q) e^{i(m\phi + qz)}. \quad (5.26)$$

For  $m \neq 0$  the only allowed boundary condition is simply that the wave-function remain finite as  $r \rightarrow 0$ , but the boundary condition on  $\psi_0(r, q)$  can be non-trivial. Those boundary conditions that lead to a self-adjoint Hamiltonian are parameterized by a positive real parameter  $\Lambda$  and read

$$\lim_{r \rightarrow 0} \left( \frac{\psi_0(r, q)}{r \partial_r \psi_0(r, q)} - \log \frac{\sqrt{\Lambda} r}{2} \right) = \gamma, \quad (5.27)$$

where  $\gamma$  is the Euler-Mascheroni constant. One can then solve the time-independent Schrödinger equation with these boundary conditions to find scattering states and a bound state:

$$\psi_{0,v,q}(r, q') = \frac{2\pi\delta(q - q')\sqrt{v}}{|i\pi + \log \frac{\Lambda}{v^2}|} \left( \pi Y_0(vr) + \log \frac{\Lambda}{v^2} J_0(vr) \right), \quad (5.28)$$

$$\psi_{m,v,q}(r, q') = 2\pi\delta(q - q')\sqrt{v} J_m(vr) \quad , \quad m \neq 0, \quad (5.29)$$

$$\psi_b(r, q) = 2\pi\delta(q)\sqrt{\frac{\Lambda}{\pi}} K_0(\sqrt{\Lambda}r). \quad (5.30)$$

The scattering states have energy  $E_{m,v,q} = v^2 + q^2 = p^2$  while the bound-state has energy  $E_b = -\Lambda$ . Matching the bound state energy with the perturbative calculation above allows to identify the parameter  $\Lambda$  of the self-adjoint extension with the renormalization invariant scale (5.24). The non-trivial test is then to compare the scattering amplitude as defined by the scattering states (5.28,5.29) with the perturbative on-shell T-matrix (5.25). A short calculation, since only  $m = 0$  leads to non-trivial scattering, provides perfect agreement.

### 5.3. A Renormalon Diagram in Quantum Mechanics

This section discusses a first diagram for an example potential. In the next section we will discuss the totality of all diagrams, both for more general potentials as well as the example considered here.

With the aim to generate a renormalon and motivated by the discussion of Section 2.1, we add to the 2D  $\delta$ -potential an extra potential that couples non-trivially to the 3<sup>th</sup> direction:

$$H = p^2 + \lambda_0 V_* + \kappa V_*. \quad (5.31)$$

A simple choice is to take as the extra piece a 1D  $\delta$  potential. To make sure the theory does not simply factorize we put the support of the 1D  $\delta$  at an angle to the  $xy$ -plane

as in Figure 5.2 and choose the potential as

$$V_* = \delta(\cos \theta z - \sin \theta y). \quad (5.32)$$

Keeping the angle  $\theta$  a free parameter will allow a check on our results since through the limit  $\theta \rightarrow 0$  we can compare to the case where the S-matrix factorizes:

$$S_{\theta=0}(\mathbf{p}_f, \mathbf{p}_i) = S_{1D\delta}(q_f, q_i) S_{2D\delta}(\mathbf{v}_f, \mathbf{v}_i). \quad (5.33)$$

By adding a new part to the potential and introducing a second coupling  $\kappa$  we introduce a whole new set of diagrams to the calculation of the perturbative S-matrix. For our discussion, in this and the following sections, it will be sufficient to focus only diagrams quadratic in  $\kappa$ . Formally we could say that the observable of our interest is  $\frac{1}{2} \frac{\partial^2}{\partial \kappa^2} S(\mathbf{p}_f, \mathbf{p}_i; \lambda, \kappa) \Big|_{\kappa=0}$ , in practice it means we will work to all order in  $\lambda$  and at second order in  $\kappa$ .

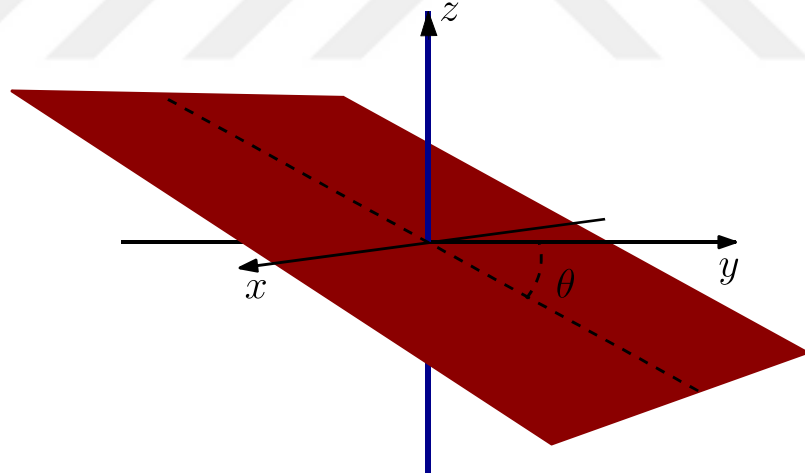


Figure 5.2. Support of our example potential. The blue line, which coincides with the  $z$ -axis, corresponds to  $V_* = \delta(x)\delta(y)$ , while the red plane corresponds to

$$V_* = \delta(\cos \theta z - \sin \theta y).$$

In this two parameter perturbation theory there are two types of vertices:  $\star$  and  $*$ . The Feynmann rules (5.4) get extended by

$$\star : \kappa \hat{V}_*(\mathbf{p}_{k-1} - \mathbf{p}_k). \quad (5.34)$$

Given the  $(\log v^2)^n$  behaviour of the diagram  $\star - \star - \dots - \star$  established in (5.19), one expects a renormalon might appear once this diagram finds itself inside a bigger loop. This can be done by squeezing the diagram between two additional  $\star$  vertices, see also figure 5.3, and explains why it is the second order in  $\kappa$  where we expect the phenomenon to first appear.

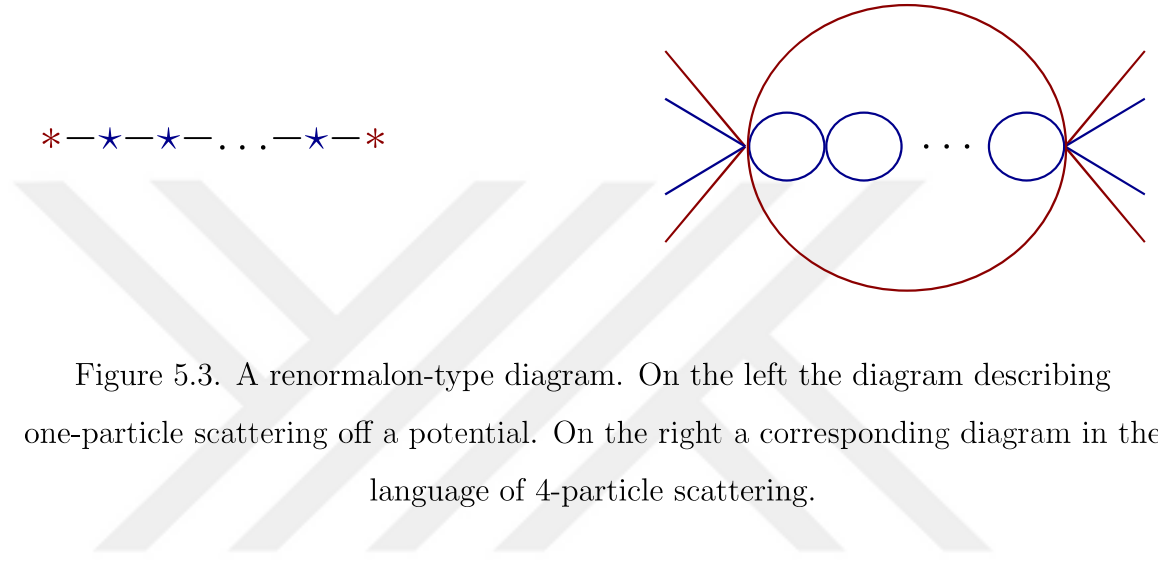


Figure 5.3. A renormalon-type diagram. On the left the diagram describing one-particle scattering off a potential. On the right a corresponding diagram in the language of 4-particle scattering.

Let us now show that indeed this intuition is correct by explicit computation. For the example (5.32) one has ( $\mathbf{p} = (r, w, q)$ )

$$* : \kappa (2\pi)^2 \delta(r_{k-1} - r_k) \delta(\cos \theta(w_{k-1} - w_k) + \sin \theta(q_{k-1} - q_k)). \quad (5.35)$$

Applying the Feynmann rules, performing some integration and applying the renormalization (5.17) it follows that

$$* - \star - \star - \dots - \star - * = \lambda^n \kappa^2 \cos^2 \theta \int \frac{dq}{2\pi} \frac{l(p_f^2 - q^2)^{n-1}}{((q_f - q)(q + \tilde{q}_f) + i\epsilon)((q_i - q)(q + \tilde{q}_i) + i\epsilon)}, \quad (5.36)$$

where we used the shorthand

$$\tilde{q}_\alpha = \cos 2\theta q_\alpha - \sin 2\theta w_\alpha, \quad (\alpha = f, i). \quad (5.37)$$

We remind the reader that the function  $l$  is essentially the logarithm, see (5.12). Equation (5.36) is indeed of the generic renormalon type integral. The logarithm becomes large when  $q^2 \approx p_f^2$  or  $q^2 \rightarrow \infty$ . A careful analysis, see Appendix B, reveals that factorial contributions to the integral (5.36) around  $|q| = p_f$  cancel each other while

this is not the case at large momentum. Using that the rational part of the integrand in (5.36) decays like  $q^{-4} = q^{-2 \times \frac{3}{2} - 1}$  for large  $q$  and via formula (B.1) we find that for large  $n$

$$* - \star - \star - \dots - \star - * \sim 2\kappa^2 \cos^2 \theta \mu^{-\frac{3}{2}} \left( \frac{\lambda}{6\pi} \right)^n (n-1)! , \quad (5.38)$$

where the factor  $6\pi = \frac{3}{2} \times 4\pi$  is to be interpreted as a multiple of the (inverse of the)  $\beta$ -function coefficient (5.15). The appearance of  $\frac{3}{2}$  is no coincidence and set by dimensional analysis. In 3D the on-shell T-matrix  $t$  has dimension of length while  $\kappa$  has dimension of inverse length. So the only way the other scale  $\mu$ , with dimension of inverse length squared, can appear is with a power  $-\frac{3}{2}$ , fixing  $\rho = \frac{3}{2}$  in (B.1).

The result (5.38) is important in that it manifestly shows that also in non-relativistic 1-particle QM renormalon diagrams appear and that they lead to factorial growth through exactly the same mechanism as in QFT, i.e. integration in momentum space over an integrand that includes a high power of a logarithmic momentum dependence due to a large number of renormalized 1-loop diagrams inside a larger loop. Given the discussion in Section 2.2, we conclude there is a pole at  $s = 6\pi$  in the Borel plane when summing all the  $* - \star - \star - \dots - \star - *$  diagrams. When  $\lambda$  is positive this will lead to an ambiguity of the form

$$\text{amb} \left( \sum_n * - \star - \star - \dots - \star - * \right) = \mp 2\pi i \kappa^2 \cos^2 \theta \mu^{-\frac{3}{2}} e^{-\frac{\lambda}{6\pi}} \quad (5.39)$$

$$= \mp 2\pi i \kappa^2 \cos^2 \theta \Lambda^{-\frac{3}{2}}. \quad (5.40)$$

It is interesting to note that while (5.38) appears not manifestly renormalization invariant, the corresponding ambiguity (5.40) obtained from resummation is manifestly renormalization invariant as it can be expressed purely in terms of the renormalization invariant scale  $\Lambda$ , defined in (5.24).

Before one draws conclusions it should be realized that the diagrams considered above form only a subset of all the diagrams contributing to the S-matrix, and so

one cannot directly extrapolate these results to the actual physical observable. Indeed, note that the growth (5.38) and the corresponding non-perturbative contribution (5.40) do *not* vanish as  $\theta \rightarrow 0$ . But because in that limit the full S-matrix is simply the product of the 1D and 2D  $\delta$  S-matrices there should be no divergence nor an extra non-perturbative contribution. This indicates that there are further factorially growing sets of diagrams in the theory and that, at least at  $\theta = 0$ , these will cancel the growth (5.38). This motivates us to carefully work through all diagrams in the next section, which will confirm such a cancellation at  $\theta = 0$  but will also show that when  $\theta \neq 0$  the cancellation is not complete and a total factorial growth remains.

## 5.4. Renormalons: All Order Perturbation Theory

As illustrated in the last section, renormalon diagrams leading to factorial growth appear also in 1-particle QM. In this section we investigate this in more detail, carefully working out all diagrams for the model (5.31). We will start with the potential  $V_*$  arbitrary so we can understand more generally under which conditions renormalons can appear. We then specialize again to (5.32) to provide an explicit fully worked out example. After exhibiting the factorial growth we will consider the Borel summation and its ambiguity, show how it can be rephrased as an ambiguity of a momentum space integral and how that ambiguity is naturally resolved through the Feynman  $i\epsilon$  prescription. An exact treatment in the next section confirms the perturbative results of this section.

### 5.4.1. First Order in $\kappa$

We'll analyze all diagrammatic contributions to the on-shell T-matrix to arbitrary order in  $\lambda$  and second order in  $\kappa$ , using the Feynman rules (5.4, 5.34) together with the renormalization (5.17). Although our interest is in the part of the S-matrix quadratic in  $\kappa$  it will be useful to first consider the linear part, as some structures appearing there will have a role to play at second order. The first order consists of all diagrams

with a single  $*$  vertex, they can be easily listed and computed to be

$$* = \kappa \hat{V}_*(\mathbf{p}_f - \mathbf{p}_i) \quad (5.41)$$

$$\star - \dots - \star - * = l(v_f^2)^{n-1} \lambda^n \kappa I^{(1,1)}(q_f, \mathbf{p}_i) \quad (5.42)$$

$$* - \star - \dots - \star = l(v_f^2)^{n-1} \lambda^n \kappa I^{(1,1)}(q_i, \mathbf{p}_f)^* \quad (5.43)$$

$$\underbrace{\star - \dots - \star - * - \star - \dots - \star}_{n-a} = l(v_f^2)^{n-a-1} l(v_i^2)^{a-1} \lambda^n \kappa I^{(1,2)}(q_f, q_i), \quad (5.44)$$

where the complex conjugate of the integral in (5.43) should be performed *without* changing the sign of the  $i\epsilon$  term.

Here two integrals appear:

$$I^{(1,1)}(\mathbf{p}_\alpha, q_\beta) = \int \frac{d^2\mathbf{v}}{(2\pi)^2} \frac{\hat{V}_*(\mathbf{v}_\alpha - \mathbf{v}, q_\alpha - q_\beta)}{p_f^2 - q_\alpha^2 + i\epsilon - v^2}. \quad (5.45)$$

$$I^{(1,2)}(q_\alpha, q_\beta; z) = \int \frac{d^2\mathbf{v}}{(2\pi)^2} \frac{d^2\mathbf{v}'}{(2\pi)^2} \frac{\hat{V}_*(\mathbf{v} - \mathbf{v}', q_\alpha - q_\beta)}{(p_f^2 - q_\alpha^2 + i\epsilon - v^2)(p_f^2 - q_\beta^2 + i\epsilon - v'^2)}. \quad (5.46)$$

In the particular example (5.32) these integrals evaluate to

$$I^{(1,1)}(\mathbf{p}_\alpha, q_\beta) = \frac{\cos \theta}{\cos^2 \theta (p_f^2 - p_\alpha^2) + (q_\alpha - q_\beta)(q_\beta + \tilde{q}_\alpha)}, \quad (5.47)$$

$$I^{(1,2)}(q_\alpha, q_\beta) = \frac{\cos \theta}{2\pi |q_\alpha^2 - q_\beta^2| F} \log \frac{2\sqrt{(p_f^2 - q_\alpha^2)(p_f^2 - q_\beta^2)}}{2p_f^2 - q_\alpha^2 - q_\beta^2 + \sec^2 \theta |q_\alpha^2 - q_\beta^2| F - \tan^2 \theta (q_\alpha - q_\beta)^2}, \quad (5.48)$$

where

$$F = \sqrt{1 - 4 \sin^2 \theta \frac{q_1 q_2 + p_f^2 \cos^2 \theta}{(q_1 + q_2)^2}} \quad (5.49)$$

and  $\tilde{q}$  was defined in (5.37).

Table 5.1. Expressions for all 8 types of diagrams at order  $\kappa^2$ . Only the diagrams in the last four rows can lead to renormalons.

Diagrams	Integrals
$* - *$	$\kappa^2 \int \frac{dq}{2\pi} I^{(2,1)}(\mathbf{p}_f, \mathbf{p}_i, q)$
$* - \dots - \star - * - *$	$l(u_f^2)^{n-1} \kappa^2 \lambda^n \int \frac{dq}{2\pi} I^{(2,2)}(q_f, \mathbf{p}_i, q)$
$* - * - \star - \dots - *$	$l(v_i^2)^{n-1} \kappa^2 \lambda^n \int \frac{dq}{2\pi} I^{(2,2)}(q_i, \mathbf{p}_f, q)^*$
$\overbrace{\star - \dots - \star - * - \star - \dots - \star}^a$	$l(v_f^2)^{a-1} l(v_i^2)^{n-a-1} \kappa^2 \lambda^n \int \frac{dq}{2\pi} I^{(2,3)}(q_f, q_i, q)$
$* - \star - \dots - \star - *$	$\kappa^2 \lambda^n \int \frac{dq}{2\pi} I^{(1,1)}(\mathbf{p}_f, q) I^{(1,1)}(\mathbf{p}_i, q)^* l(p_f^2 - q^2)^{n-1}$
$\overbrace{\star - \dots - \star - * - \star - \dots - \star}^a$	$l(v_f^2)^{a-1} \kappa^2 \lambda^n \int \frac{dq}{2\pi} I^{(1,2)}(q_f, q) I^{(1,1)}(\mathbf{p}_i, q)^* l(p_f^2 - q^2)^{n-a-1}$
$\overbrace{* - \star - \dots - \star}^a$	$l(v_i^2)^{a-1} \kappa^2 \lambda^n \int \frac{dq}{2\pi} I^{(1,2)}(q_i, q)^* I^{(1,1)}(\mathbf{p}_f, q) l(p_f^2 - q^2)^{n-a-1}$
$\overbrace{* - \dots - \star - * - \star - \dots - \star}^a$	$l(v_f^2)^{a-1} l(v_i^2)^{b-1} \kappa^2 \lambda^n \int \frac{dq}{2\pi} I^{(1,2)}(q_f, q) I^{(1,2)}(q_i, q)^* l(p_f^2 - q^2)^{n-a-b-1}$

### 5.4.2. Second Order in $\kappa$

This is the order where we expect renormalon diagrams to appear. As a starting point for our discussion we present the integral expressions for all diagrams with two  $*$  vertices and an arbitrary number  $n$  of  $\star$  vertices in Table 5.1, where, along with the definitions in Equations 5.45 and 5.46,  $I^{(2,1)}$ ,  $I^{(2,2)}$  and  $I^{(2,3)}$  are defined as

$$I^{(2,1)}(\mathbf{p}_\alpha, \mathbf{p}_\beta, q) = \int \frac{d^2\mathbf{v}}{(2\pi)^2} \frac{\hat{V}_*(\mathbf{v}_\alpha - \mathbf{v}, q_\alpha - q) \hat{V}_*(\mathbf{v} - \mathbf{v}_\beta, q - q_\beta)}{(p_f^2 - q^2 + i\epsilon - v^2)}, \quad (5.50)$$

$$I^{(2,2)}(q_\alpha, \mathbf{v}_\beta, q) = \int \frac{d^2\mathbf{v}_1}{(2\pi)^2} \frac{d^2\mathbf{v}_2}{(2\pi)^2} \frac{\hat{V}_*(\mathbf{v}_1 - \mathbf{v}_2, q_\alpha - q) \hat{V}_*(\mathbf{v}_2 - \mathbf{v}_\beta, q - q_\beta)}{(p_f^2 - q_\alpha^2 + i\epsilon - v_1^2)(p_f^2 - q^2 + i\epsilon - v_2^2)}, \quad (5.51)$$

$$I^{(2,3)}(q_\alpha, q_\beta, q) = \frac{1}{(2\pi)^6} \int \frac{d^2\mathbf{v}_1 d^2\mathbf{v}_2 d^2\mathbf{v}_3}{(p_f^2 - q_\alpha^2 + i\epsilon - v_1^2)(p_f^2 - q^2 + i\epsilon - v_2^2)(p_f^2 - q_\beta^2 + i\epsilon - v_3^2)}. \quad (5.52)$$

The first four types of diagrams are given in the first four rows of Table 5.1. These diagrams cannot grow factorially in  $n$ , since the integrands of the  $q$  integral are  $n$  independent. This implies we can safely ignore them at large  $n$  and so we will not consider them further. We are interested in the four remaining types that are given in the last four rows in Table 5.1. They contain an integral over  $q$  of an integrand containing  $(\log \frac{q^2}{\mu})^n$  and can lead to factorial growth in  $n$ . Indeed the diagrams in the fifth row are the ones we worked out in an example in the previous section confirming this factorial growth.

First let us point out that the loop integrals in Table 5.1 containing the logarithms is over  $q$ , the momentum associated to the  $z$ -direction. Now observe that if we would choose the potential  $V_*$  to be independent of this direction, so that  $\hat{V}_* \propto \delta(q)$ , then this loop integral, via (5.45, 5.46), would become trivial and no factorial growth is generated. This shows that although the renormalization of the 2D  $\delta$  potential  $V_*$  is crucial, so is the coupling to an additional potential that depends on a 3<sup>rd</sup> direction. It appears to be the analog in one-particle mechanics of the need for more than 2 particles to generate renormalons in a multi-particle scattering setup, which is due to particle number conservation in QM (as opposed to QFT).

To understand if factorial growth does in fact appear one needs to be more precise about the non-logarithmic parts of the integrands. These are formed by products of the first order integrals (5.45, 5.46) which are in turn determined through  $\hat{V}_*$ . Possible factorial growth for large  $n$  originates in the momentum regions where the logarithm is large, either  $q^2 \approx p_f^2$  or  $q^2 \gg \mu$ . As we show in Appendix B there is no net contribution from the first region while the contribution of the second region is fully determined by the large momentum behaviour of the non-logarithmic part of the integrand:

$$\int_{-\infty}^{\infty} \frac{dq}{2\pi} f(q) l(p_f^2 - q^2)^{n-1} \sim \frac{2\mu^{-\rho}}{(4\pi\alpha)^n} \left(\frac{n}{\rho}\right)^{\sigma} (n-1)! , \quad (5.53)$$

when for large  $|q|$  the function  $f(q)$  decays as

$$f(q) \sim |q|^{-2\rho-1} (\log q^2)^{\sigma}. \quad (5.54)$$

The upshot is that the presence of renormalons is a feature of the large  $|q_\beta|$  behaviour of the integrals (5.45, 5.46) which in turn is fully determined by the large  $|q|$  behaviour of the potential  $\hat{V}_*(\mathbf{v}, q)$ . For this reason we expect the presence of renormalons to be a robust feature, not at all specific to the concrete example (5.32) that we will analyze in detail below. Indeed, if one would slightly change (5.32) in a way that the second  $\delta$ -function in (5.35) is replaced by another function, say a Gaussian, that is peaked around  $|q| \approx |\mathbf{v}|$  then this will not drastically change the large  $|q|$  behaviour of the integrals (5.45, 5.46) and one would expect renormalons to remain present. Understanding the precise mathematical conditions on  $\hat{V}_*(\mathbf{v}, q)$  for which a non-zero, non-cancelling set of renormalons appears would be interesting, but we leave it for future work.

### 5.4.3. Concrete Example

Let us now specialize to the specific example (5.32), for which we computed the expressions (5.47, 5.48). Their large  $|q|$  decay is given by

$$I^{(1,1)}(\mathbf{p}_\alpha, q_\beta) = -\cos \theta q_\beta^{-2} + \mathcal{O}(q_\beta^{-3}) \quad (5.55)$$

$$I^{(1,2)}(q_\alpha, q_\beta) = \frac{\cos \theta}{4\pi} q_\beta^{-2} \left( \log \frac{q_\beta^2}{\mu} - 4\pi l(p_f^2 - q_\alpha^2) + \log \cos^2 \theta \right) + \mathcal{O}(q_\beta^{-3}). \quad (5.56)$$

Note that in the second line we also included a first subleading term as this will come to play a role. Using these formulas and (5.53, 5.54) it is straightforward to compute the growth of the 4 relevant diagrams in Table 5.1:

$* - \star - \dots - \star - *$

$$\sim C_n (n-1)! (1 + \mathcal{O}(n^{-1})) \quad , \quad C_n = 2 \cos^2 \theta \kappa^2 \mu^{-\frac{3}{2}} \left( \frac{\lambda}{6\pi} \right)^n \quad (5.57)$$

$\underbrace{\star - \dots - \star}_{a} - * - \underbrace{\star - \dots - \star}_{n-a} - *$

$$\sim -C_n l(v_f^2)^{a-1} \left( (n-a)! - (6\pi l(v_f^2) + \frac{3}{2} \log \cos^2 \theta)(n-a-1)! \right) (1 + \mathcal{O}(n^{-1})) \quad (5.58)$$

$* - \underbrace{\star - \dots - \star}_{n-a} - * - \underbrace{\star - \dots - \star}_{a}$

$$\sim -C_n l(v_i^2)^{a-1} \left( (n-a)! - (6\pi l(v_i^2) + \frac{3}{2} \log \cos^2 \theta)(n-a-1)! \right) (1 + \mathcal{O}(n^{-1})) \quad (5.59)$$

$\underbrace{\star - \dots - \star}_{a} - * - \underbrace{\star - \dots - \star}_{n-a-b} - * - \underbrace{\star - \dots - \star}_{b}$

$$\begin{aligned} & \sim C_n l(v_f^2)^{a-1} l(v_i^2)^{b-1} ((n-a-b+1)! - (6\pi l(v_f^2) + 6\pi l(v_i^2) + 3 \log \cos^2 \theta)(n-a-b)! \\ & + (6\pi l(v_f^2) + \frac{3}{2} \log \cos^2 \theta)(6\pi l(v_i^2) + \frac{3}{2} \log \cos^2 \theta)(n-a-b-1)!) (1 + \mathcal{O}(n^{-1})). \end{aligned} \quad (5.60)$$

The common factor  $(1 + \mathcal{O}(n^{-1}))$  is due to  $1/n$  corrections to (5.53), but these will be irrelevant when we sum the 4 types of diagrams and keep only the leading contribution. We already presented (5.57) in (5.38) but now have all other contributions listed as

well. This allows us to finally analyze the growth of  $\tau^{(n,2)}(\mathbf{p}_f, \mathbf{p}_i) \propto \lambda^n \kappa^2$  by summing the contributions from the various diagrams. The leading growth goes like  $(n-1)!$ , we get contributions from (5.57), (5.58, 5.59) with  $a = 1$  and (5.60) with  $a = b = 1$ , but in such a way that their sum cancels! So instead we should look for growth of order  $(n-2)!$ . There are contributions from (5.58, 5.59) with  $a = 2$  and (5.60) with  $a = 2, b = 1$  and  $a = 1, b = 2$ , but also from the subleading terms in (5.58, 5.59) with  $a = 1$  and (5.60) with  $a = b = 1$ . Again their sum vanishes. Without being discouraged we investigate growth of the form  $(n-3)!$ . Now there are quite a few contributions: (5.58, 5.59) with  $a = 3$  and (5.60) with  $a = 3, b = 1, a = 1, b = 3$  and  $a = 2, b = 2$ , the subleading term of (5.58, 5.59) with  $a = 2$  and (5.60) with  $a = 2, b = 1$  and  $a = 1, b = 2$  and also the subsubleading term of (5.60) with  $a = b = 1$ . When we sum them again various cancellations happen but finally a non-zero contribution remains. The result is

$$\tau^{(n,2)}(\mathbf{p}_f, \mathbf{p}_i) \sim \frac{9}{2} (\cos \theta \log \cos^2 \theta)^2 \kappa^2 \mu^{-\frac{3}{2}} \left( \frac{\lambda}{6\pi} \right)^n (n-3)!. \quad (5.61)$$

This formula for the asymptotic growth of the on-shell T-matrix of the model (5.31) is the key technical result of this paper. It establishes that non-relativistic 1-particle QM can exhibit a renormalon divergence in its perturbative series. In our derivation we saw that the  $(n-1)!$  growth of (5.38) gets cancelled against diagrams with similar growth. As we remarked earlier this is as expected since (5.38) doesn't vanish at  $\theta = 0$  while the total result should, due to factorization and obvious absence of divergence at this value. Now observe that indeed the total result (5.61) vanishes at  $\theta = 0$ , thus passing an important consistency check.

#### 5.4.4. Borel Summation: Ambiguity and Resolution

The factorial growth (5.61), which for positive  $\lambda$  is non sign-oscillating, leads to a pole on the positive real axis of the Borel plane leading to an ambiguity in the Borel summation of  $\tau^{(2)}$ , the on-shell T-matrix at all order in  $\lambda$  and second order in  $\kappa$ . Then,

the ambiguity due to (5.61) is

$$\text{amb } \tau^{(2)}(\mathbf{p}_f, \mathbf{p}_i) = \mp \frac{9\pi i}{2} (\cos \theta \log \cos^2 \theta)^2 \kappa^2 \mu^{-\frac{3}{2}} e^{-\frac{6\pi}{\lambda}} \left( \frac{\lambda}{6\pi} \right)^2 \quad (5.62)$$

$$= \mp 2\pi i (\cos \theta \log \cos^2 \theta)^2 \kappa^2 \Lambda^{\frac{3}{2}} \left( \frac{\lambda}{4\pi} \right)^2. \quad (5.63)$$

Given this ambiguity of the Borel summation procedure one needs to identify a physical principle to either decide the sign or cancel this extra imaginary part.

To (re-)introduce this principle, let us revisit the terms that lead to the growth (5.61). Let us collect those diagrams in Table 5.1 with integration of the  $m$ 'th power of the logarithm. We can write their sum as follows

$$\tilde{\tau}_m^{(2)}(\mathbf{p}_f, \mathbf{p}_i) = \int_{-\infty}^{\infty} dq f(q; \lambda; \mathbf{p}_f, \mathbf{p}_i) \left( \frac{\lambda}{4\pi} \log \frac{q^2 - p_f^2}{\mu} \right)^m. \quad (5.64)$$

As we argued above such an integral grows like  $(m - 3)!$ . Instead of performing the integrals and then summing over  $m$  we could consider first summing and then integrating:

$$\tilde{\tau}^{(2)}(\mathbf{p}_f, \mathbf{p}_i) = \int_{-\infty}^{\infty} dq \frac{f(q; \lambda; \mathbf{p}_f, \mathbf{p}_i)}{1 - \frac{\lambda}{4\pi} \log \frac{q^2 - p_f^2}{\mu}}. \quad (5.65)$$

The divergence of the series of  $\tilde{\tau}_m^{(2)}$  is now reflected in the divergence of the above integral. To make this a bit more explicit let us rewrite the integral above as

$$\tilde{\tau}^{(2)}(\mathbf{p}_f, \mathbf{p}_i) = \int_{-p_f^2}^{\infty} \frac{dE}{\sqrt{E + p_f^2}} \frac{2f_e(\sqrt{E + p_f^2}; \lambda; \mathbf{p}_f, \mathbf{p}_i)}{1 - \frac{\lambda}{4\pi} \log \frac{E}{\mu}}, \quad (5.66)$$

where  $f_e(q) = \frac{1}{2}(f(q) + f(-q))$ . The divergence is then due to the simple pole at  $E = \Lambda$  and so can be avoided by moving it slightly below or above the real axis:

$$\tilde{\tau}_{\pm}^{(2)}(\mathbf{p}_f, \mathbf{p}_i) = \int_{-p_f^2}^{\infty} \frac{dE}{\sqrt{E + p_f^2}} \frac{2f_e(\sqrt{E + p_f^2}; \lambda; \mathbf{p}_f, \mathbf{p}_i)}{1 - \frac{\lambda}{4\pi} \log \frac{E \pm i\epsilon}{\mu}}. \quad (5.67)$$

Of course this also introduces an ambiguity, which, as we'll now discuss, is the same as the ambiguity of the Borel summation. Apart from regularizing the integral as a principal value the  $i\epsilon$  prescription in (5.67) also introduces an extra positive/negative

imaginary part proportional to half the residue at  $E = \Lambda$ . This leads to

$$\text{amb } \tilde{\tau}^{(2)}(\mathbf{p}_f, \mathbf{p}_i) = \mp 2\pi i \Lambda \frac{f_e(\sqrt{\Lambda + p_f^2}; \lambda; \mathbf{p}_f, \mathbf{p}_i)}{\sqrt{\Lambda + p_f^2}}. \quad (5.68)$$

In the limit  $\lambda \rightarrow 0^+$  the renormalization invariant scale grows large,  $\Lambda \rightarrow \infty$ , and the ambiguity (5.68) is fully determined by the large  $q$ , small  $\lambda$  behaviour of  $f_e(q; \lambda; \mathbf{p}_f, \mathbf{p}_i)$ . Using (5.55, 5.56) and accounting for various cancellations, identical to those observed previously, the result is

$$f_e(q; \lambda; \mathbf{p}_f, \mathbf{p}_i) \sim \frac{\kappa^2}{2\pi} (\cos \theta \log \cos^2 \theta)^2 q^{-4} (\log q^2)^{-2}. \quad (5.69)$$

Combining this expression with (5.68) reproduces the Borel ambiguity (5.63) and shows explicitly that Borel summation with a prescription for the contour is in this case equivalent to a momentum integral with  $i\epsilon$  prescription.

The key point is that the  $i\epsilon$  regularization introduced above is really that of Feynman. The physical choice, which corresponds to the correct choice of ingoing-outgoing scattering boundary conditions, is  $p_f^2 + i\epsilon$  in the propagator and translates to  $-i\epsilon$  in (5.67), since  $E = q^2 - p_f^2$ . Although we reintroduced  $i\epsilon$  in (5.67) it was in some sense always there, in that if we would have kept the  $i\epsilon$  of our original Feynman rules (5.4) it would have appeared just like in (5.67) with the minus choice. Although at a given order it might have seemed to be perfectly valid to take the limit  $\epsilon \rightarrow 0$  since this provided a sensible finite answer, we now see that this is more subtle and actually causes the renormalon pole to be on the positive real axis. In other words this limit does not commute with summation of the series:

$$\lim_{\epsilon \rightarrow 0} \int dq \sum_n a_n(q, \epsilon) \lambda^n \neq \sum_n \lim_{\epsilon \rightarrow 0} \int dq a_n(q, \epsilon) \lambda^n. \quad (5.70)$$

The left hand side provides a finite answer while the right hand side is a factorially diverging series. One can equivalently recover the finite answer on the left from the diverging series on the right by Borel summation, where the prescription in the Borel plane corresponding to the physical choice  $-i\epsilon$  in (5.67) is to integrate along a contour

that deforms the real axis *below* the renormalon pole, selecting the + sign in (5.63).

This observation indicates that renormalons of the perturbative on-shell T-matrix lead to an extra imaginary non-perturbative contribution to this on-shell T-matrix, that will not get canceled by additional non-perturbative corrections, but whose presence on the contrary is required by causality, i.e. outgoing waves only after scattering. In the next section we will recalculate  $\tau^{(2)}(\mathbf{p}_f, \mathbf{p}_i)$ , exact and fully non-perturbatively in  $\lambda$ . As we will see this reproduces the results discussed here and also highlights more directly the role of the  $i\epsilon$  prescription.

### 5.5. Rederivation Using Exact Green's Operator

In this section we will recompute  $\tau^{(2)}(\mathbf{p}_f, \mathbf{p}_i)$ , the part of the on-shell T-matrix quadratic in  $\kappa$ , but now using operator formalism to do this exactly in  $\lambda$ . We first shortly review the relation between the operator formalism and the Born series in the standard perturbative setting and then point out how this can be easily adapted to find a series for the S-matrix which is perturbative in  $\kappa$  but exact in  $\lambda$ . The key step is replacing the free Green's operator by the Green's operator of the 2D  $\delta$  potential, which can be computed exactly.

#### 5.5.1. Operator Formalism and the Born Series

We start by reminding the reader of the relation between the on-shell T-matrix  $\tau$  and the off-shell T-operator  $T$  [42]:

$$\tau(\mathbf{p}_f, \mathbf{p}_i) = \langle \mathbf{p}_f | T(p_f^2 + i\epsilon) | \mathbf{p}_i \rangle. \quad (5.71)$$

The off-shell T-operator, defined for an arbitrary complex number  $z$  not on the positive real axis, is in turn determined in terms of the Green's operator/resolvent  $G(z)$  and the potential  $V = H - p^2$ :

$$T(z) = V + V G(z) V \quad , \quad G(z) = (z - H)^{-1}. \quad (5.72)$$

To connect to the standard perturbative Born series, used in the previous sections, one first rewrites the Green's function for the interacting Hamiltonian in terms of that of the free Hamiltonian:

$$G(z) = (1 - G_0(z)V)^{-1}G_0 \quad , \quad G_0 = (z - p^2)^{-1}. \quad (5.73)$$

It follows that  $T(z) = V(1 - G_0(z)V)^{-1}$ . Inserting this expression in (5.71) and expanding the inverse as a geometric series then yields the Born-series:

$$\tau(\mathbf{p}_f, \mathbf{p}_i) = \sum_{n=0}^{\infty} \langle \mathbf{p}_f | V \left( G_0(p_f^2 + i\epsilon)V \right)^n | \mathbf{p}_i \rangle. \quad (5.74)$$

### 5.5.2. Operator Formalism and the $\lambda$ -Exact Series

Let us now consider our model (5.31), where  $V = V_* + V_*$ . Note that in this section, for notational simplicity, we absorb in this subsection the coupling constants  $\lambda_0$  and  $\kappa$  into  $V_*$  and  $V_*$  respectively. Because we know the exact Green's operator  $G_*$  of the 2D  $\delta$  Hamiltonian, see below, we might consider expressing the Green's function of the total Hamiltonian in terms of  $G_*$  and  $V_*$  rather than  $G_0$  and  $V$ :

$$G(z) = (1 - G_*(z)V_*)^{-1}G_* \quad , \quad G_*(z) = (z - p^2 - V_*)^{-1}. \quad (5.75)$$

The expression for the T-operator obtained by inserting this formula in the definition (5.72) is a bit more involved:

$$\begin{aligned} T(z) = & T_*(z) + V_*(1 - G_*(z)V_*)^{-1} + V_*(1 - G_*(z)V_*)^{-1}G_*(z)V_* \\ & + (1 - V_*G_*(z))^{-1}V_*\tilde{G}_*(z)V_* + V_*(1 - G_*(z)V_*)^{-1}G_*(z)V_*G_*V_*, \end{aligned} \quad (5.76)$$

where  $T_*(z)$  is the off-shell T-operator of the 2D  $\delta$  potential. As before we can now expand the inverses as geometric series, with the important and crucial difference that

now this will give an expansion only in  $V_*$ , i.e.  $\kappa$ , while being exact in  $\lambda$ . The result is

$$\begin{aligned} T(z) = & T_*(z) + V_* \sum_{n=0}^{\infty} (G_*(z)V_*)^n + V_* \sum_{n=1}^{\infty} (G_*(z)V_*)^n \\ & + \sum_{n=1}^{\infty} (V_* G_*(z))^n V_* + V_* \sum_{n=1}^{\infty} (G_*(z)V_*)^n G_*(z)V_*. \end{aligned} \quad (5.77)$$

The above might be more clear when expressed in diagrammatic language. Apart from  $T_*$  there is a contribution from each diagram made out of an arbitrary number of vertices connected by propagators  $\sim$  representing  $G_*$ , with each vertex being a  $*$ , except the first or last vertex, which can also be  $\star$ . One has the following set of diagrams:

$$\begin{aligned} * \sim \dots \sim * & , \quad \star \sim * \sim \dots \sim * \\ * \sim \dots \sim * \sim \star & , \quad \star \sim * \sim \dots \sim * \sim \star. \end{aligned} \quad (5.78)$$

We stress again that this is a calculation perturbative in  $\kappa$  while being exact in  $\lambda$ . By further expanding  $G_*$  in terms of  $V_*$  and  $G_0$  one recovers the double expansion of the previous sections. The expansion of  $G_*$  has the diagrammatic form

$$\sim = - + -\star - + -\star -\star - + \dots. \quad (5.79)$$

The above, computed via the renormalized Feynmann rules (5.4, 5.17), is a series that converges to

$$\langle \mathbf{p}_1 | G_*(z) | \mathbf{p}_2 \rangle = \frac{(2\pi)^3 \delta^3(\mathbf{p}_1 - \mathbf{p}_2)}{(z - p_2^2)} + 2\pi \frac{\delta(q_1 - q_2)}{(z - p_1^2)(z - p_2^2)} \tau_*(z - q_2^2), \quad (5.80)$$

where we refer to (5.21) for the definition of  $\tau_*$ . That this is indeed the exact Greens function of the 2D  $\delta$  model can be checked by comparing to results obtained through the non-perturbative definition of that model through self-adjoint extension.

We have now collected all ingredients to work out an alternative perturbation theory in  $\kappa$ , which is exact in  $\lambda$ . It consists of the diagrams (5.78) with the Feynmann

rules:

$$\star : 2\pi\lambda\delta(q_{k-1} - q_k) \quad , \quad * : \kappa\hat{V}_*(\mathbf{p}_{k-1} - \mathbf{p}_k) \quad (5.81)$$

$$\sim : \int \frac{d^3\mathbf{p}_k}{(2\pi)^3} \langle \mathbf{p}_{k-1} | G_\star(p_f^2 + i\epsilon) | \mathbf{p}_k \rangle. \quad (5.82)$$

Using the above rules one readily computes the four diagrams of order  $\kappa^2$ :

$$\begin{aligned} * \sim * &= \int \frac{dq}{2\pi} \left( I^{(2,1)}(\mathbf{p}_f, \mathbf{p}_i, q) + I^{(1,1)}(\mathbf{p}_f, q) I^{(1,1)}(\mathbf{p}_i, q)^* \tau_\star(p_f^2 - q^2 + i\epsilon) \right). \\ \star \sim * \sim * &= \tau_\star(u_f^2) \int \frac{dq}{2\pi} \left( I^{(2,2)}(q_f, \mathbf{p}_i, q) \right. \\ &\quad \left. + I^{(1,2)}(q_f, q) I^{(1,1)}(\mathbf{p}_i, q)^* \tau_\star(p_f^2 - q^2 + i\epsilon) \right). \\ * \sim * \sim \star &= \tau_\star(u_i^2) \int \frac{dq}{2\pi} \left( I^{(2,2)}(q_i, \mathbf{p}_f, q)^* \right. \\ &\quad \left. + I^{(1,2)}(q, q_i) I^{(1,1)}(\mathbf{p}_f, q) \tau_\star(p_f^2 - q^2 + i\epsilon) \right). \\ \star \sim * \sim * \sim \star &= \tau_\star(u_f^2) \tau_\star(u_i^2) \int \frac{dq}{2\pi} \left( I^{(2,3)}(q_f, q_i, q) \right. \\ &\quad \left. + I^{(1,2)}(q_f, q) I^{(1,2)}(q, q_i; z) \tau_\star(p_f^2 - q^2 + i\epsilon) \right). \end{aligned}$$

Let us now focus on the parts of the above result containing an integral over  $\tau_\star$ . Collecting the four contributions we can write them as

$$\tilde{\tau}^{(2)}(\mathbf{p}_f, \mathbf{p}_i) = \int_{-\infty}^{\infty} dq f(q; \lambda, \mathbf{p}_f, \mathbf{p}_i) \frac{\lambda}{1 - \frac{\lambda}{4\pi} \log \frac{q^2 - p_f^2 - i\epsilon}{\mu}}. \quad (5.83)$$

This reproduces (5.65, 5.67) and confirms the resolution of the summation ambiguity by the  $i\epsilon$  prescription discussed there, making it fully transparent via (5.71) and (5.82). Additionally it shows that there are no further non-perturbative effects that could cancel the extra imaginary contribution the  $i\epsilon$  prescription introduces.

## 6. CONCLUSION

In this thesis, we investigated how both perturbative and non-perturbative physical information arises from the singularities of integrals. Upon a technical introduction that we presented in Chapter 2 on how the singularity on coupling plane plays a role in the perturbative and non-perturbative sectors of a quantum theory and the intimate connection between them, which is the subject of resurgence theory, in three separate chapters, which constitutes the main part of the thesis, we presented three different examples that previously published in [26–28].

First two of these examples [26, 27], which are the contents of Chapters 3 and 4, are centered around the spectral problem and its application to the semi-classical expansion and the pair-production problem. In both cases, focusing on the quantum action, we showed that the physical information, which is perturbative in the previous one and non-perturbative in the latter one, can be obtained from the singularities of the integrals that represent the action. In this way, in Chapter 3, focusing on the perturbative sector, we provide a generalization of the WKB related methods, which was discussed in Chapter 2.3.2, to arbitrary dimensions. In addition to that in Chapter 3, we complement the perturbative expansion discussion in Chapter 4, by obtaining the non-perturbative pair-production probabilities.

The  $i\varepsilon$  prescription provided us a guideline for handling the singularities and in this way, in Chapter 4, we have been able to obtain the pair production probability without any Borel-like ambiguity. We presented this resolution both using perturbative expansions and their summations via the recursion relation that presented in Chapter 3 and using Lefschetz thimbles associated to the exact leading order approximation in the derivative expansion.

In Chapter 5, on the other hand, we focused on a scattering problem in 3 dimensions centered around 2D  $\delta$ -potential. We showed that the perturbative expansion of

the  $S$ -matrix of this non-relativistic model has renormalon divergences that leads to a non-perturbative contribution to the full  $S$ -matrix. We also showed that this divergence is, in fact, associated to a singularity on the momentum space, and again using the  $i\varepsilon$  prescription, it is possible to obtain the non-perturbative information without any ambiguity.



## REFERENCES

1. Eden, R. J., P. V. Landshoff, D. I. Olive and J. C. Polkinghorne, *The Analytic S-matrix*, Cambridge Univ. Press, Cambridge, 1966.
2. White, A. R., “The Past and Future of S-Matrix Theory”, *Scattering*, pp. 1483–1504, Academic Press, London, 2002.
3. Rajaraman, R., *Solitons and Instantons: An Introduction to Solitons and Instantons in Quantum Field Theory*, North-Holland Publishing Company, 1982.
4. Shifman, M., *Advanced Topics in Quantum Field Theory.: A Lecture Course*, Cambridge Univ. Press, Cambridge, UK, 2012.
5. Zinn-Justin, J., *Path Integrals in Quantum Mechanics*, Oxford Graduate Texts, OUP Oxford, 2010.
6. Dyson, F. J., “Divergence of Perturbation Theory in Quantum Electrodynamics”, *Physical Review*, Vol. 85, pp. 631–632, 1952.
7. Bender, C. M. and T. T. Wu, “Statistical Analysis of Feynman Diagrams”, *Physical Review Letters*, Vol. 37, pp. 117–120, 1976.
8. Parisi, G., “Asymptotic Estimates of Feynman Diagrams”, *Physical Letters B*, Vol. 68, pp. 361–364, 1977.
9. Dorigoni, D., “An Introduction to Resurgence, Trans-Series and Alien Calculus”, *Annals of Physics*, Vol. 409, p. 167914, 2019.
10. Aniceto, I., G. Basar and R. Schiappa, “A Primer on Resurgent Transseries and Their Asymptotics”, *Physics Reports*, Vol. 809, pp. 1–135, 2019.

11. Bogomolny, E., “Calculation of Instanton Anti-instanton Contributions in Quantum Mechanics”, *Physics Letters B*, Vol. 91, No. 3, pp. 431–435, 1980.
12. Zinn-Justin, J., “Multi-Instanton Contributions in Quantum Mechanics”, *Nuclear Physics B*, Vol. 192, pp. 125–140, 1981.
13. Zinn-Justin, J. and U. D. Jentschura, “Multi-instantons and Exact Results I: Conjectures, WKB Expansions, and Instanton Interactions”, *Annals of Physics*, Vol. 313, No. 1, p. 197–267, 2004.
14. Zinn-Justin, J. and U. D. Jentschura, “Multi-instantons and Exact Results II: Specific Cases, Higher Order Effects and Numerical Calculations”, *Annals of Physics*, Vol. 313, No. 2, p. 269–325, 2004.
15. Aniceto, I. and R. Schiappa, “Non-perturbative Ambiguities and the Reality of Resurgent Transseries”, *Communications in Mathematical Physics*, Vol. 335, No. 1, pp. 183–245, 2015.
16. Dunne, G. V. and M. Ünsal, “Uniform WKB, Multi-instantons and Resurgent Transseries”, *Physical Review D*, Vol. 89, No. 10, 2014.
17. Cherman, A., D. Dorigoni and M. Unsal, “Decoding Perturbation Theory Using Resurgence: Stokes Phenomena, New Saddle Points and Lefschetz thimbles”, *Journal of High Energy Physics*, Vol. 10, p. 056, 2015.
18. Kozcaz, C., T. Sulejmanpasic, Y. Tanizaki and M. Ünsal, “Cheshire Cat Resurgence, Self-resurgence and Quasi-Exact Solvable Systems”, *Communications in Mathematical Physics*, Vol. 364, No. 3, pp. 835–878, 2018.
19. Dunne, G. V. and M. Unsal, “Deconstructing Zero: Resurgence, Supersymmetry and Complex Saddles”, *Journal of High Energy Physics*, Vol. 12, p. 002, 2016.
20. Dunne, G. V. and M. Ünsal, “What is QFT? Resurgent Transseries, Lefschetz

Thimbles and New Exact Saddles”, *Proceedings, 33rd International Symposium on Lattice Field Theory*, Vol. LATTICE2015, p. 010, 2016.

21. Parisi, G., “Asymptotic Estimates in Perturbation Theory”, *Physics Letters B*, Vol. 66, pp. 167–169, 1977.
22. Bogomolny, E. B., “Calculation of the Green Functions by the Coupling Constant Dispersion Relations”, *Physics Letters B*, Vol. 67, pp. 193–194, 1977.
23. Chadha, S. and P. Olesen, “On Borel Singularities in Quantum Field Theory”, *Physics Letters B*, Vol. 72, pp. 87–90, 1977.
24. Olesen, P., “On Vacuum Instability in Quantum Field Theory”, *Physics Letters B*, Vol. 73B, pp. 327–329, 1978.
25. Dunne, G. V., 2004, “Heisenberg-Euler Effective Lagrangians: Basics and Extensions”, arXiv:0406216 [hep-th].
26. Pazarbaşı, C., “Recursive Generation of the Semi-classical Expansion in Arbitrary Dimension”, *Physical Review D*, Vol. 103, No. 8, p. 085011, 2021.
27. Pazarbaşı, C., 2021, “Pair Production in Real Proper Time and Unitarity Without Borel Ambiguity”, arXiv:2111.06204 [hep-th].
28. Pazarbaşı, C. and D. Van Den Bleeken, “Renormalons in Quantum Mechanics”, *Journal of High Energy Physics*, Vol. 08, p. 096, 2019.
29. Gross, D. J. and A. Neveu, “Dynamical Symmetry Breaking in Asymptotically Free Field Theories”, *Physical Review D*, Vol. 10, p. 3235, 1974.
30. Lautrup, B. E., “On High Order Estimates in QED”, *Physics Letters B*, Vol. 69, pp. 109–111, 1977.

31. 't Hooft, G., "Can We Make Sense Out of Quantum Chromodynamics?", *The Subnuclear Series*, Vol. 15, p. 943, 1979.
32. Le Guillou, J.-C. and J. Zinn-Justin, *Large Order Behaviour of Perturbation Theory*, Elsevier, 2012.
33. Itzykson, C. and J.-B. Zuber, *Quantum Field Theory*, McGraw-Hill, 1980.
34. Beneke, M., "Renormalons", *Physics Reports*, Vol. 317, pp. 1–142, 1999.
35. Zinn-Justin, J., *Quantum Field Theory and Critical Phenomena*, Clarendon Press, Oxford, 2002.
36. Beneke, M. and V. M. Braun, "Renormalons and Power Corrections", *At The Frontier of Particle Physics: Handbook of QCD (In 3 Volumes)*, pp. 1719–1773, World Scientific, 2001.
37. Shifman, M., "New and Old about Renormalons: in Memoriam Kolya Uraltsev", *International Journal of Modern Physics A*, Vol. 30, No. 10, p. 1543001, 2015.
38. Watson, G. N., "A Theory of Asymptotic Series", *Philosophical Transactions of the Royal Society of London*, Vol. 211, pp. 279–313, 1912.
39. Sternin, B. and V. Shatalov, *Borel-Laplace Transform and Asymptotic Theory: Introduction to Resurgent Analysis*, Taylor & Francis, 1995.
40. Brent, P., "Resurgence in Geometry and Physics", 2016, <https://www.math.mcgill.ca/bpym/courses/resurgence/>, accessed on May 20, 2022.
41. Landau, L. D. and E. M. Lifshitz, *Quantum Mechanics: Nonrelativistic Theory*, Elsevier, 2013.

42. Taylor, J. R., *Scattering Theory: The Quantum Theory of Nonrelativistic Collisions*, Courier Corporation, 2006.
43. Voros, A., “The Return of the Quartic Oscillator: The Complex WKB Method”, *Annales de l'IHP Physique théorique*, Vol. 39, No. 3, pp. 211–338, 1983.
44. Balian, R., G. Parisi and A. Voros, “Discrepancies from Asymptotic Series and Their Relation to Complex Classical Trajectories”, *Physical Review Letters*, Vol. 41, No. 17, p. 1141, 1978.
45. Delabaere, E. and F. Pham, “Resurgent Methods in Semi-classical Asymptotics”, *Annales de l'IHP Physique théorique*, Vol. 71, No. 1, pp. 1–94, 1999.
46. Mironov, A. and A. Morozov, “Nekrasov Functions and Exact Bohr Sommerfeld Integrals”, *Journal of High Energy Physics*, Vol. 2010, No. 4, 2010.
47. Basar, G., G. V. Dunne and M. Ünsal, “Quantum Geometry of Resurgent Perturbative/Non-perturbative relations”, *Journal of High Energy Physics*, Vol. 2017, No. 5, 2017.
48. Kreshchuk, M. and T. Gulden, “The Picard-Fuchs Equation in Classical and Quantum Physics: Application to Higher Order WKB Method”, *Journal of Physics A*, Vol. 52, No. 15, p. 155301, 2019.
49. Fischbach, F., A. Klemm and C. Nega, “WKB Method and Quantum Periods Beyond Genus One”, *Journal of Physics A*, Vol. 52, No. 7, p. 075402, 2019.
50. Raman, M. and P. Bala Subramanian, “Chebyshev Wells: Periods, Deformations and Resurgence”, *Physical Review D*, Vol. 101, No. 12, p. 126014, 2020.
51. Codesido, S. and M. Mariño, “Holomorphic Anomaly and Quantum Mechanics”, *Journal of Physics A*, Vol. 51, No. 5, p. 055402, 2017.

52. Codesido, S., M. Marino and R. Schiappa, “Non-Perturbative Quantum Mechanics from Non-Perturbative Strings”, *Annales Henri Poincaré*, Vol. 20, No. 2, pp. 543–603, 2019.

53. Nekrasov, N. A. and S. L. Shatashvili, “Quantization of Integrable Systems and Four Dimensional Gauge Theories”, *16th International Congress on Mathematical Physics*, pp. 265–289, 2009.

54. Eynard, B. and N. Orantin, “Invariants of Algebraic Curves and Topological Expansion”, *Communications in Number Theory and Physics*, Vol. 1, pp. 347–452, 2007.

55. Norbury, P., “Quantum Curves and Topological Recursion”, *Proceedings of Symposia in Pure Mathematics*, Vol. 93, p. 41, 2015.

56. Gutzwiller, M. C., “Energy Spectrum According to Classical Mechanics”, *Journal of Mathematical Physics*, Vol. 11, No. 6, pp. 1791–1806, 1970.

57. Gutzwiller, M. C., “Periodic Orbits and Classical Quantization Conditions”, *Journal of Mathematical Physics*, Vol. 12, No. 3, pp. 343–358, 1971.

58. Voros, A., “Aspects of Semiclassical Theory in the Presence of Classical Chaos”, *Progress of Theoretical Physics Supplement*, Vol. 116, pp. 17–44, 1994.

59. Schwinger, J. S., “On Gauge Invariance and Vacuum Polarization”, *Physical Review*, Vol. 82, pp. 664–679, 1951.

60. DeWitt, B. S., “Quantum Field Theory in Curved Space-Time”, *Physics Reports*, Vol. 19, pp. 295–357, 1975.

61. Avramidi, I., *Heat Kernel Method and Its Applications*, Springer International Publishing, 2019.

62. Moss, I. and S. Poletti, “Finite Temperature Effective Actions for Gauge Fields”, *Physical Review D*, Vol. 47, pp. 5477–5486, 1993.

63. Moss, I. G. and W. Naylor, “Diagrams for Heat Kernel Expansions”, *Classical and Quantum Gravity*, Vol. 16, No. 8, p. 2611–2624, 1999.

64. Bender, C. and S. Orszag, *Advanced Mathematical Methods for Scientists and Engineers I: Asymptotic Methods and Perturbation Theory*, Advanced Mathematical Methods for Scientists and Engineers, Springer, 1999.

65. Voros, A., “Spectral Functions, Special Functions and the Selberg Zeta Function”, *Communications in Mathematical Physics*, Vol. 110, No. 3, pp. 439–465, 1987.

66. NIST Digital Library of Mathematical Functions, <http://dlmf.nist.gov/>, accessed on May 20, 2022.

67. Dunne, G. V. and M. Ünsal, “Generating Non-perturbative Physics from Perturbation Theory”, *Physical Review D*, Vol. 89, p. 041701(R), 2014.

68. Gahramanov, I. and K. Tezgin, “Remark on the Dunne-Ünsal Relation in Exact Semiclassics”, *Physical Review D*, Vol. 93, p. 065037, 2016.

69. Matone, M., “Instantons and Recursion Relations in N=2 SUSY Gauge Theory”, *Physics Letters B*, Vol. 357, pp. 342–348, 1995.

70. Gorsky, A. and A. Milekhin, “RG-Whitham Dynamics and Complex Hamiltonian Systems”, *Nuclear Physics B*, Vol. 895, pp. 33–63, 2015.

71. Heisenberg, W. and H. Euler, “Folgerungen aus der Diracschen Theorie des Positrons”, *Zeitschrift fur Physik*, Vol. 98, pp. 714–732, 1936.

72. Dunne, G. V. and T. M. Hall, “Borel Summation of the Derivative Expansion and Effective Actions”, *Physical Review D*, Vol. 60, p. 065002, 1999.

73. Florio, A., “Schwinger Pair Production from Padé-Borel Reconstruction”, *Physical Review D*, Vol. 101, No. 1, p. 013007, 2020.
74. Dunne, G. V. and C. Schubert, “Worldline Instantons and Pair Production in Inhomogeneous Fields”, *Physical Review D*, Vol. 72, p. 105004, 2005.
75. Dunne, G. V., Q. Wang, H. Gies and C. Schubert, “Worldline instantons II: The Fluctuation prefactor”, *Physical Review D*, Vol. 73, p. 065028, 2006.
76. Dunne, G. V. and Q. Wang, “Multidimensional Worldline Instantons”, *Physical Review D*, Vol. 74, p. 065015, 2006.
77. Dumlu, C. K. and G. V. Dunne, “Complex Worldline Instantons and Quantum Interference in Vacuum Pair Production”, *Physical Review D*, Vol. 84, p. 125023, 2011.
78. Dumlu, C. K., “Multidimensional Quantum Tunneling in the Schwinger Effect”, *Physical Review D*, Vol. 93, No. 6, p. 065045, 2016.
79. Ilderton, A., G. Torgrimsson and J. Wardh, “Non-perturbative Pair Production in Interpolating Fields”, *Physical Review D*, Vol. 92, No. 6, p. 065001, 2015.
80. Vassilevich, D. V., “Heat Kernel Expansion: User’s Manual”, *Physics Reports*, Vol. 388, pp. 279–360, 2003.
81. Fliegner, D., M. G. Schmidt and C. Schubert, “The Higher Derivative Expansion of the Effective Action by the String Inspired Method: Part 1”, *Zeitschrift für Physik C Particles and Fields volume*, Vol. 64, pp. 111–116, 1994.
82. Fliegner, D., P. Haberl, M. G. Schmidt and C. Schubert, “The Higher Derivative Expansion of the Effective Action by the String Inspired Method: Part 2”, *Annals of Physics*, Vol. 264, pp. 51–74, 1998.

83. Schubert, C., “Perturbative Quantum Field Theory in the String Inspired Formalism”, *Physics Reports.*, Vol. 355, pp. 73–234, 2001.
84. Keldysh, L. V., “Ionization in the Field of a Strong Electromagnetic Wave”, *Soviet Journal of Experimental and Theoretical Physics*, Vol. 20, No. 5, pp. 1307–1314, 1965.
85. Brezin, E. and C. Itzykson, “Pair Production in Vacuum by An Alternating Field”, *Physical Review D*, Vol. 2, pp. 1191–1199, 1970.
86. Popov, V. S., “Pair Production in A Variable External Field (Quasiclassical Approximation)”, *Soviet Journal of Experimental and Theoretical Physics*, Vol. 34, p. 709, 1972.
87. Kim, S. P. and D. N. Page, “Schwinger Pair Production via Instantons in A Strong Electric Field”, *Physical Review D*, Vol. 65, p. 105002, 2002.
88. Kim, S. P. and D. N. Page, “Schwinger Pair Production in Electric and Magnetic Fields”, *Physical Review D*, Vol. 73, p. 065020, 2006.
89. Kim, S. P. and D. N. Page, “Improved Approximations for Fermion Pair Production in Inhomogeneous Electric Fields”, *Physical Review D*, Vol. 75, p. 045013, 2007.
90. Dumlu, C. K. and G. V. Dunne, “The Stokes Phenomenon and Schwinger Vacuum Pair Production in Time-Dependent Laser Pulses”, *Physical Review Letters*, Vol. 104, p. 250402, 2010.
91. Taya, H., T. Fujimori, T. Misumi, M. Nitta and N. Sakai, “Exact WKB Analysis of the Vacuum Pair Production by Time Dependent Electric Fields”, *Journal of High Energy Physics*, Vol. 03, p. 082, 2021.
92. Affleck, I. K., O. Alvarez and N. S. Manton, “Pair Production at Strong Coupling

in Weak External Fields”, *Nuclear Physics B*, Vol. 197, pp. 509–519, 1982.

93. Schneider, C. and R. Schützhold, “Dynamically Assisted Sauter-Schwinger Effect in Inhomogeneous Electric Fields”, *Journal of High Energy Physics*, Vol. 02, p. 164, 2016.

94. Akal, I. and G. Moortgat-Pick, “Quantum Tunnelling from Vacuum in Multidimensions”, *Physical Review D*, Vol. 96, No. 9, p. 096027, 2017.

95. Dietrich, D. D. and G. V. Dunne, “Gutzwiller’s Trace Formula and Vacuum Pair Production”, *Journal of Physics A*, Vol. 40, pp. F825–F830, 2007.

96. Dunne, G. V., “Worldline Instantons, Vacuum Pair Production and Gutzwiller’s Trace Formula”, *Journal of Physics A*, Vol. 41, p. 164041, 2008.

97. Gutzwiller, M. C., “Periodic Orbits and Classical Quantization Conditions”, *Journal of Mathematical Physics*, Vol. 12, pp. 343–358, 1971.

98. Muratore-Ginanneschi, P., “Path Integration Over Closed Loops and Gutzwiller’s Trace Formula”, *Physics Reports*, Vol. 383, pp. 299–397, 2003.

99. Sueishi, N., S. Kamata, T. Misumi and M. Ünsal, “On Exact WKB Analysis, Resurgent Structure and Quantization Conditions”, *Journal of High Energy Physics*, Vol. 12, p. 114, 2020.

100. Tanizaki, Y. and T. Koike, “Real Time Feynman Path Integral with Picard–Lefschetz Theory and Its Applications to Quantum Tunneling”, *Annals of Physics*, Vol. 351, pp. 250–274, 2014.

101. Feldbrugge, J., J.-L. Lehners and N. Turok, “Lorentzian Quantum Cosmology”, *Physical Review D*, Vol. 95, No. 10, p. 103508, 2017.

102. Feldbrugge, J., J.-L. Lehners and N. Turok, “No Smooth Beginning for Space-

time”, *Physical Review Letters*, Vol. 119, No. 17, p. 171301, 2017.

103. Millington, P., Z.-G. Mou, P. M. Saffin and A. Tranberg, “Statistics on Lefschetz Thimbles: Bell-Leggett-Garg Inequalities and the Classical Statistical Approximation”, *Journal of High Energy Physics*, Vol. 03, p. 077, 2021.

104. Rajeev, K., “Lorentzian Worldline Path Integral Approach to Schwinger Effect”, *Physical Review D*, Vol. 104, No. 10, p. 105014, 2021.

105. Nikishov, A. I., “Barrier Scattering in Field Theory Removal of Klein Paradox”, *Nuclear Physics B*, Vol. 21, pp. 346–358, 1970.

106. Cohen, T. D. and D. A. McGady, “The Schwinger Mechanism Revisited”, *Physical Review D*, Vol. 78, p. 036008, 2008.

107. Costin, O. and G. V. Dunne, “Resurgent Extrapolation: Rebuilding A Function from Asymptotic Data. Painlevé I”, *Journal of Physics A*, Vol. 52, No. 44, p. 445205, 2019.

108. Costin, O. and G. V. Dunne, “Physical Resurgent Extrapolation”, *Physics Letters B*, Vol. 808, p. 135627, 2020.

109. Costin, O. and G. V. Dunne, “Uniformization and Constructive Analytic Continuation of Taylor Series”, *Communications in Mathematical Physics*, Vol. 392, pp. 863–906, 2022.

110. Basar, G. and G. V. Dunne, “Resurgence and the Nekrasov-Shatashvili Limit: Connecting Weak and Strong Coupling in the Mathieu and Lamé Systems”, *Journal of High Energy Physics*, Vol. 2015, No. 2, 2015.

111. Gusynin, V. P. and I. A. Shovkovy, “Derivative Expansion for the One Loop Effective Lagrangian in QED”, *Canadian Journal of Phys.*, Vol. 74, pp. 282–289, 1996.

112. Gusynin, V. P. and I. A. Shovkovy, “Derivative Expansion of the Effective Action for QED in (2+1) Dimensions and (3+1) Dimensions”, *Journal of Mathematical Physics*, Vol. 40, pp. 5406–5439, 1999.
113. Berndt, B. and A. Ramanujan, *Ramanujan’s Notebooks: Part 3.*, Springer, Germany, 1991.
114. Witten, E., “Analytic Continuation Of Chern-Simons Theory”, *AMS/IP Studies in Advanced Mathematics*, Vol. 50, pp. 347–446, 2011.
115. Witten, E., 2010, “A New Look At The Path Integral Of Quantum Mechanics”, arXiv:1009.6032 [hep-th].
116. Jackiw, R., *Diverse Topics in Theoretical and Mathematical Physics*, Advanced Series in Mathematical Physics, World Scientific, 1995.
117. Albeverio, S., F. Gesztesy, R. Hoegh-Krohn and H. Holden, *Solvable Models in Quantum Mechanics*, Theoretical and Mathematical Physics, Springer Berlin Heidelberg, 2012.

## APPENDIX A: NOTATIONS AND CONVENTIONS

Our conventions for the Fourier transform in  $D$  dimensions are the followings

$$\langle \mathbf{x}|\mathbf{p}\rangle = e^{i\mathbf{x}\cdot\mathbf{p}/\hbar} \quad , \quad \langle \mathbf{x}|\mathbf{x}'\rangle = \delta^D(\mathbf{x} - \mathbf{x}'), \quad (\text{A.1})$$

$$\langle \mathbf{p}|\mathbf{x}\rangle = \frac{e^{-i\mathbf{x}\cdot\mathbf{p}/\hbar}}{(2\pi\hbar)^D} \quad , \quad \langle \mathbf{p}|\mathbf{p}'\rangle = (2\pi\hbar)^D \delta^D(\mathbf{p} - \mathbf{p}'). \quad (\text{A.2})$$

Then, the identity operator is

$$\mathbf{1} = \int d^Dx |\mathbf{x}\rangle\langle\mathbf{x}| = \int \frac{d^Dp}{(2\pi\hbar)^D} |\mathbf{p}\rangle\langle\mathbf{p}|. \quad (\text{A.3})$$

and trace of an operator is

$$\text{Tr } O = \int d^Dx \langle \mathbf{x}|O|\mathbf{x}\rangle = \int \frac{d^Dp}{(2\pi\hbar)^D} \langle \mathbf{p}|O|\mathbf{p}\rangle. \quad (\text{A.4})$$

In Chapter 5, we set  $\hbar = 2m = 1$  which implies that only the length dimension remains and some objects appearing in this chapter have the following dimensions:

$$\begin{aligned} [E] &= [p^2] = L^{-2} \quad , \quad [S] = L^3 \quad , \quad [\tau] = L, \\ [\lambda_0] &= [\lambda] = 1 \quad , \quad [\kappa] = L^{-1} \quad , \quad [\mu] = [\Omega] = L^{-2}. \end{aligned} \quad (\text{A.5})$$

## APPENDIX B: ASYMPTOTICS OF A KEY RENORMALON INTEGRAL

In this appendix, we will discuss the integral appears in the renormalon discussion in Chapter 5. The following content is identical to Appendix B of [28].

For large  $n$  there is the following asymptotic formula

$$I = \int_{-\infty}^{\infty} dq f(q) (\log(q^2 - q_0) + a)^n \sim e^{\rho a} \rho^{-(n+1)} \left(\frac{n}{\rho}\right)^{\sigma} n!, \quad (\text{B.1})$$

where the parameters  $\rho$  and  $\sigma$  are determined by the large  $|q|$  behaviour of  $f$ ,  $q_0$  a positive constant and  $a$  a complex number. More precisely the formula above is valid when  $f$  decays for large  $|q|$  as

$$f(q) \sim |q|^{-2\rho-1} (\log q^2)^{\sigma}. \quad (\text{B.2})$$

Let us sketch how this formula is derived and why only the large  $|q|$  region contributes while the contributions around  $q^2 \approx q_0^2$  cancel.

One starts by rewriting the integral as an integral over the even part of  $f$  and splitting it over the regions  $[0, q_0]$ ,  $[q_0, \sqrt{2}q_0]$ ,  $[\sqrt{2}q_0, \infty]$ . In the first two regions one changes integration variables as  $q = q_0\sqrt{1+e^{-t}}$  while in the third region  $q = q_0\sqrt{1+e^t}$ , so that  $I = I_1 + I_2 + I_3$  with

$$I_1 = - \int_{0-i\pi}^{\infty-i\pi} dt e^{-t} g(t) (\tilde{a} - t)^n, \quad \tilde{a} = a + \log q_0^2, \quad (\text{B.3})$$

$$I_2 = \int_0^{\infty} dt e^{-t} g(t) (\tilde{a} - t)^n, \quad g(t) = \frac{q_0 f_e(q_0 \sqrt{1+e^{-t}})}{\sqrt{1+e^{-t}}}, \quad (\text{B.4})$$

$$I_3 = \int_0^{\infty} dt e^t h(t) (\tilde{a} + t)^n, \quad h(t) = \frac{q_0 f_e(q_0 \sqrt{1+e^t})}{\sqrt{1+e^t}}. \quad (\text{B.5})$$

where  $f_e = \frac{1}{2}(f(q) + f(-q))$  is the even part of  $f$ . Each of these integrals will at large  $n$  be dominated by the large  $t$  region. Note that the first two integrals are very similar, except that the first is over a complex contour parallel to the real axis. Although

each of these integrals grows like  $n!$  these contributions cancel each other. One way to see this is that both integrals together are equal to a closed contour integral – up to two vertical pieces which can be estimated not to grow factorially – and the resulting residue contributions will only grow only with a powerlaw in  $n$ .

This leaves us with the third contribution, using the assumed decay (B.2) for  $f$  one reproduces (B.1) by standard saddle point evaluation:

$$I_3 \sim q_0^{-2\rho} \int_0^\infty dt e^{-\rho t} t^\sigma (\tilde{a} + t)^n \sim e^{\rho a} \rho^{-(n+1)} \left(\frac{n}{\rho}\right)^\sigma n!. \quad (\text{B.6})$$

## APPENDIX C: NUMERICAL RESULTS

Here, we present the results for several anharmonic oscillators in one, two and three dimensions. The computations are done by the implementation of the recursive formula in (4.28) to *Mathematica*. The results for one dimension match exactly with the ones in the literature [49, 51, 68] and for two and three dimension, to our knowledge, these results appeared for the first time in [26] and this appendix is identical to Appendix C of that paper.

### C.1. Cubic Oscillator:

We consider  $V(\mathbf{x}) = \frac{x^2}{2} + \lambda x_1 \mathbf{x}^2$ .

- 1 Dimension:

$$\begin{aligned}\Delta\Gamma_0(u) &= u + \frac{15u^2\lambda^2}{4} + \frac{1155u^3\lambda^4}{16} + \frac{255255u^4\lambda^6}{128} + \frac{66927861u^5\lambda^8}{1024}. \\ \Delta\Gamma_2(u) &= \frac{7\lambda^2}{16} + \frac{1365u\lambda^4}{64} + \frac{285285u^2\lambda^6}{256} + \frac{121246125u^3\lambda^8}{2048}. \\ \Delta\Gamma_4(u) &= \frac{119119\lambda^6}{2048} + \frac{156165009u\lambda^8}{16384} + \frac{67931778915u^2\lambda^{10}}{65536}.\end{aligned}$$

- 2 Dimensions:

$$\begin{aligned}\Delta\Gamma_0(u) &= \frac{u^2}{2} + 2u^3\lambda^2 + 30u^4\lambda^4 + 672u^5\lambda^6 + 18480u^6\lambda^8. \\ \Delta\Gamma_2(u) &= -\frac{1}{12} + \frac{u\lambda^2}{3} + 10u^2\lambda^4 + \frac{1120u^3\lambda^6}{3} + 15400u^4\lambda^8. \\ \Delta\Gamma_4(u) &= \frac{11\lambda^4}{105} + \frac{92u\lambda^6}{3} + 3240u^2\lambda^8 + 265408u^3\lambda^{10} + 19347328u^4\lambda^{12}.\end{aligned}$$

- 3 Dimensions:

$$\begin{aligned}\Delta\Gamma_0(u) &= \frac{u^3}{6} + \frac{35u^4\lambda^2}{48} + \frac{3003u^5\lambda^4}{320} + \frac{46189u^6\lambda^6}{256} + \frac{26558675u^7\lambda^8}{6144}. \\ \Delta\Gamma_2(u) &= -\frac{u}{8} - \frac{5u^2\lambda^2}{96} + \frac{77u^3\lambda^4}{128} + \frac{36465u^4\lambda^6}{1024} + \frac{37182145u^5\lambda^8}{24576}. \\ \Delta\Gamma_4(u) &= -\frac{2369\lambda^2}{80640} - \frac{2869u\lambda^4}{5120} - \frac{265551u^2\lambda^6}{28672} + \frac{30808063u^3\lambda^8}{294912}.\end{aligned}$$

### C.2. Quartic Oscillator:

We consider  $V(\mathbf{x}) = \frac{\mathbf{x}^2}{2} + \lambda(\mathbf{x}^2)^2$ .

- 1 Dimension:

$$\begin{aligned}\Delta\Gamma_0(u) &= u - \frac{3u^2\lambda}{2} + \frac{35u^3\lambda^2}{4} - \frac{1155u^4\lambda^3}{16} + \frac{45045u^5\lambda^4}{64} - \frac{969969u^6\lambda^5}{128}. \\ \Delta\Gamma_2(u) &= -\frac{3\lambda}{8} + \frac{85u\lambda^2}{16} - \frac{2625u^2\lambda^3}{32} + \frac{165165u^3\lambda^4}{128} - \frac{10465455u^4\lambda^5}{512}. \\ \Delta\Gamma_4(u) &= -\frac{1995\lambda^3}{256} + \frac{400785u\lambda^4}{1024} - \frac{26249223u^2\lambda^5}{2048} + \frac{1419711293u^3\lambda^6}{4096}.\end{aligned}$$

- 2 Dimensions:

$$\begin{aligned}\Delta\Gamma_0(u) &= \frac{u^2}{2} - \frac{4u^3\lambda}{3} + 8u^4\lambda^2 - 64u^5\lambda^3 + \frac{1792u^6\lambda^4}{3}. \\ \Delta\Gamma_2(u) &= -\frac{1}{12} - \frac{2u\lambda}{3} + 8u^2\lambda^2 - \frac{320u^3\lambda^3}{3} + \frac{4480u^4\lambda^4}{3}. \\ \Delta\Gamma_4(u) &= \frac{4\lambda^2}{9} - \frac{2752u\lambda^3}{105} + \frac{17536u^2\lambda^4}{21} - \frac{192512u^3\lambda^5}{9}.\end{aligned}$$

- 3 Dimensions:

$$\begin{aligned}\Delta\Gamma_0(u) &= \frac{u^3}{6} - \frac{5u^4\lambda}{8} + \frac{63u^5\lambda^2}{16} - \frac{1001u^6\lambda^3}{32} + \frac{36465u^7\lambda^4}{128}. \\ \Delta\Gamma_2(u) &= -\frac{u}{8} - \frac{5u^2\lambda}{16} + \frac{455u^3\lambda^2}{96} - \frac{8085u^4\lambda^3}{128} + \frac{435435u^5\lambda^4}{512}. \\ \Delta\Gamma_4(u) &= \frac{269\lambda}{4480} + \frac{523u\lambda^2}{1280} - \frac{67479u^2\lambda^3}{2560} + \frac{7501923u^3\lambda^4}{10240}.\end{aligned}$$

### C.3. Quintic Oscillator:

We consider  $V(\mathbf{x}) = \frac{\mathbf{x}^2}{2} + \lambda x_1(\mathbf{x}^2)^2$ .

- 1 Dimension:

$$\begin{aligned}\Delta\Gamma_0(u) &= u + \frac{315u^4\lambda^2}{16} + \frac{692835u^7\lambda^4}{128} + \frac{9704539845u^{10}\lambda^6}{4096}. \\ \Delta\Gamma_2(u) &= \frac{1085u^2\lambda^2}{32} + \frac{15570555u^5\lambda^4}{512} + \frac{456782651325u^8\lambda^6}{16384}. \\ \Delta\Gamma_4(u) &= \frac{1107\lambda^2}{256} + \frac{96201105u^3\lambda^4}{2048} + \frac{4140194663605u^6\lambda^6}{32768}.\end{aligned}$$

- 2 Dimensions:

$$\begin{aligned}\Delta\Gamma_0(u) &= \frac{u^2}{2} + 8u^5\lambda^2 + 1440u^8\lambda^4 + 465920u^{11}\lambda^6 + 198451200u^{14}\lambda^8. \\ \Delta\Gamma_2(u) &= -\frac{1}{12} + \frac{56u^3\lambda^2}{3} + 9408u^6\lambda^4 + \frac{17937920u^9\lambda^6}{3} + 4213780480u^{12}\lambda^8. \\ \Delta\Gamma_4(u) &= \frac{44u\lambda^2}{7} + 20704u^4\lambda^4 + \frac{235023360u^7\lambda^6}{7} + \frac{222716628992u^{10}\lambda^8}{5}.\end{aligned}$$

- 3 Dimensions:

$$\begin{aligned}\Delta\Gamma_0(u) &= \frac{u^3}{6} + \frac{77u^6\lambda^2}{32} + \frac{323323u^9\lambda^4}{1024} + \frac{1302340845u^{12}\lambda^6}{16384}. \\ \Delta\Gamma_2(u) &= -\frac{u}{8} + \frac{805u^4\lambda^2}{128} + \frac{2263261u^7\lambda^4}{1024} + \frac{34659070875u^{10}\lambda^6}{32768}. \\ \Delta\Gamma_4(u) &= \frac{83819u^2\lambda^2}{23040} + \frac{1121359525u^5\lambda^4}{172032} + \frac{1891956467895u^8\lambda^6}{262144}.\end{aligned}$$